ADVANCED MASTERS IN STRUCTURAL ANALYSIS
OF MONUMENTS AND HISTORICAL CONSTRUCTIONS

Master's Thesis

Dwipayana Ali Muhammad Hanafiah

Numerical Analysis of Bell Tower of St. Jakub Church in Kutná Hora

Czech Technical University in Prague

Education and Culture

Erasmus Mundus

ADVANCED MASTERS IN STRUCTURAL ANALYSIS
OF MONUMENTS AND HISTORICAL CONSTRUCTIONS

Master's Thesis

Numerical Analysis of Belltower of St. Jakub Church in Kutná Hora

This Masters Course has been funded with support from the European Commission. This publication reflects the views only of the author, and the Commission cannot be held responsible for any use which may be made of the information contained therein.

Czech Republic | 2017

CZECH TECHNICAL UNIVERSITY IN PRAGUE
Faculty of Civil Engineering
Thákurova 7, 166 29 Prague 6, Czech Republic

MASTER'S THESIS PROPOSAL

study programme: FS

study branch: Advanced Masters in Structural Analysis of Monuments and Historical Constructions

academic year: 2016/2017

Student's name and surname: Dwipayana Ali Muhammad Hanafiah

Department: Department of Mechanics

Thesis supervisor: Petr Fajman

Thesis title: Numerická analýza kostelní věže sv. Jakuba v Kutné Hoře

Thesis title in English Numerical Analysis of Belltower of St. Jakub Church in Kutna Hora

Framework content: The first part of the thesis will be discussing about the historical aspect of St. Jakub Church in Kutnà Hora, especially to the bell tower. The next part will be discussing about the Masonry Quality Index method to determine the bell tower's structural parameters. Lastly, , numerical method is performed to model the bell tower and to obtain the values of natural frequencies as well as whether the swinging of the bell tower is giving a resonance effect to the whole structure.

Assignment date: 7/04/2017 Submission date: 06/07/2017

If the student fails to submit the Master's thesis on time, they are obliged to justify this fact in advance in writing, if this request (submitted through the Student Registrar) is granted by the Dean, the Dean will assign the student a substitute date for holding the final graduation examination (2 attempts for FGE remain). If this fact is not appropriately excused or if the request is not granted by the Dean, the Dean will assign the student a date for retaking the final graduation examination, FGE can be retaken only once. (Study and Examination Code, Art 22, Par 3, 4.)

The student takes notice of the obligation of working out the Master's thesis on their own, without any outside help, except for consultation. The list of references, other sources and names of consultants must be included in the Master's thesis.

Master's thesis supervisor

Head of department

Date of Master's thesis proposal take over: July 2017

Student

This form must be completed in 3 copies – 1x department, 1x student, 1x Student Registrar (sent by department)

No later than by the end of the 2nd week of instruction in the semester, the department shall send one copy of BT Proposal to the Student Registrar and enter data into the faculty information system KOS. (Dean's Instruction for Implementation of Study Programmes and FGE at FCE CTU Art. 5, Par. 7)

DECLARATION

Name: Dwipayana Ali Muhammad Hanafiah

Email: dwipayana.hanafiah@gmail.com

Title of the Msc Dissertation: Numerical Analysis of Bell Tower of St. Jakub Church in Kutnà Hora

Supervisor(s): Doc. Ing. Petr Fajman. Csc.

Year: 2016/2017

I hereby declare that all information in this document has been obtained and presented in accordance with academic rules and ethical conduct. I also declare that, as required by these rules and conduct, I have fully cited and referenced all material and results that are not original to this work.

I hereby declare that the MSc Consortium responsible for the Advanced Masters in Structural Analysis of Monuments and Historical Constructions is allowed to store and make available electronically the present MSc Dissertation.

University: Czech Technical University in Prague

Date: 6th July 2017

Signature:

This master thesis report is dedicated to my parents, my wife, and all my family who always believe in me.

ACKNOWLEDGEMENTS

The writer would like to acknowledge Erasmus consortium for providing the scholarship. I would like to express my gratitude to my advisor Prof. Petr Fajman for all his support, useful questions and comments through the learning process of this master thesis. Special appreciation is also given to all teaching staffs, professors, university staffs, and SAHC colleagues in both of University of Padova and Czech Technical University in Prague for making this this amazing experience possible. Finally, I thank my parents, my lovely wife, sister, and brother for their unlimited support and encouragement throughout the years in all possible ways.

ABSTRACT

It is a great advantage, as in our case, if a numerical model can support the results of experimental measurements obtained from the measurement of real structure. It will allow us to get better knowledges of the structural behavior as well as to prepare for any intervention required in the future. This thesis will be discussing about numerical modelling of bell tower and the bell itself (is now in production) of St. Jakub Church in Kutnà Hora, Czech Republic. The structural parameters of the material are estimated using the Masonry Quality Index (MQI) method. The result of the structural analysis shows that the MQI method is giving a quite accurate representation of the structural material, it could be seen from the values of the first three natural frequencies of the bell tower that matched the previously done on field modal analysis. Furthermore, the bell tower is also checked for effect of the bell swing. The swinging of the bell could induce a resonance effect that could cause the structure to deform in a larger magnitude than what it supposed to be. The effect of using heavier bell is also being analyzed on the structure to avoid the resonance effect. Moreover, the lateral displacement caused by static wind load will also be counted into comparison between those load and displacement caused by the bell swing

ABSTRAKTY

Numerická analýza kostelní věže sv. Jakuba v Kutné Hoře

Je velkou výhodou (jako v našem případě), pokud lze numerický model konstrukce podpořit výsledky experimentálních měření získaných na skutečné konstrukci. To dovoluje získat lepší znalosti o chování konstrukce případně zjistit její problémy a přípravit její rekonstrukci. Práce se zaměřuje na numerický model zvonu (nyní je ve výrobě) a věže kostela sv. Jakuba v Kutné Hoře. Vzhledem k tomu, že nebylo možné experimentálně získát vstupní hodnoty materiálových vlastností , byl použit postup MQI (index kvality zdiva). Výsledná odezva konstrukce ukazuje na správné určení materiálových hodnot. Hodnoty prvních tři vlastních frekvencí jsou v souladu s naměřenými hodnotami. Následně byla hledána odezva kostelní věže od vynuceného kmitání od zvonění navrhovaného zvonu a byla kontrolována možnost resonance jiných težších zvonů. Nakonec byl proveden statický výpočet od zatížení větrem a byly porovnány hodnoty posunů s hodnotami od dynamického zatížení zvonem.

ABSTRAKSI

Analisis numerik menara bel dari Gereja St. Jakub, Kutná Hora

Pemodelan struktur secara numerik merupakan suatu metode yang berguna sebagai alat verifikasi terhadap pengujian analisis modal yang telah dilakukan di lapangan. Metode ini memberikan kita suatu pengetahuan yang lebih mendalam tentang perilaku struktur suatu bangunan dan juga sebagai bahan persiapan untuk rencana perbaikan struktur yang diperlukan di masa mendatang. Thesis ini akan membahas tentang analisis numerik dari menara dan bel dari Gereja St. Jakub yang berlokasi di Kutnà Hora, Republik Ceko. Parameter struktural dari material batu bata diestimasi dengan menggunakan metode Masonry Quality Index (MQI). Hasil dari analisis struktur yang dilakukan menunjukkan jika metode MQI dalam menentukan parameter struktur suatu material memberikan hasil yang cukup akurat sebagai representasi dari material yang digunakan, ini bisa dilihat dari nilai tiga frekuensi natural dari menara yang mempunyai hasil menyerupai dengan pengujian analisis modal yang telah dilakukan sebelumnya. Lebih jauh lagi, perilaku struktural menara juga dicek terhadap efek dari ayunan bel yang digunakan. Ayunan dari bel dapat memberikan efek resonansi yang bisa menimbulkan deformasi dengan nilai yang lebih besar dari seharusnya. Efek dari penggunaan bel dengan berat yang berbeda juga dianalisis untuk menghindari fenomena resonansi. Deformasi lateral akibat beban angin juga dilibatkan sebagai perbandingan deformasi antara beban angin dengan beban dari ayunan bel.

This page is left blank on purpose.

TABLE OF CONTENTS

LIST OF FIGURES

LIST OF TABLES

1. INTRODUCTION

Church of St. James (Kostel sv. Jakuba) is a Gothic style church located in Kutná Hora, a city situated in the Central Bohemian Region of Bohemia, Czech Republic. Its tower is one of the most defining landmark of the city. Constructed in 1330, it took 90 for the church to be completed in 1420. The church was originally designed with two towers, but the construction of the southern tower was canceled due to the fact that the ground beneath the church area was too unstable due to silver mining tunnels. The unfinished part of the second tower is clearly visible on the church exterior. For the unusual height of its tower, the church was also referred to as the Tall or High Church until the 17th century. The interior of the church combines Gothic, Renaissance, and Baroque architecture. In 1995, together with other buildings and monuments on the historic center of the city, Church of St. Jakub was registered to UNESCO World Heritage Site. This thesis report will present a numerical analysis of the church’s bell tower. A good numerical modeling of a structure will be a very useful tool and can support the results of experimental measurements obtained from the measurement of a real structure. It will allow us to get better knowledges of the structural behavior as well as to prepare for any intervention required in the future.

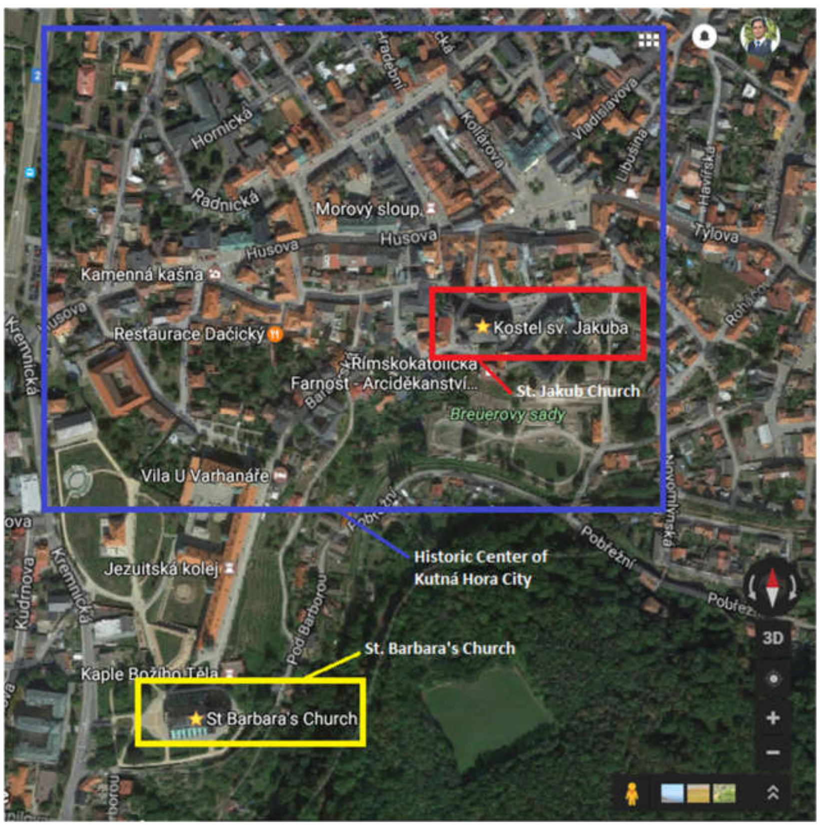

Figure 1 - Location of St. Jakub Church within the area of Kutná Hora city

1.1 History and alterations of the Church

The Church of St James is the oldest stone church in Kutná Hora, and was intended as the spiritual center of the entire town since the beginning of its establishment. Located in the heart of the medieval town, the distance to all other churches is approximately the same, which is an expression of the sacred nature of this area. The tower of the Church of St James is thus visible from afar and serves as a crucial point of orientation for the wider area.

Construction of the church began somewhere around 1330s and its most important donors were the coiners and minters from the adjacent Italian Court, the seat of the Central Mint (coin manufacturer) of Prague. The presbytery was vaulted and held its first church service as early as in 1356. The Sedlec Cistercian monastery had a major influence on the early part of the church‘s construction, both structurally and symbolically. This is also why the church was originally dedicated to the Virgin Mary. Construction work was completed in 1420. Parler's building workshop, which at that time already working on the construction of the Cathedral of St. Barbara, participated in the later construction stages. The work of this workshop is particularly noticeable in the rich flamboyant tracery used in the large window on the west facade of the church. The original plan of the church was to construct two towers. This initial plan was abandoned during construction phase due to the serious problems with the subsoil, which caused the structure to be unable to bear the load of a second church tower. Nevertheless, the north tower was built to a respectable height of 86 meters, afterwards the church simply began to be called the tall church.

In 1410, a separate parish district was established at the High Church, with the church remaining at its center to this day. However, the Catholic tradition was interrupted for two centuries by the actions of Utraquist priests, who administered the church from 1424 until 1620. During this time, the church was placed under the protection of St James.

Over the years, the church has been through several periods of renovation and repair. In 1650, the roof was repaired after 200 years. The bell tower also frequently repaired due to high frequency of lightning strike. In 1698, the dome of the bell was repaired but it was heavily damaged by a storm in 1740. During the 1st and 2nd World War periods, all five bells of the St. Jakub Church was seized for military purposes.

Figure 2 – Church of St. Jakub, Kutná Hora, Czech Republic

The long history of the church has left many unique relics from various periods. The end of the presbytery is decorated with Late Gothic frescoes, with one of the sanctuaries even bearing the oldest surviving inscription in Kutná Hora (1356). The aisle bears preserved frescoes from the mid-15th century, which position distinctly Catholic motifs next to Utraquist symbols, thus uncovering, in an interesting manner, the intricate ideological situation prevailing at that time. Also of interest is the rare predella of the otherwise destroyed main altar from 1515 and, finally, a painting of The Holy Trinity by Petr Brandl, which is part of the current altar, built in the Baroque style.

1.2 Bell Tower of the Church

The bell tower of St. Jakub Church standing at 86 meters high and become a crucial point of orientation of the surrounding area. The tower consists of six floors with various inter story height. On the south and east side of the tower, there are two points of contacts that attaches the tower to the main structure of the church. To counter the thrust from the church, there are three buttresses constructed on the west and north side of the tower. One buttress is located on the west façade, and the remaining two buttresses are located on the northern façade of the tower. These buttresses go from ground to the height of 20.4 meter.

Figure 3 - View of the north (left) and west (right) side of the tower

The bell tower has regular rectangular plan for each floor. From ground floor to third floor (28-meter-high), the tower is measured 10.2 x 9.0 m with the thickness of the wall varies between 1920 to 2210 mm. From the fourth floor to the roof, the tower is measured 9.4 x 9.0 m with the thickness of the wall varies between 1130 to 1180 mm. There are presence of vaults below the floor from the first floor up until the third floor. On the fourth floor, a wooden platform for the bell was installed as well as the clocks on all side of the facade.

The main materials of the wall are made of double leaf masonry wall. The outer part of the wall is made of cut natural stone while the inner part of the wall is made from masonry brick. Lime mortar is used on both side of the wall as a binding agent, though in the inner part of the wall it seems that some of the mortar are degraded. The buttresses and tower's top floor are made from only one layer of cut natural stone, while the vaults are made from masonry brick. The mechanical properties of the wall will be further determined using Masonry Quality Index (MQI) method.

Figure 4 – Inside layer of the double leaves masonry wall

1.3 Present Condition of the Bell Tower

The bell tower is accessible through a staircase door on the south side of the church. After walking through the rounded staircases, then crossing through the attic of the church, the bell tower can be entered on its second floor. On the Third floor, there is a room used for the main mechanical machine of the clocks.

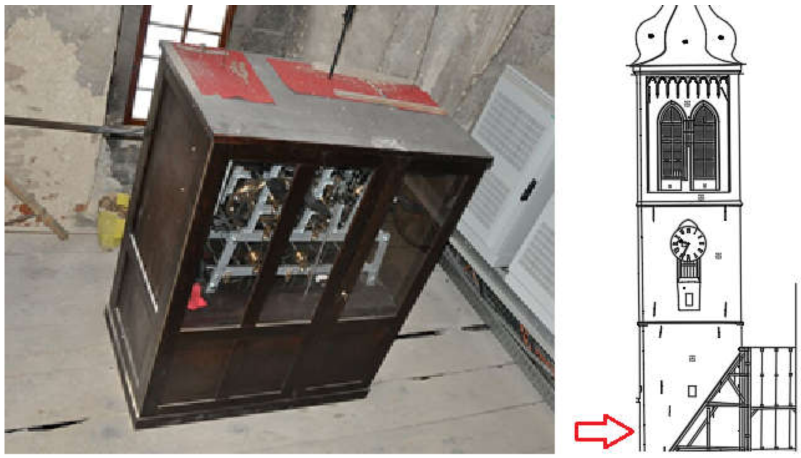

Figure 5 – Mechanical machine for the clocks

The bell and clocks room on the fourth floor is divided with a wooden platform in the middle. Lastly, the room on the fifth floor is used for what is appearing to be a structural health monitoring system for the tower.

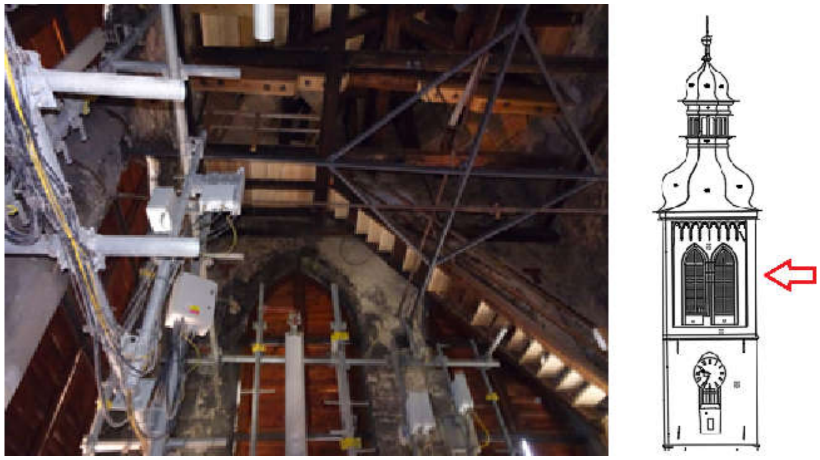

Figure 6 – Condition on the fifth floor with the installed device

During the site visit to the St. Jakub Church, the bell was not in place. But in the future the bell will be reinstalled and during the course of the report, the effect of bell swing will be taken into account for structural analysis, especially to see whether the bell will cause resonance effect to the structure or not. There are presence of cracks on the strucure. Most of the cracks on the tower appear on the inner side of the wall. Moreover, the cracks are having a vertical pattern suggesting that the cause of the cracks is from compressive load.

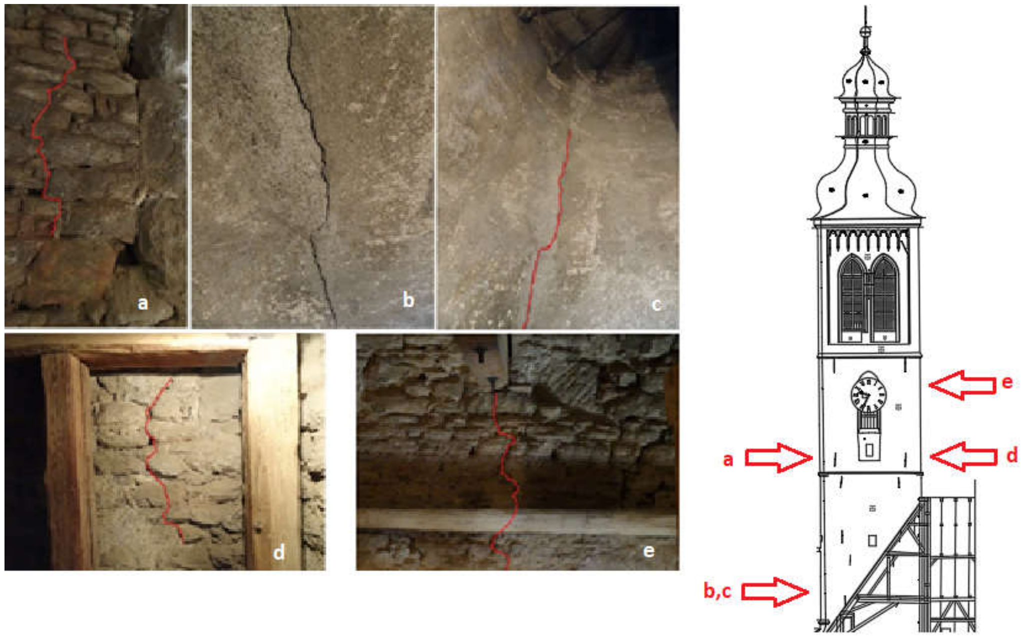

Figure 7 – Vertical cracks spotted during the site visit

2. LITERATURE REVIEW

2.1 Natural Frequencies and Mode Shape

Free vibration is a vibration of a structure that occurs at its natural frequency, which is the frequency which a system tends to oscillate without any presence of driving force. Free vibration of any elastic body is called natural vibration and happens at a frequency called natural frequency. Natural vibration is difference with forced vibration which happen at frequency of applied force. When the forced frequency is equal to the natural frequency, the amplitude of vibration will increase by multiple times. This phenomenon is also known as resonance.

The free vibration of an undamped system in one of its natural vibration modes mathematically described by

$$m\ddot{u} + ku = 0 \tag{2.1}$$

$$u(t) = q_n(t).\phi_\mathrm{n} \tag{2.2}$$

Where Φ_n denotes the deformed shape, which does not vary with time, and $q_n(t)$ provides the amplitude or the scale factor. The system's displacement as a function of time can be described by simple harmonic function of

$$q_n(t) = A_n.cos\omega_n.t + B_n.sin\omega_n.t \tag{2.3}$$

Where A_n ad B_n are constants of integration given by the initial conditions that initiate the motion. Combining equation *(2.2)* and *(2.3)* will gives

$$u(t) = \phi_\mathrm{n}(A_n.cos\omega_n.t + B_n.sin\omega_n.t) \tag{2.4}$$

Where ω_n and Φ_n are unknown. Substituting this form of u(t) in equation *(2.1)* gives

$$[-\omega_\mathrm{n}^2\mathrm{m}\phi_\mathrm{n} + \mathrm{k}\phi_n]q_n(t) = 0 \tag{2.5}$$

The equation above can be satisfied in one of two ways. Either $q_n(t)=0$, or the other part of the equation equals zero. Here we can see that when $q_n(t)=0$, it implies that $u(t)=0$ and there is no motion of the system (trivial solution). The other one being that the natural frequencies and modes must satisfy the following algebraic equation:

$$\mathrm{k}\phi_n = \omega_\mathrm{n}^2\mathrm{m}\phi_\mathrm{n}$$

$$[\mathrm{k} - \omega_\mathrm{n}^2\mathrm{m}]\phi_n = 0 \tag{2.6}$$

This algebraic equation is called the matrix eigen value problem. We know that the stiffness and mass matrices, k and m, are known. This problem is to determine the value of ω_n^2 and Φ_n. The set has the trivial solution of $\Phi_n = 0$, which is useless because it implies no motion. The nontrivial solution of this problem is present if

$$det\,[\mathrm{k} - \omega_\mathrm{n}^2\mathrm{m}] = 0 \tag{2.7}$$

When the determinant is expanded, the equation has N number of real and positives roots for ω_n^2 because the structural mass and stiffness, m and k, are symmetric and positive definite. The roots ω_n^2

determine the N number of natural frequencies ω_n (n=1, 2, 3, …. N) of vibrations, and conventionally arranged from smallest to largest ($\omega_1 < \omega_2 < \omega_3 < \dots \omega_N$).

Each structure, depending on its physical and mechanical characteristics, possesses unique ways of vibrating as many as its number of DOF called natural mode of vibration. A mode of vibration is characterized by a modal frequency and a mode shape. This mode shape describes the expected displacement of a structure vibrating at a particular mode. For each ω_n, it is possible to compute the respective Φ_n from the equation *(2.6)*. The eigen value problem does not fix the amplitude of the vectors Φ_n, only the shape of the vector given by the relative values of the N displacements. There are N independent vectors Φ_n corresponding to the N natural vibration frequencies ω_n of an N-DOF system. This Φ_n vectors are known as natural modes of vibration, or natural mode shapes of vibration.

2.2 Masonry Quality Index

The quality of masonry has a fundamental role in determining the capacity of a structure in withstanding the acting loads, and in providing a sound structural behavior under seismic loads. This problem cannot be studied only in terms of stress and strain, but also qualitatively. Masonry that can resist and transfer vertical and seismic forces without failing must have geometric and physical characteristics that allow as much as possible a monolithic behavior. Among the characteristics that a “good quality” masonry should have, as identified by Borri et De Maria (2009), and Borri et al., (2015), are:

- Presence of horizontal courses
- Presence of not-aligned mortar head joints
- Presence of parallelepiped-shaped and big stones or bricks
- Presence of transversal connections in multi-leaf walls (traditionally made with big stones)
- Good quality of mortar
- Adequate strength of bricks or stones.

Seven parameters are to be considered for an estimation of the mechanical properties of a masonry wall. The estimation requires an in-depth knowledge of historical construction methods due to the demands placed upon the engineer to categorize each parameter under three possible outcomes: Fulfilled (F), Partially Fulfilled (PF), Not Fulfilled (NF). During the structural survey, engineer must be able to identify a specific qualitative value for each parameter. Those seven parameters are:

a. SM, conservation state and the mechanical properties of the bricks or stones. This parameter considering several problems including the common phenomenon of erosion of porous stone.
b. SD, stone/brick dimension properties.
c. SS, stone/brick shape. This parameter ranges from perfectly cut stones to pebbles

d. WC, wall leaf connection. Connection between adjacent leaves have considerable effect on the global behavior of masonry structure. This varies from cases where there is no connection between the wall leaves to ones with well-constructed connection between the leaves

e. HJ, horizontal bed joints characteristics. Depending on the type of masonry and construction techniques, horizontal bed joints are sometimes non-continuous. This may highly affect the lateral and compression strength of a masonry wall panel

f. VJ, vertical bed joints characteristics. The vertical joint of a masonry wall could be well staggered, partially staggered or not staggered

g. MM, mortar mechanical properties. Mortars used in historical buildings are usually lime-based. However, the variation in the volumetric ratio of binder: aggregate, the quality of the lime and the type of lime (hydraulic or aerial) does have considerable effect on the mechanical properties of the mortar. The quality of the bonding between mortar and the stones/bricks should also be considered

All the parameters above can be interpreted numerically according to table 1 below to compose values of the masonry quality index (MQI) using equation (1).

Table 1 - Numerical values for MQI analysis

	Vertical loading (V)			Horizontal in-plane loading (I)			Horizontal out-of-plane loading (O)		
	NF	PF	F	NF	PF	F	NF	PF	F
HJ	0	1	2	0	0.5	1	0	1	2
WC	0	1	1	0	1	2	0	1.5	3
SS	0	1.5	3	0	1	2	0	1	2
VJ	0	0.5	1	0	1	2	0	0.5	1
SD	0	0.5	1	0	0.5	1	0	0.5	1
MM	0	0.5	2	0	1	2	0	0.5	1
SM	0.3	0.7	1	0.3	0.7	1	0.5	0.7	1

$$MQI = SM\,(SD+SS+WC+HJ+VJ+MM) \qquad (2.8)$$

From the obtained MQI values, the mechanical parameters of the masonry wall can be determined based on the graphics provided below. The determined mechanical parameters are compressive strength, modulus of elasticity, and shear strength.

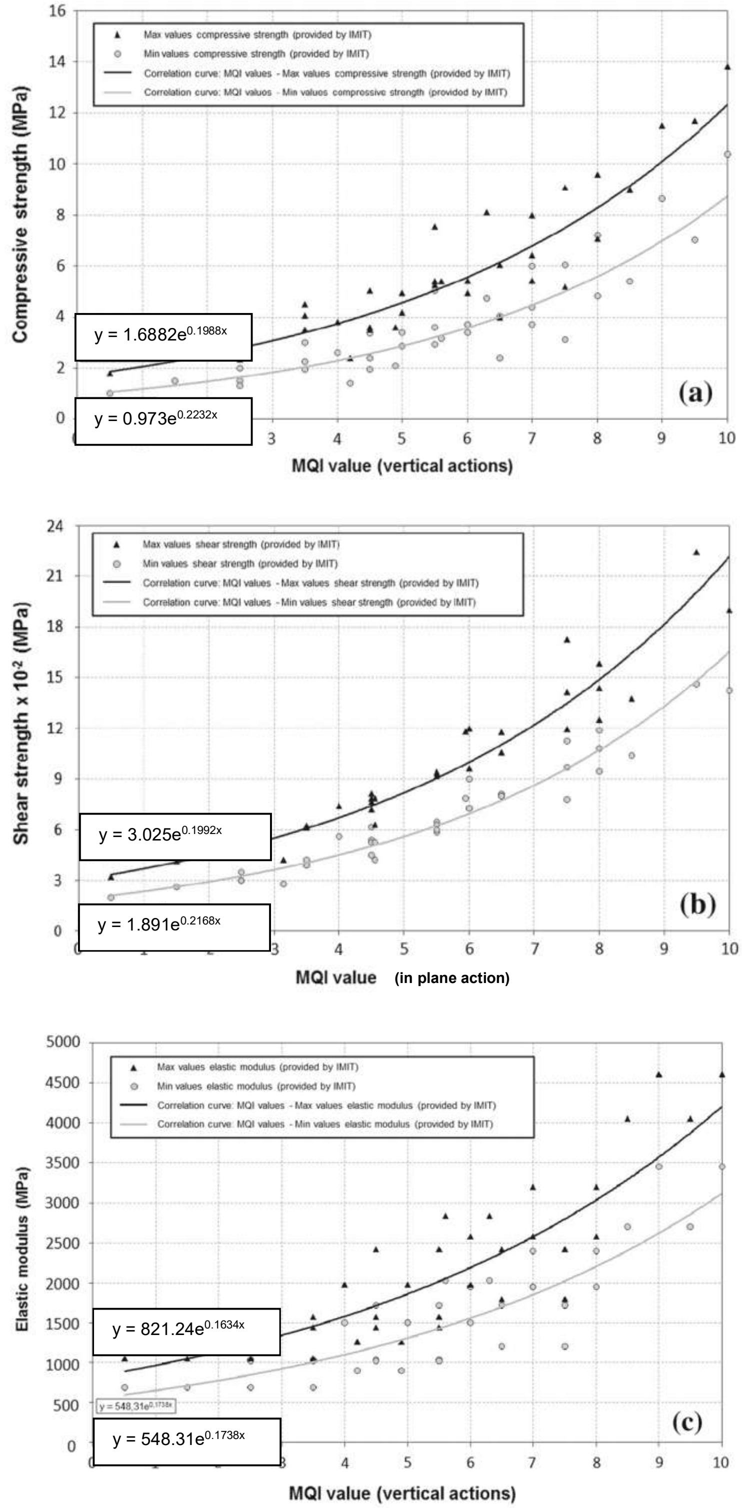

Figure 8 – Values of mechanical properties of existing masonry buildings as a function of MQI values

2.3 Mechanic of the Bell Swing

One of the important forces to which bell tower are subjected is the one caused by the turning/oscillation of the bells. These forces and their value depends on the way in which the bells are made to ring. There are three most frequently used systems, the Central European, the English and the Spanish method (Ivorra et al., 2006). In the Central European system, the bells are swung around their axes through an angle that can vary from 55° to 90°. In the English system, the bells are swinging in a complete circle (360°), while changing the direction of the swing in each cycle. In both systems, the bells are very much out of balance and rest on specially designed bell frames inside the tower. Lastly in the Spanish system, the bells are provided with a large counterweight, which means they are well balanced. In addition, they are usually fixed directly to the tower windows and always turn in the same direction.

The load from the bell swing will be working on the structure in a dynamic way. According to DIN 4178, German standard regulating bell tower, the horizontal and vertical forces on the structure as a result of the bell swing can be expressed with the equations below:

$$H = \frac{m.g}{1+k^2}\left(2\frac{cos\varphi_0}{cos\varphi} - 3\right)cos\varphi.sin\varphi \tag{2.9}$$

$$V = \frac{m.g}{1+k^2}(k^2 + 3.cos^2\varphi - 2.cos\varphi.cos\varphi_0) \tag{2.10}$$

Where m is the mass of the bell, φ is the angle of the swinging bell with a vertical line as a reference point, and φ_0 is the maximum angle which the bell could attain. As for k, it is a coefficient composed from the equation below:

$$k = \frac{is}{r} \ or \ \sqrt{\left(\frac{T_0^2}{r}\frac{g}{4\pi^2} - 1\right)} \tag{2.11}$$

Where “is” (m) is the mass radius of inertia of the bell to its horizontal axis, and “r” (m) is the distance between bell rotational point to its center of mass.

2.4 Structural Resonance

In general physics, resonance is a phenomenon in which an external force drives another system to oscillate with greater amplitude at specific frequencies. Frequencies at which the response amplitude is a relative maximum are known as the system's resonant frequencies or resonance frequencies. At resonant frequencies, small periodic driving forces could produce large amplitude oscillations, this large amplitudes (displacements) happen due to the storage of vibrational energy. In structural engineering, it may cause violent swaying motions and failure in structures that it designed improperly such as bridges, buildings, trains, and aircraft.

Avoiding resonance disasters is a major concern in every building, tower, and bridge construction project. As a countermeasure, oftenly a damping system can be installed to absorb resonant frequencies and thus dissipate the absorbed energy. For example, the Taipei 101 building in Taiwan relies on a 660-ton pendulum, a tuned mass damper, to cancel resonance. Furthermore, the structure is designed to resonate at a frequency that does not typically occur. Buildings in seismic zones are often constructed to consider the oscillating frequencies of expected ground motion. In addition, engineers designing objects having engines must ensure that the mechanical resonant frequencies of the component parts do not match driving vibrational frequencies of the motors or other strongly oscillating parts.

2.5 Structural Modal Testing

Modal analysis corresponds to the study of the dynamic properties of structures under vibration excitation. Experimental modal analysis is the field of measuring and analyzing the dynamic response of structures when excited by an input. It combines vibration test data and analytical methods to determine modal parameter of a structural system. Dynamic properties obtained from experimental modal analysis are the frequencies, mode shapes, and damping. These properties related to physical and mechanical characteristic of the analyzed structure (mass, stiffness, and energy dissipation).

Dynamic testing performed to historical structure can be useful for several reasons:

a. Assessment of safety and structural reliability of a long history under various loads
b. Discovering reasons of damages
c. To verify strengthening/repair efficiency
d. To evaluate dynamic characteristics of buildings
e. Validation of behavioral models in their elastic range. For successive structural analysis and verification
f. Troubleshooting of a structural response problem
g. Structural health monitoring

Modal analysis is a procedure that combines vibration test data and analytical methods to determine modal parameters including frequencies, mode shapes, and damping of a structural system. It is a valuable tool used to understand the dynamic response of a structure. Typically, three types of vibration tests are applied; impact, sinusoidal, and random. An ideal impact to a structure will cause a constant amplitude in the frequency domain, resulting in all modes of vibration being excited with equal energy. The sinusoidal test consists of certain acceleration level combined with a frequency sweep at a range from an initial frequency to a final frequency. The objective of most sinusoidal tests is to find the resonant frequencies of the structure and then dwell on those frequencies in further tests. Lastly, structure at the random vibration test is exposed to energies at all frequencies in the bandwidth selected and test requires statistical description.

A transducer is an equipment able to transform a physic quantity, that usually defines the system response, such as displacements, velocities, accelerations, strains, forces, etc., into a proportional electrical signal, ready to be processed by the data acquisition system. In what concerns civil engineering structures, measuring displacements requests all sensors to be related to an external reference point and, often it is costly to do it. Therefore, test equipment based on accelerometers are usually preferred, providing accurate results with relatively low cost. Moreover, it is possible to calculate displacements by numerical integration of the acceleration records.

A piezoelectric accelerometer is one spring-mass-damper system which produces signals proportional to the acceleration in a frequency band below their resonant frequency. Piezoelectric accelerometers have the advantages of not using external power source (active transducers), being stable, having a good signal-to-noise ratio and being linear over a wide frequency and dynamic range.

During the dynamic testing performed on the Bell Tower of St. Jakub Church in December 2016, several piezoelectric accelerometers were installed on the clock tower to obtain the data for structure's modal information. Below are shown the position of the accelerometers on the bell tower.

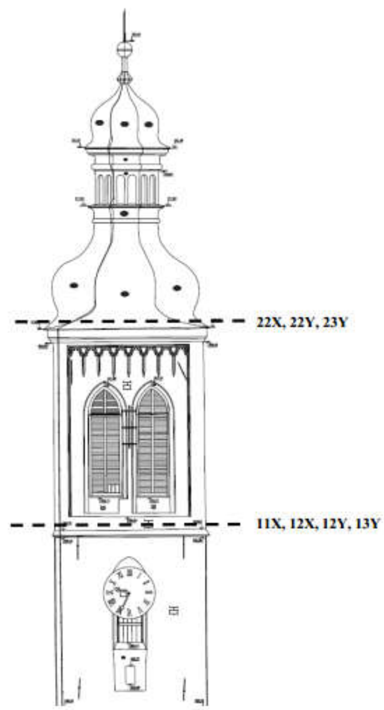

Figure 9 – Position of the accelerometers on the top part of the bell tower

During the dynamic test of the bell tower, three frequencies were evaluated in the frequency range 0 to 4 Hz. The three first natural frequencies of the structure and the mode shapes of those frequencies will be presented in the figures below.

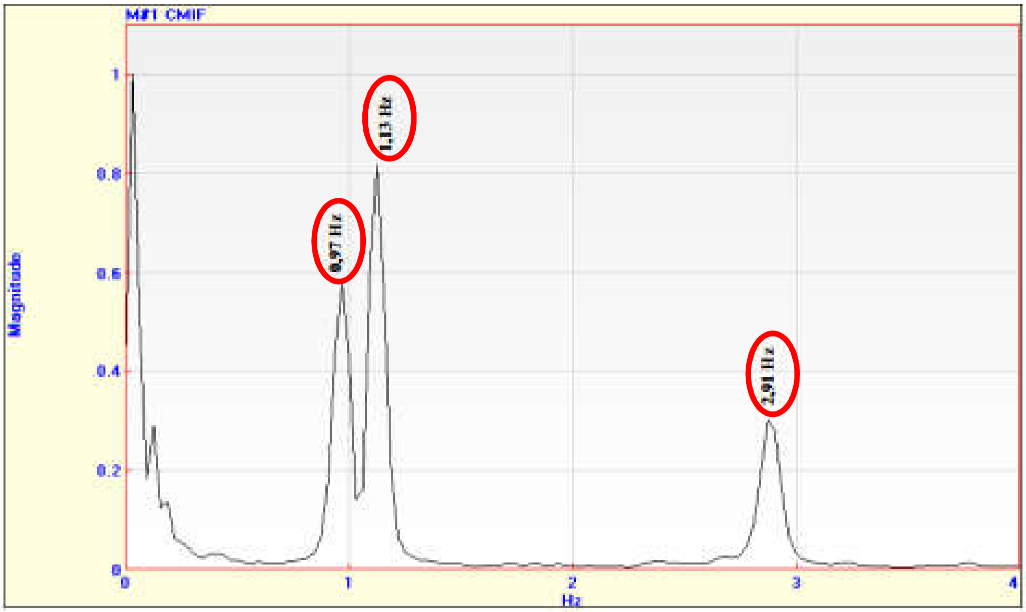

Figure 10 – First three natural frequencies of the bell tower

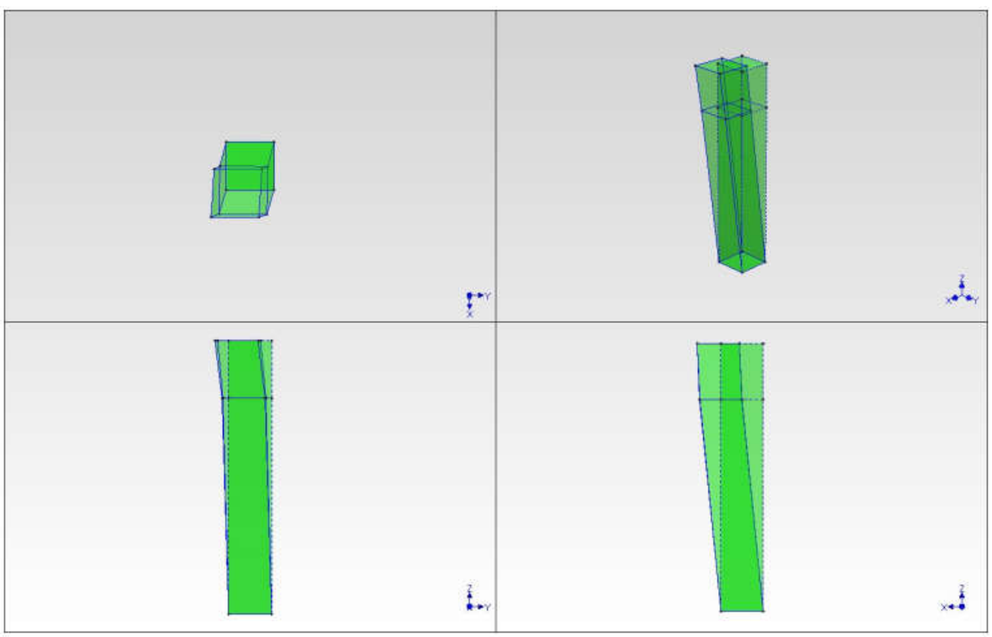

Figure 11 – Mode shape of f1 (0.97 Hz), horizontal bending in X-direction

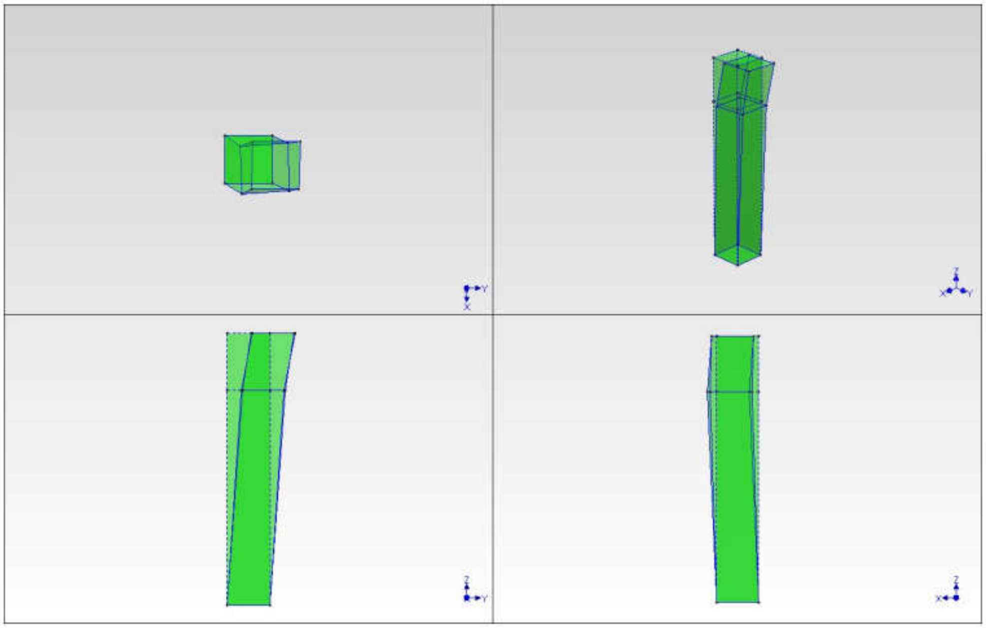

Figure 12 – Mode shape of f2 (1.13 Hz), horizontal bending in Y-direction

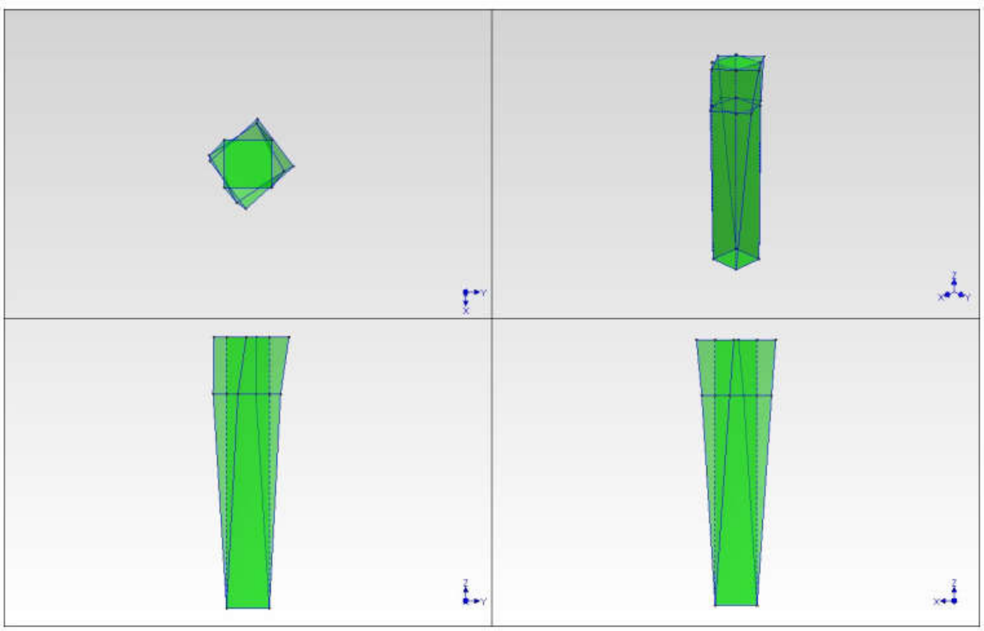

Figure 13 – Mode shape of f3 (2.91 Hz), torsional bending

The value of natural frequencies and the mode shapes obtained from the dynamic testing will be used as a point of reference on the constructing phase of numerical modeling of the bell tower which will be explained on the next chapter.

3. STRUCTURAL MODELING

3.1 Masonry Quality Index

As explained on the previous chapter, seven parameters are to be considered for an estimation of the mechanical properties of the masonry wall. The detailed values for each parameter of masonry quality index will be presented in the table below:

Table 2 – Qualitative values for each parameter of MQI

Parameter	Images	Qualitative value
SM, conservation state and the mechanical properties of the bricks or stones.		F. For solid fired bricks, hollow bricks, concrete blocks, and hardstone, a fulfilled (F) outcome can be taken
SD, stone/brick dimension properties	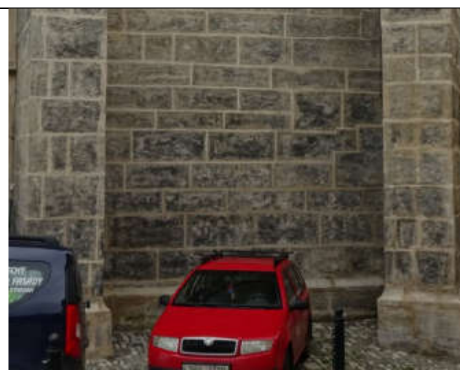	F. The bell tower could be categorized as F outcome since there are presence of more than 50% of elements with large dimension (>40 cm)
SS, stone/brick shape	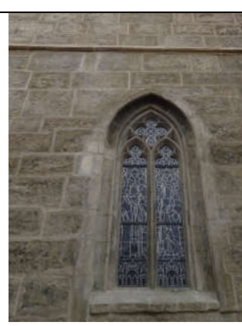 	PF. One masonry leaf made of perfectly cut stone, while there is co-presence of rounded, pebble, or barely cut stonework

WC, wall leaf connection	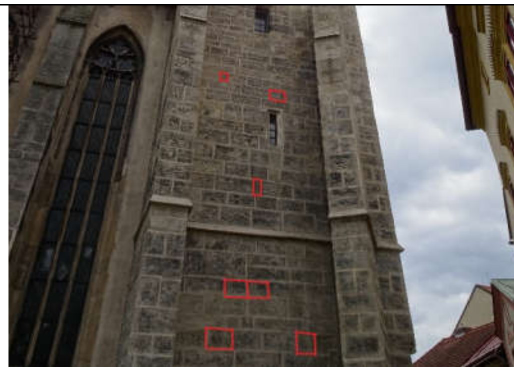	PF. For non-visible section, PF value can be taken if there are presence of some headers and when the wall thickness is larger than stone large dimension
HJ, horizontal bed joints characteristics	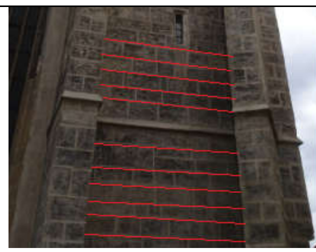 	F. Continuous horizontal bed joints
VJ, vertical bed joints characteristics		PF. Partially staggered vertical joints. vertical joint between 2 brick is not placed in the middle of adjacent upper and lower brick
MM, mortar mechanical properties		PF. Medium quality mortar, masonry made of irregular (rubble) stones and weak mortar, but with presence of pinning stones.

Using equation *(2.8)* and numerical values presented in Table 1, we can obtain the Masonry Quality Index for each action; vertical (V), out of plane action (O), and in plane action (I).

Table 3 – MQI values based on qualitative observation of the bell tower

Parameter	State	Value		
		V	I	O
SM	F	1	1	1
SD	F	1	1	1
SS	PF	1.5	1	1
WC	PF	1	1	1.5
HJ	F	2	1	2
VJ	PF	0.5	1	0.5
MM	F	0.5	1	0.5
	MQI	**6.5**	**6**	**6.5**
	category	A	A	B

Based on the MQI values above, using equation presented in figure 2.1 we can estimate the compressive strength, modulus of elasticity, and shear strength of the masonry wall used in the bell tower.

Table 4 – Structural parameters based on the MQI analysis

Parameter (MPa)	Equation		Value		
	min	max	min	max	middle
Compressive strength, fm	$0.973e^{0.2232*6.5}$	$1.6882e^{0.1988*6.5}$	4.00	6.15	5.07
Shear strength, τ_0	$1.891e^{0.2168*6}$	$3.025e^{0.1992*6}$	0.07	0.10	0.08
Modulus of elasticity, E	$548.31e^{0.1738*6.5}$	$821.24e^{0.1634*6.5}$	1696.87	2375.39	2036.13

Moreover, three types of masonry elements are used during structural modeling phase. The minimum values will be assigned to the vaults element, since from the field observation the vaults are made from only single masonry element. The middle value will be assigned to the most of the bell tower's wall, while the maximum value will be assigned to the buttresses and the top floor of the tower. This is performed because the top buttresses and the top floor are made only from the cut stone without the second layer of masonry wall, thus it is assumed that they have a better structural properties than other parts of tower.

3.2 Software Modeling

3.2.1 Material definition

The bell tower was modeled using Dlubal software. On this software, the main structural elements are the wall and floor, both are modeled using surface element. The main material used on the structural element were masonry for walls and floor, timber for some of the floor elements, roof truss, and bell supporting element, and stone for the foundation. Below are shown the material definition process for the main elements used in the structural modeling:

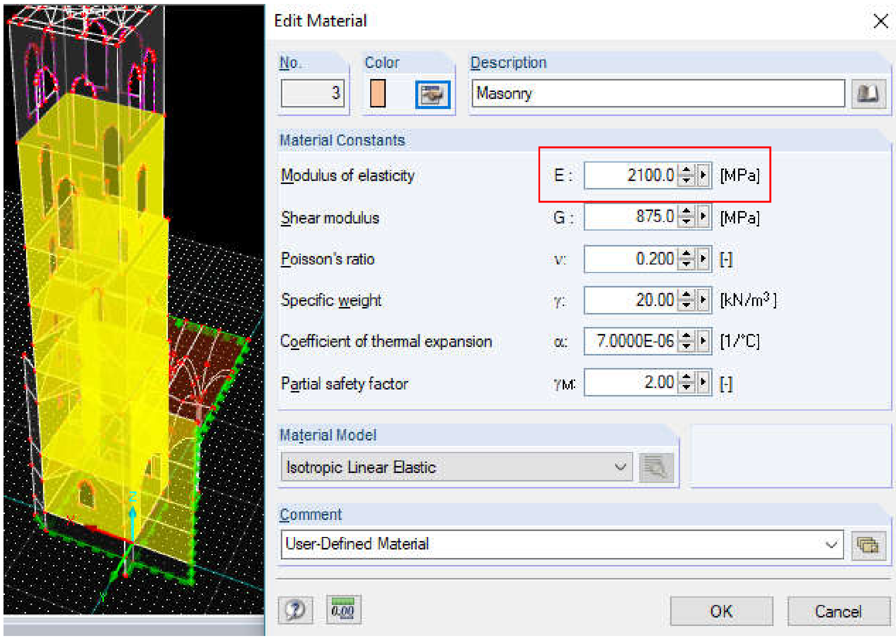

Figure 14 – Masonry material definition

Furthermore, the values of each parameters for the masonry material can be adjusted more detail to match the values obtained from the MQI analysis process.

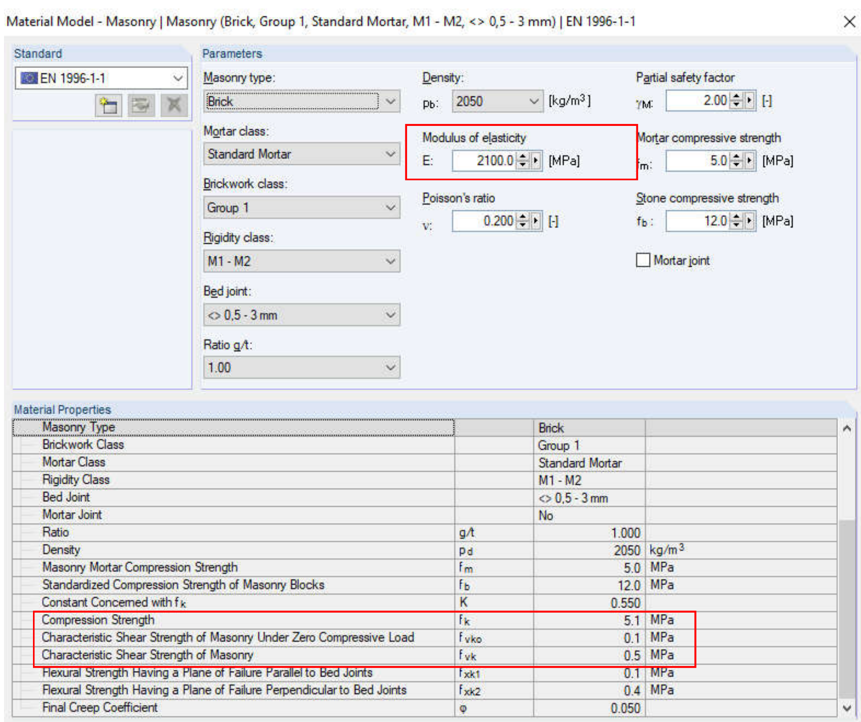

Figure 15 – Detailed section of masonry wall material definition

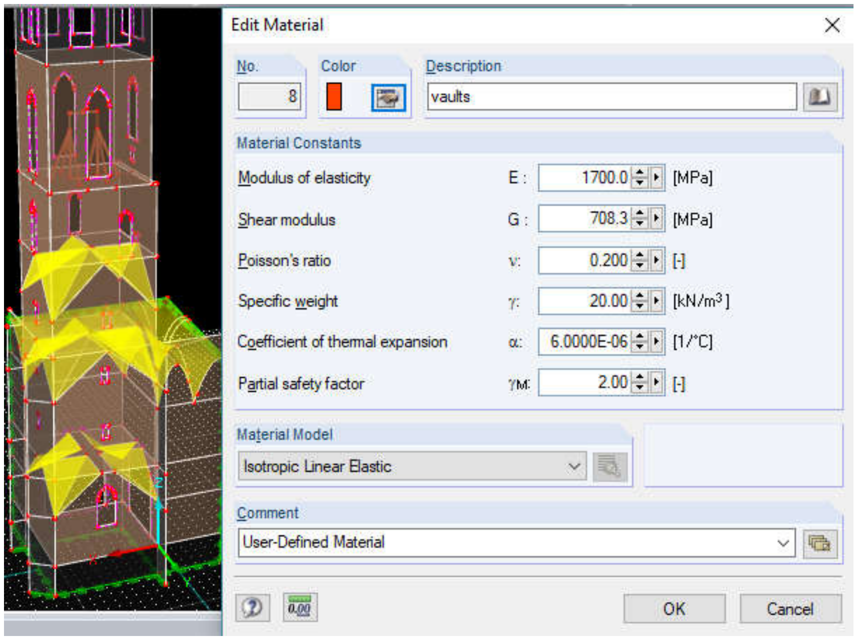

Figure 16 – Masonry vaults material definition

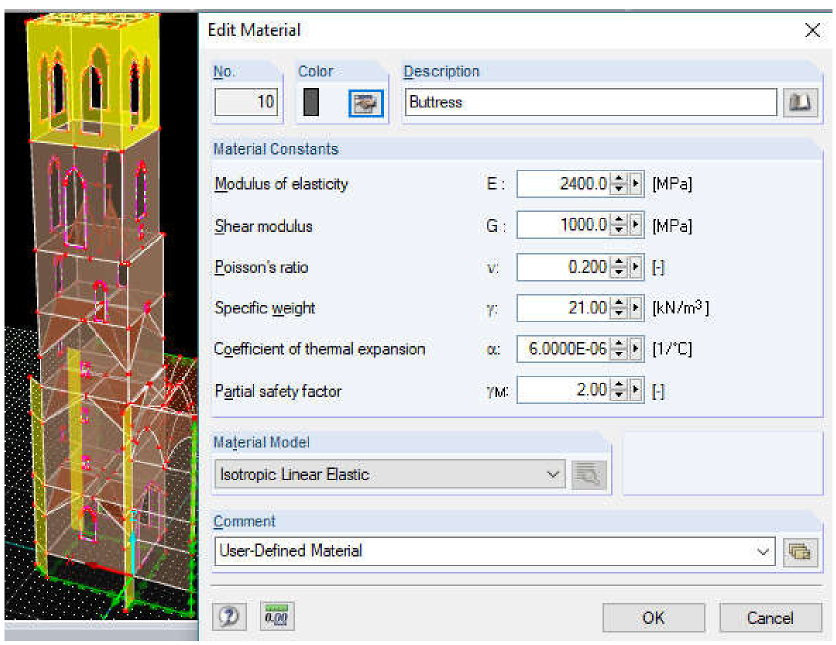

Figure 17 – Masonry buttresses material definition

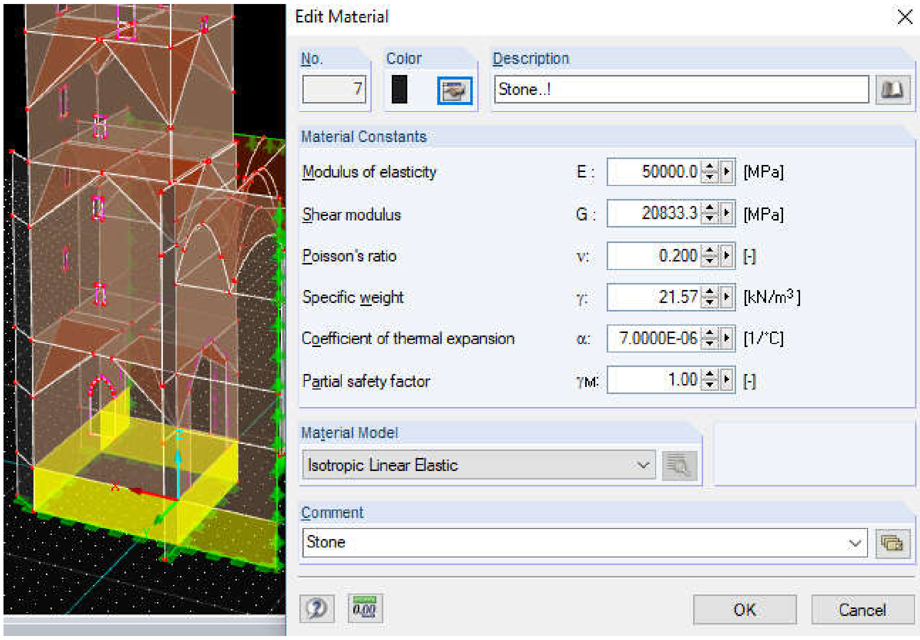

Figure 18 – Stone material definition

3.2.2 Surface Creation

On creating the surface elements, it is important to carefully measure the element thickness based on the field structural investigation. Based on the data and drawings provided, similar wall panels can be created with the thickness representing the actual condition

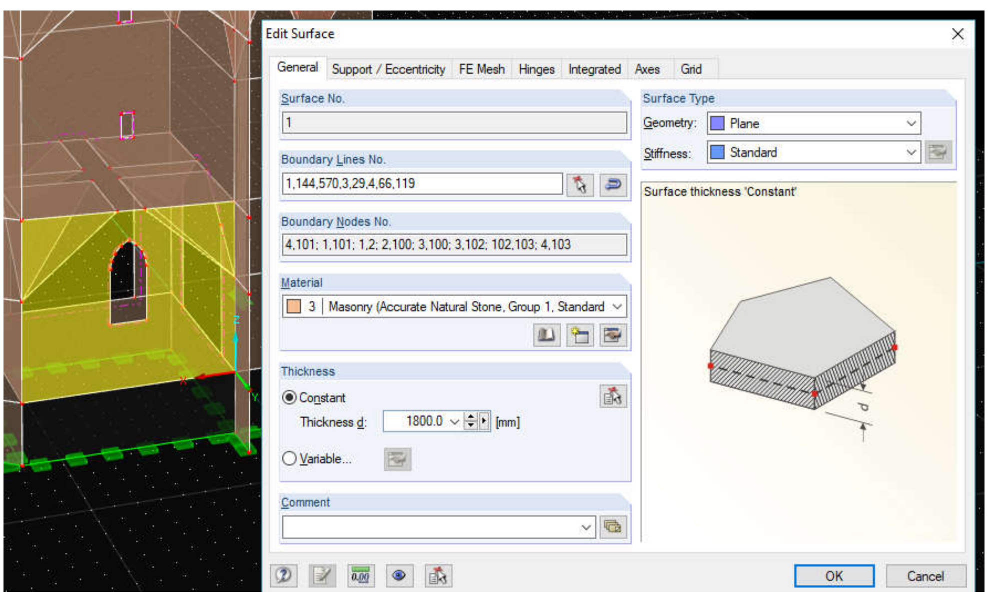

Figure 19 – Surface element creation

It is also necessary to create correct openings on the wall panel that represent the actual structural condition. This is because an opening will reduce the wall mass, geometry, and stiffness and in the end, will contribute to the natural frequencies calculation process. The creation of the opening can be done by creating a polygonal opening directly onto the wall surface. The similar shape of the opening can be achieved by editing the joint coordinates of the openings.

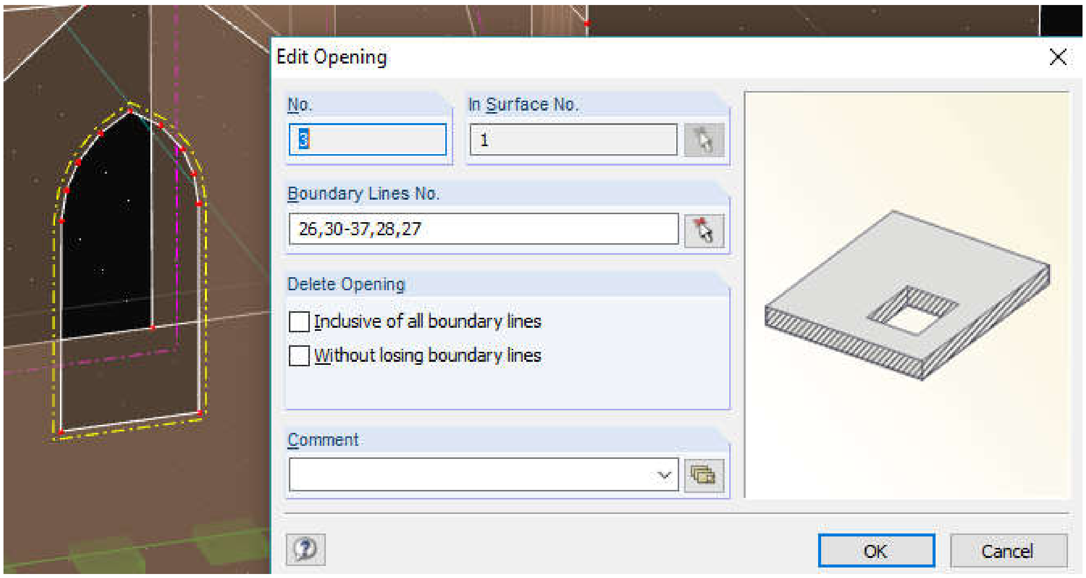

Figure 20 – Wall opening creation

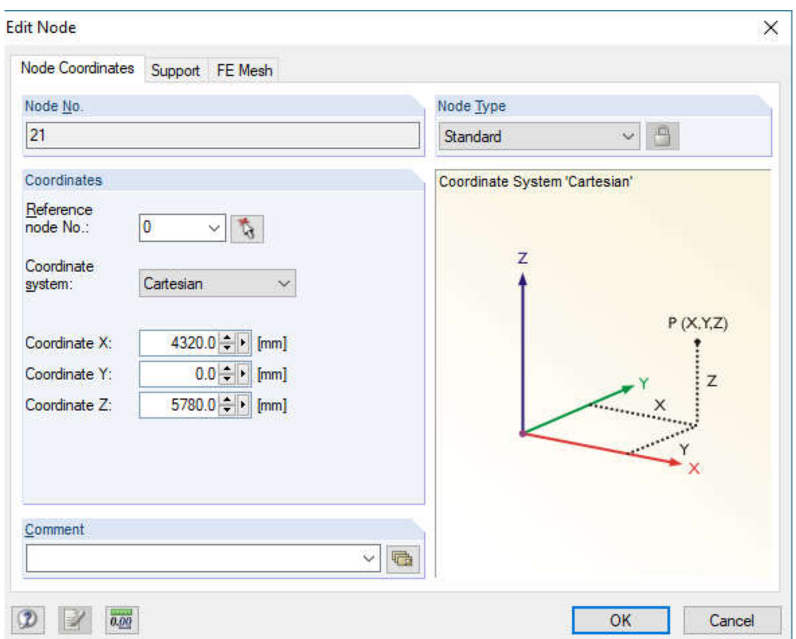

Figure 21 – Editing the nodes of an opening to match the actual shape of the opening

3.2.3 Support Definition

Defining the right restraint (support) on the structural model is important because it will affect how the structure is behave. In this case, there are two main structural supports modeled. One is in the base of the structure (below the foundation), and the other one is modeled in the end of the vaulting system of the church on the second floor (elevation +19.400). This is performed in order to give the tower a suitable restraint, thus will result in the correct dynamic behavior.

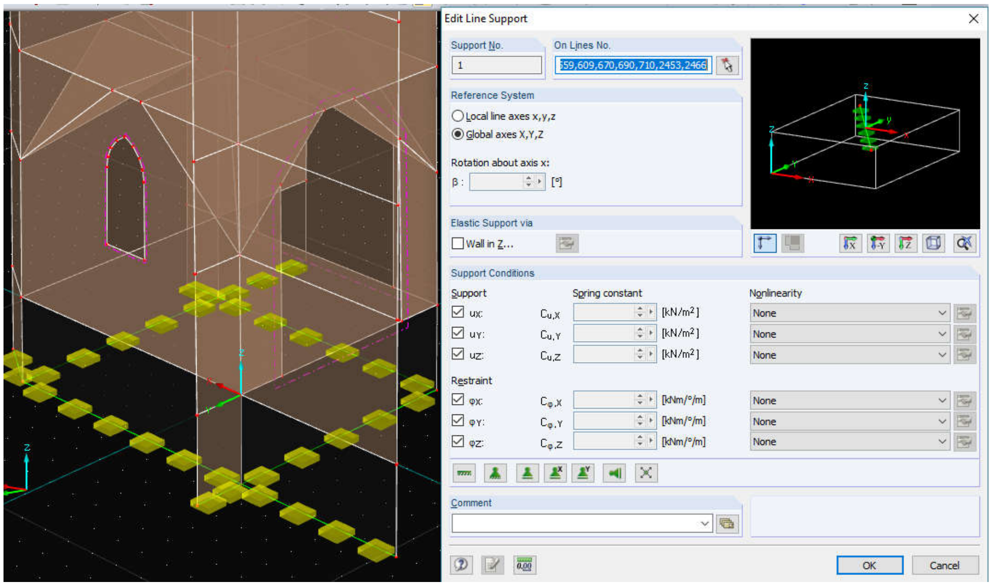

Figure 22 – Support creation (line support) on the base of the structure

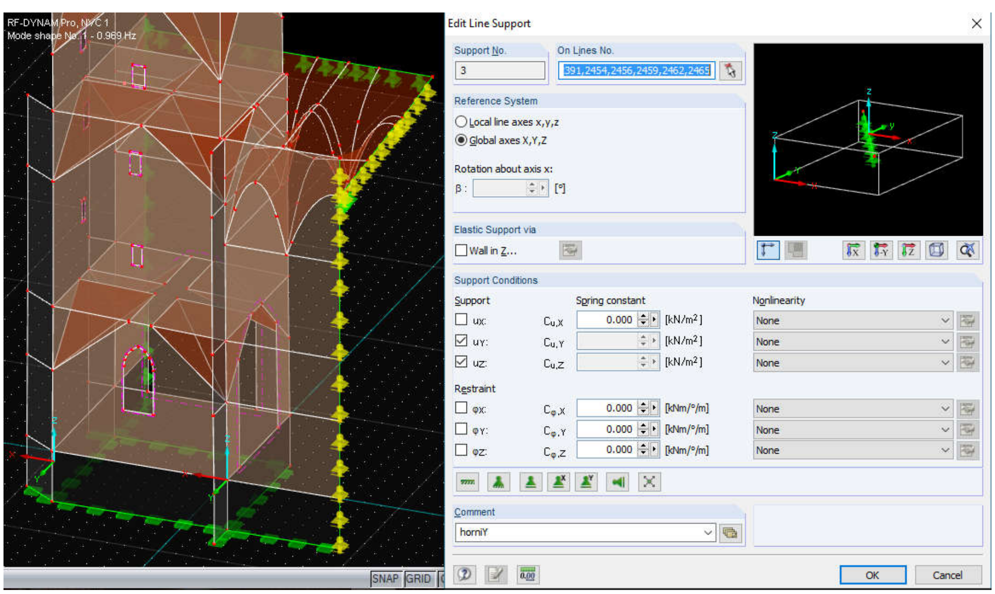

Figure 23 – Support creation (line support) on the end of the church's vault system

For the line support on the end of the church's vault system, a partially hinged support is installed in a way that the support will only be able to move to certain direction.

For sake of simplicity on the roof modelling, the roof is only modeled with line, without the section of timber frame. But in order to create a good approximation of the structure behavior, an additional mass will be applied to a point in the roof during the mass cases definition for the natural vibration analysis. This additional mass will make a better calculation of the natural vibration of the structure, since natural frequency of the structure is depend on its mass and stiffness.

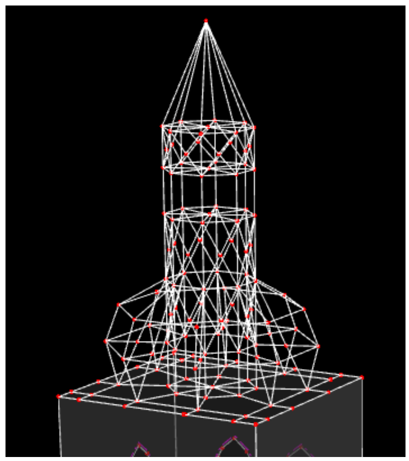

Figure 24 – Model of the roof of the bell tower

3.3 Loadings

3.3.1 Dead Load and Super Imposed Dead Load

For the deal load, the software can calculate automatically the self-weight of the all the elements created. The most important thing to do is to make sure that the software is already considering the materials self-weight.

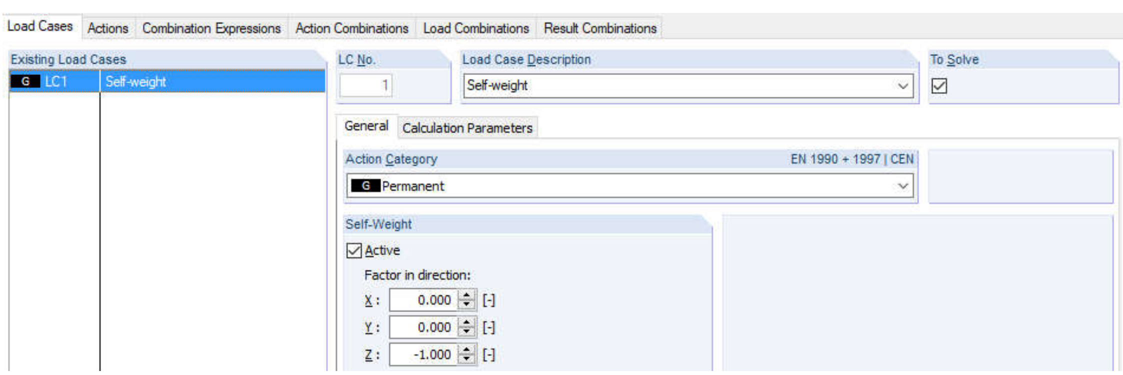

Figure 25 – Load case definition, dead load

Super imposed dead load is the dead load on the structure besides the self-weight of the structure, the load is permanent but will not contribute anything to structural strengths. This load could be present on the structure in the form of floor finishing, plumbing, cables, and permanent equipment on the structure. On the super imposed dead load definition, the storage area category was chosen because upon structural inspection, some of the rooms in the tower are still used for equipment storage or light mechanical rooms for the clocks system. The value of the load is estimated to be 3 kPa.

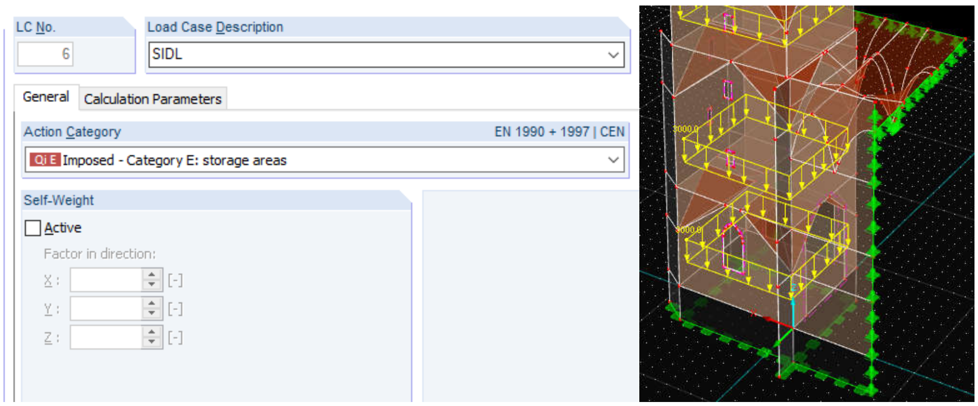

Figure 26 – Load case definition, super imposed dead load

3.3.2 Live Load

Live loads include any temporary or transient forces that act on the structural element. Typically, they include people, furniture, and almost everything else that can be moved throughout a building. Live loads can be prescribed to any structural element (floors, columns, beams, roofs) and will eventually be factored into a calculation of gravity loads. For the bell tower, it is approximated that the value of the applied live load would be 3 kPa, similar on all floors.

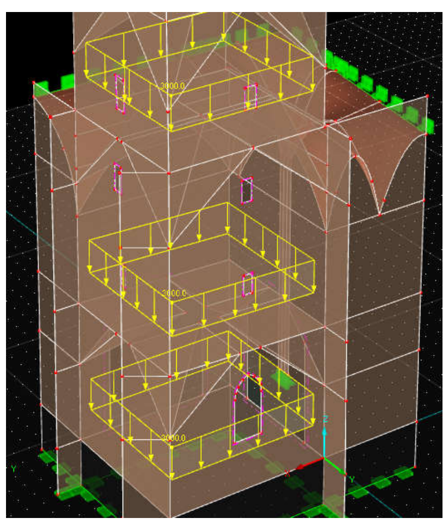

Figure 27 – Load case definition, live load

3.3.3 Swinging Bell Loads

As previously explained in chapter 2.3, to calculate the “is” variable correctly the bell needs to be discretized into several parts since there are no exact data of the bell thickness. Only the data of mass of bell is obtained, which is 2500 kg. In order to obtain an accurate “is” value, the thickness of the bell needs to be estimated so that the total mass of all the discretized section (Σmi) is equal to 2500 kg. Below are presented the calculation to obtain “is” value:

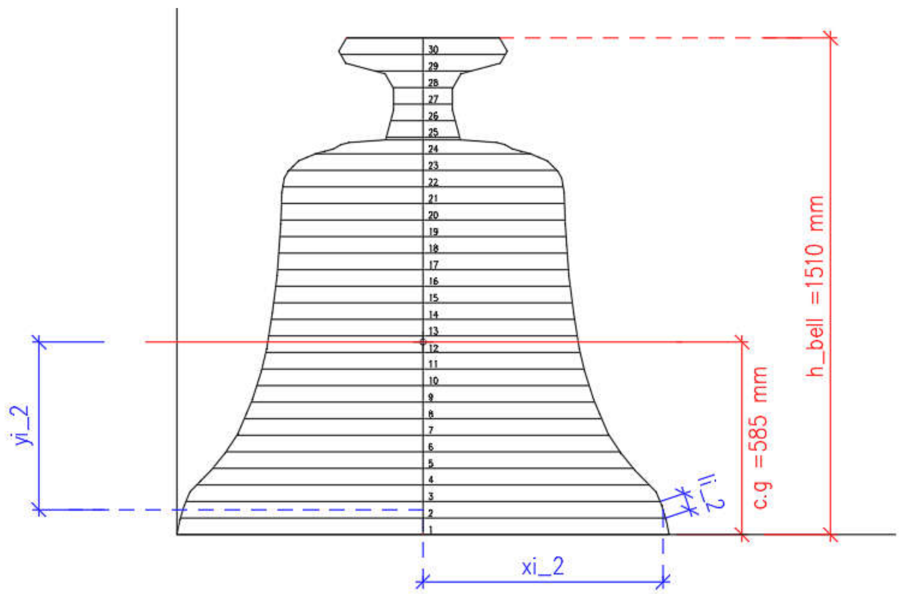

Figure 28 – Discretization of the bell section

Calculation of (is)

thickness 0.060485 m density 8600 kg/m3

h_bell 1510 mm

no.	yi (m)	li (m)	xi (m)	yi*[li*t*(2*π*xi)]	mi (kg)
1	-0.56	0.051	0.744	-69.4	124.0
2	-0.51	0.053	0.731	-64.6	126.6
3	-0.46	0.06	0.711	-64.1	139.4
4	-0.409	0.07	0.664	-62.1	151.9
5	-0.359	0.065	0.619	-47.2	131.5
6	-0.309	0.06	0.583	-35.3	114.3
7	-0.258	0.055	0.555	-25.7	99.8
8	-0.208	0.055	0.533	-19.9	95.8
9	-0.158	0.053	0.514	-14.1	89.0
10	-0.107	0.053	0.498	-9.2	86.3
11	-0.057	0.052	0.484	-4.7	82.3
12	-0.007	0.051	0.474	-0.6	79.0
13	0.044	0.051	0.466	3.4	77.7
14	0.094	0.051	0.458	7.2	76.3
15	0.144	0.051	0.451	10.8	75.2
16	0.195	0.051	0.445	14.5	74.2
17	0.245	0.05	0.441	17.7	72.1
18	0.295	0.05	0.437	21.1	71.4
19	0.346	0.05	0.434	24.5	70.9
20	0.396	0.05	0.432	28.0	70.6
21	0.447	0.051	0.43	32.0	71.7
22	0.497	0.054	0.423	37.1	74.7
23	0.547	0.096	0.382	65.6	119.9
24	0.598	0.221	0.254	109.7	183.5
25	0.648	0.052	0.105	8.0	12.3
26	0.698	0.051	0.092	7.4	10.6
27	0.749	0.05	0.0895	7.6	10.1
28	0.799	0.075	0.106	14.3	17.9
29	0.849	0.115	0.237	52.2	61.5
30	0.9	0.053	0.248	26.7	29.6
			Σ	70.6	2500.0

Yc= 70.6/2500= 28.2 mm

thickness	0.060485 m		density		8600 kg/m^3
h_bell	1510 mm				
no.	yc-yi (m)	li (m)	xi (m)	(yc-yi)^2*[li*t*(2*π*xi)]	mi (kg)
1	-0.003	0.051	0.744	0.0	124.0
2	0.047	0.053	0.731	0.3	126.6
3	0.098	0.06	0.711	1.3	139.4
4	0.148	0.07	0.664	3.3	151.9
5	0.198	0.065	0.619	5.2	131.5
6	0.249	0.06	0.583	7.1	114.3
7	0.299	0.055	0.555	8.9	99.8
8	0.349	0.055	0.533	11.7	95.8
9	0.4	0.053	0.514	14.2	89.0
10	0.45	0.053	0.498	17.5	86.3
11	0.5	0.052	0.484	20.6	82.3
12	0.551	0.051	0.474	24.0	79.0
13	0.601	0.051	0.466	28.1	77.7
14	0.651	0.051	0.458	32.4	76.3
15	0.702	0.051	0.451	37.0	75.2
16	0.752	0.051	0.445	41.9	74.2
17	0.802	0.05	0.441	46.4	72.1
18	0.853	0.05	0.437	52.0	71.4
19	0.903	0.05	0.434	57.8	70.9
20	0.953	0.05	0.432	64.1	70.6
21	1.004	0.051	0.43	72.2	71.7
22	1.054	0.054	0.423	82.9	74.7
23	1.104	0.096	0.382	146.1	119.9
24	1.155	0.221	0.254	244.7	183.5
25	1.205	0.052	0.105	17.9	12.3
26	1.255	0.051	0.092	16.7	10.6
27	1.306	0.05	0.0895	17.2	10.1
28	1.356	0.075	0.106	33.0	17.9
29	1.407	0.115	0.237	121.7	61.5
30	1.457	0.053	0.248	62.9	29.6
			Σ	1289.1	2500.0

$$is = 1510 - \left(\frac{1289.1}{2500} * 1000\right) = 994.4\ mm$$

$$r = 1510 - 585 = 925\ mm$$

The value of r above needs to be corrected because there is also presence of a yoke made from timber on top of the bell. The yoke has a mass of approximately 150 kg with the center of mass of 250 mm from the bottom of it.

$$r' = \frac{2500 * 925 + 150 * (-250)}{2500 + 150} = 858.49\ mm$$

$$k = \left(\frac{994.4}{858.49}\right) = 1.158$$

With all of parameters for equation *(2.9)* and *(2.10)* are found, the acting horizontal and vertical forces on the structure as a result of bell swinging can be presented in the form of forces vs angle function:

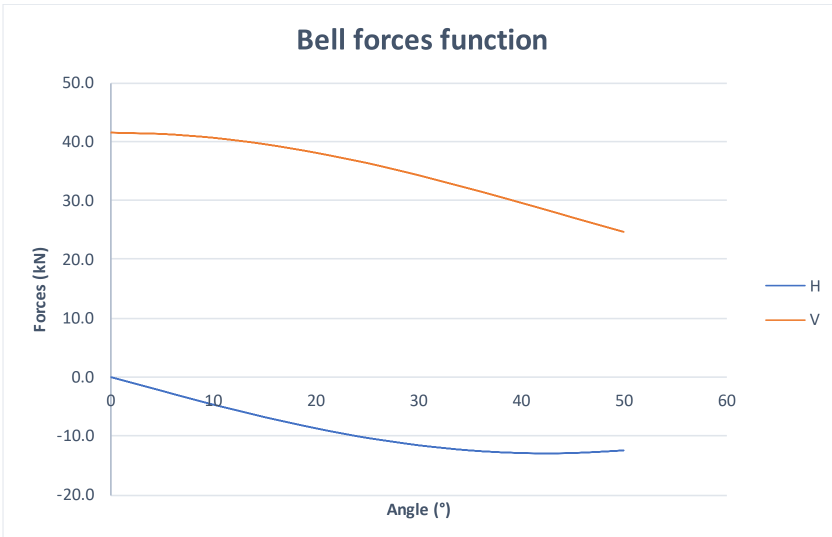

Figure 29 – Function of the bell forces vs angle of the bell swing

Furthermore, if the angle is converted into time in which the bell is rotating, the function can be presented as a force vs time functions.

$$T_0 = \frac{120}{44} = 2.73\ sec$$

$$f = \frac{44}{120} = 0.367\ Hz$$

Table 5 – Bell mass and stroke/min relation (DIN 4178)

Mass (kg)	stroke/min
4000	40
3000	42
2500	44
2000	47
1600	49
1150	51
950	52
800	54

Where 44 is the number of a possible bell stroke per minute according to DIN 4178, which has correlation with the mass of the bell. Using value of the T_0, the function in Figure 29 can be described into force vs time functions:

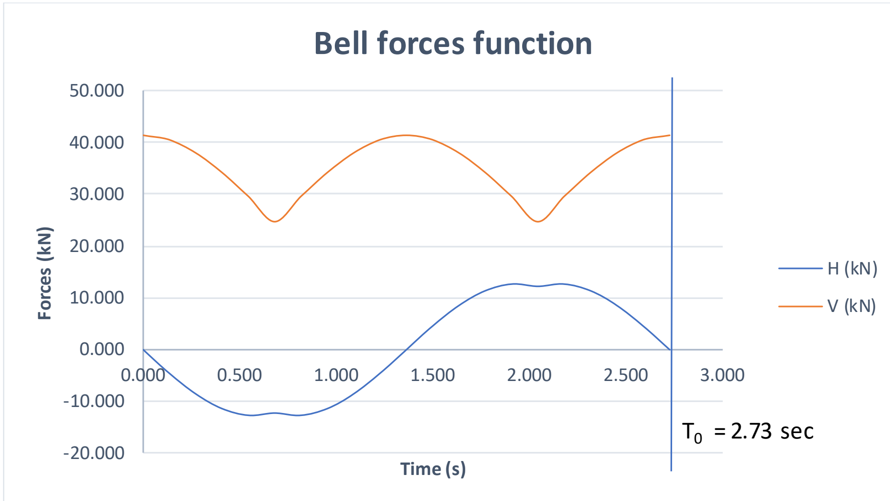

Figure 30 – Function of the bell forces vs time

3.3.4 Wind Load

For comparison between the lateral deflection occurred in the structure, the wind load is also considered to be applied to the bell tower. Based on the previous study, the basic wind speed used is 25 m/s with the terrain type IV. The scheme of wind load, in the direction of the bell, will be as follow:

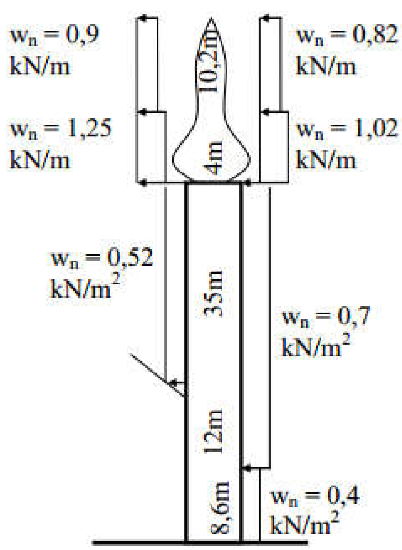

Figure 31 – Wind load in the direction of the bell swing

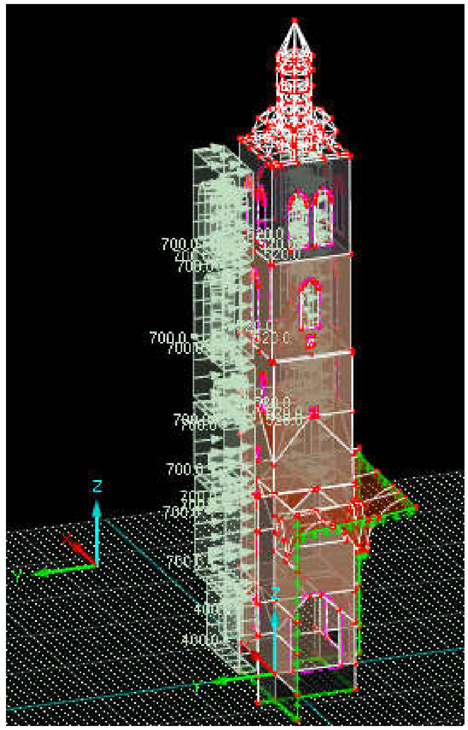

Figure 32 – Applied wind load in the direction of the bell swing

3.4 Natural Vibration Analysis and Dynamic Analysis

The natural vibration and dynamic analysis of the clock tower is performed using an additional add-on of the software called RF-DynamPro. For natural vibration analysis, all the mass cases that will be counted are defined then combined using mass combination. They are the self-weight, super imposed dead load, live load, and the mass of the bell. On the mass combinations definition, the live load is reduced. This is normally done on the structure to represent the state of actual condition of the structure.

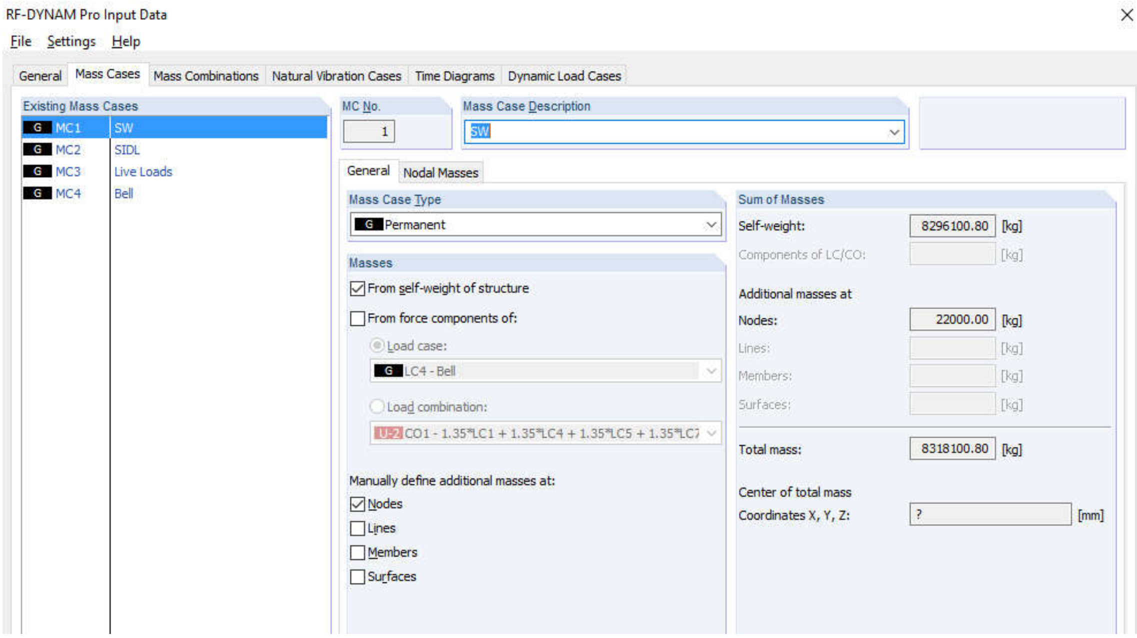

Figure 33 – Mass cases definition for natural vibration analysis

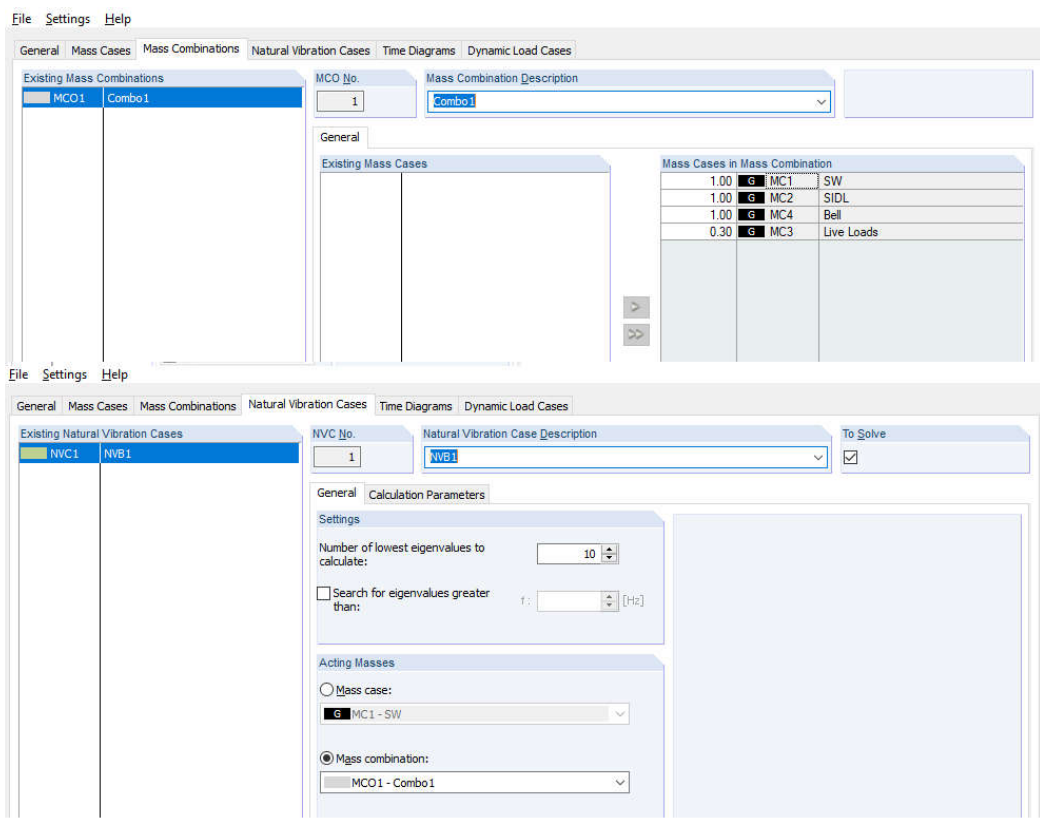

Figure 34 – Mass combinations and natural vibration cases definition

On the mass cases definition, there are additional points load added on the top floor as the roof load. The added load for roof structure are taken as 22000 kg based on the calculation performed during the previous study. Additionally, the dynamic analysis of the bell tower force is also performed using the same add-on. First the loads of the bell swing have to be inserted into the structure as a static load. The values of the load are inserted as the maximum loads for horizontal and vertical direction caused by the bell swing, which according to equation *(2.9)* and *(2.10)* are 13.13 kN for horizontal load, and 41.84 kN for vertical load. Later in the time diagram definition, a multiplier factor (k) will be used to create the change of the load's magnitude during the course of time. Below are presented the dynamic load cases definition for the structure:

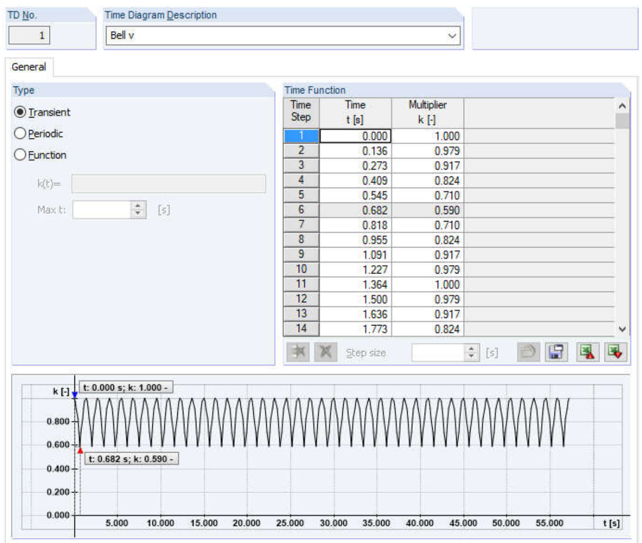

Figure 35 – Time diagram for vertical load from the bell swing

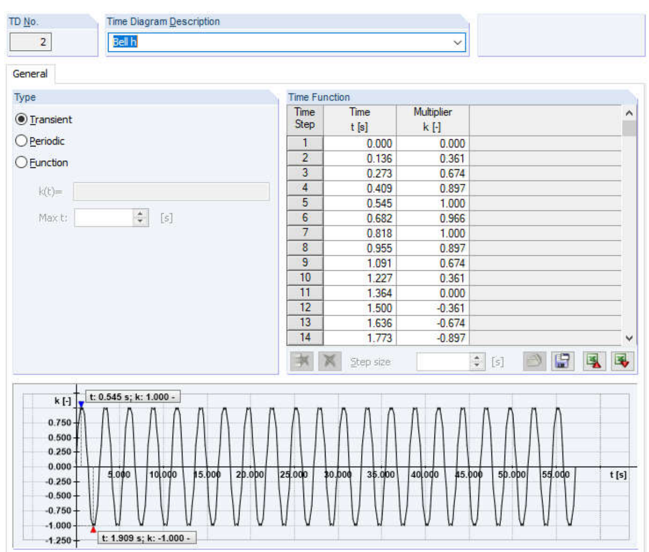

Figure 36 – Time diagram for horizontal load from the bell swing

The time diagrams will be attached to the corresponding static loads to create a dynamic time-dependent loads that will be working on the structure.

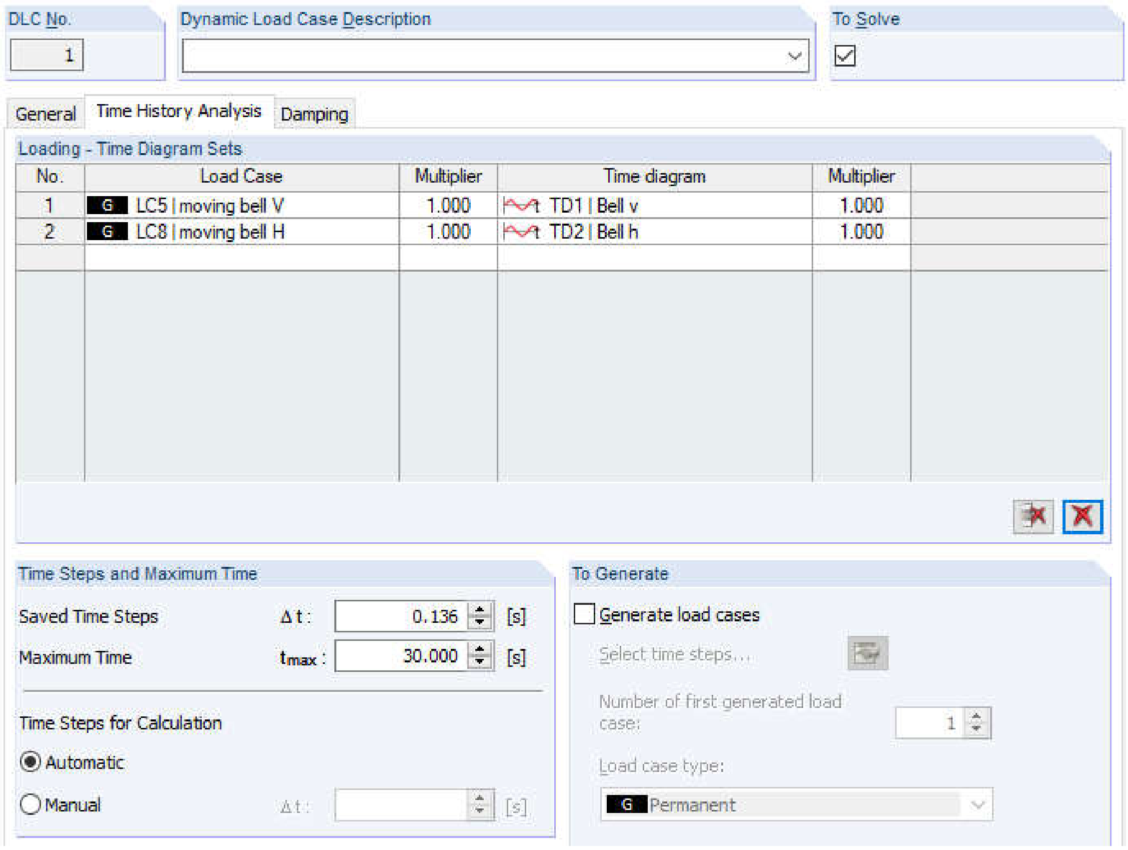

Figure 37 – Dynamic load case definition

After the dynamic load case definition, the structural model can be run to obtained the result.

4. RESULT AND ANALYSIS

Based on the analysis of natural vibration and the time dependent performed, below are presented the results of the analysis as well as other matters that could be up for discussion.

4.1 Result of Natural Vibration Analysis

The first three natural frequencies and the mode shapes of the tower will be presented in the images below:

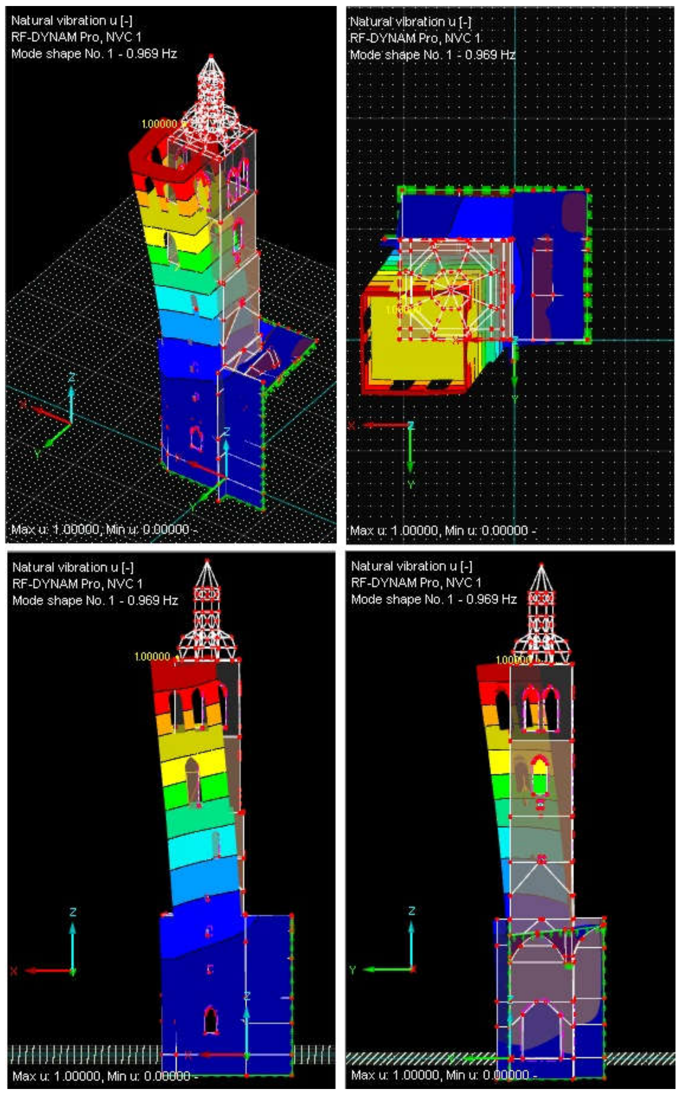

Figure 38 – Natural vibration of the 1st mode (f1 = 0.969 Hz, 1st shape of the horizontal bending in the east-west direction)

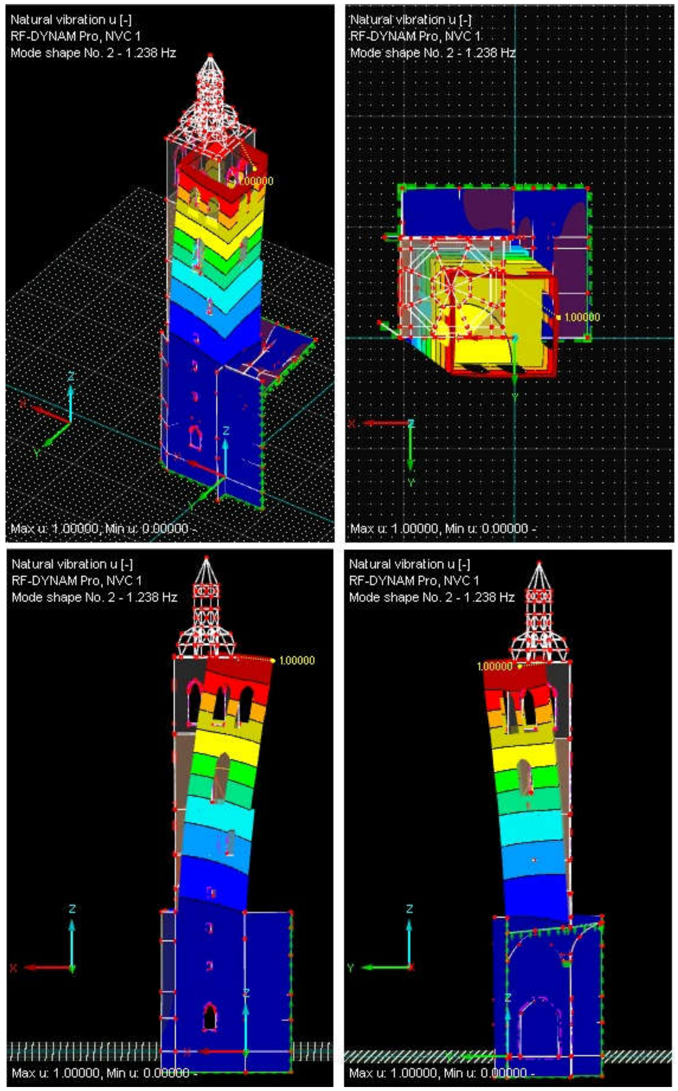

Figure 39 – Natural vibration of the 2nd mode (f2 = 1.238 Hz, 1st shape of the horizontal bending in the north-south direction)

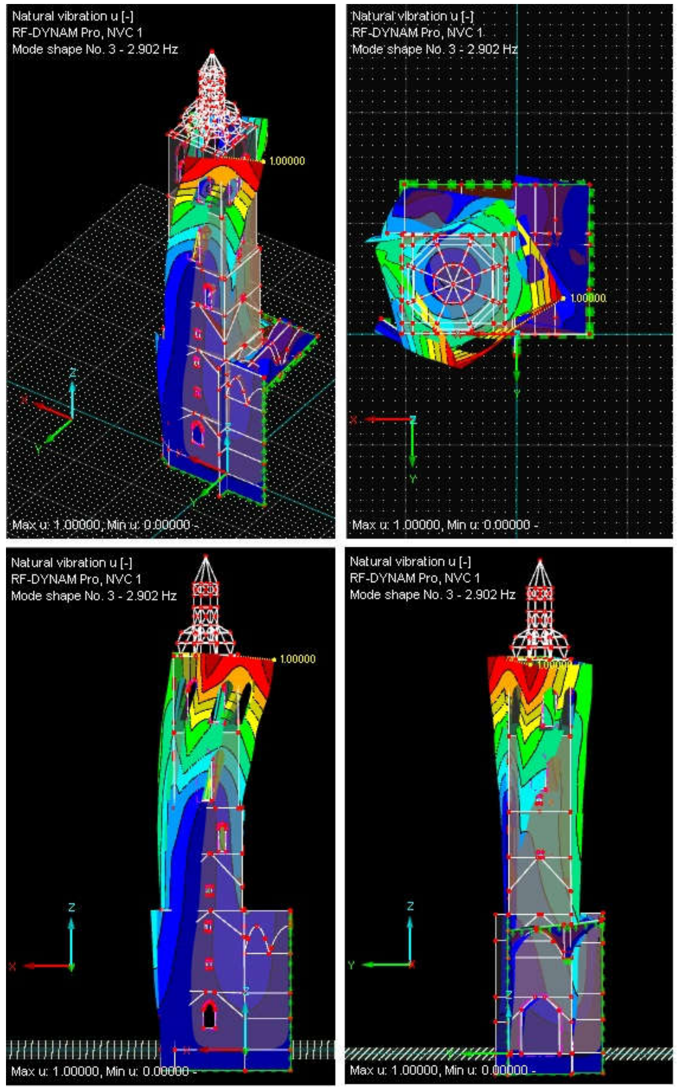

Figure 40 – Natural vibration of the 3rd mode (f3 = 2.902 Hz, torsional bending of the structure)

Table 6 – Three first natural frequencies of the bell tower

5.1 Natural Frequencies

Mode No.	A: Eigenvalue λ	B: Angular Frequency ω [rad/s]	C: Natural frequency f [Hz]	D: Natural period T [s]
1	37.072	6.0887	0.969	1.032
2	60.516	7.7792	1.238	0.808
3	332.453	18.2333	2.902	0.345

From the picture and table above, it can be seen that the natural vibration of the bell tower based on the analysis result match the result obtained from dynamic testing on the field (section 2.5). The first mode showed a horizontal bending to east-west direction, then the second mode also showed a horizontal bending to north-south direction, while the third mode showed a torsional bending of the tower.

For the lateral bending, it can be noticed that the direction of the bending is not perfectly towards one direction. This can be observed more detail in the effective modal mass factor table below

Table 7 – Effective modal mass factor of the first three natural frequencies

5.7 Effective Modal Mass Factors

NVC1 - NVB1 | Mode Shape 1 (f : 0.969 Hz)

	A	B	C	D	E	F	G	H	I	J
Mode No.	Modal Mass	Effective Modal Mass						Effective Modal Mass Factor		
	M_i [kg]	m_{eX} [kg]	m_{eY} [kg]	m_{eZ} [kg]	$m_{\varphi X}$ [kg.m²]	$m_{\varphi Y}$ [kg.m²]	$m_{\varphi Z}$ [kg.m²]	f_{meX} [-]	f_{meY} [-]	f_{meZ} [-]
1	937665.98	1173958.88	2320695.26	765.90	723476294.54	362726992.21	1756548.066	0.139	0.275	0.000
2	777035.26	2028038.28	1000978.57	53.74	368614978.37	740536692.47	1264.634	0.240	0.119	0.000
3	669328.02	900717.51	45916.69	10188.92	343793.321	46103818.469	107300637.03	0.107	0.005	0.001

Natural Frequencies | Mode Shapes by Member | Mode Shapes by Surface | Mode Shapes by Mesh Node | Masses in Mesh Points | Effective Modal Mass Factors

If the first mode is taken as an example, it can be seen that the effective modal mass factor on Y direction (corresponds to east-west direction) has a factor larger than on the X direction (corresponds to north-south direction). Thus, it can be said that the main direction of bending for the first mode is to the east-west direction. Same thing could be applied to the second mode the show that the main bending direction for the second mode is to the north-south direction.

Furthermore, this case of bending direction could have occurred due to different restraint condition off the tower as well as the irregularity of tower's layout. From the structural layout, it can be seen that on the north and west side, structure is restrained by three buttresses up until the second floor, also one of the buttress has an asymmetrical position. While on the east and south side, structure is restrained by the main structure of the church. These different states of restraint could be the cause of structural lateral natural bending not being perfectly to one certain direction

4.2 Result of Time Dependent Analysis of the Bell Swing

There are three variables monitored on the time dependent analysis of the bell swing. They are joint displacements, rotation, and velocities. The reason to the inclusion of velocities parameter is to monitor whether the occupants of the structure will feel discomfort caused by the dynamic load, in this case the bell swing. Below are presented the result of the analysis:

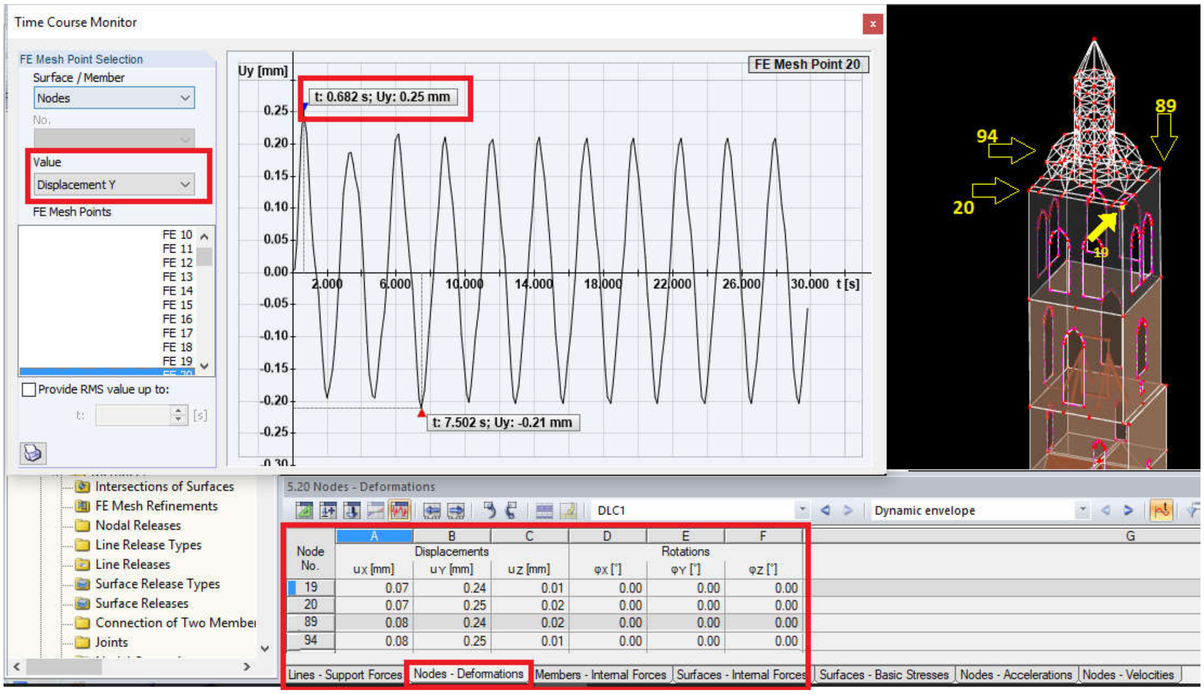

Figure 41 – Top nodal displacements and rotations caused by the swing of the bell

Table 8 – Top nodal velocities caused by the swing of the bell

5.26 Nodes - Velocities

DLC1

Node No.	Velocities u'x [m/s]	u'Y [m/s]	u'z [m/s]	Angular Velocities φ'x [rad/s]	φ'Y [rad/s]	φ'z [rad/s]
19	0.00	0.00	0.00	0.00	0.00	0.00
20	0.00	0.00	0.00	0.00	0.00	0.00
89	0.00	0.00	0.00	0.00	0.00	0.00
94	0.00	0.00	0.00	0.00	0.00	0.00

Figure 41 above showing the top nodal displacement in the direction by the bell swing, parallel to Y-global direction of the structural model. While in the table included on the image are the values of top nodal displacements and rotation on the other directions. From the values presented on the Figure 41 and Table 8 above, it can be seen that resonance did not occur on the bell tower and the maximum lateral displacement caused by the swinging of the bell is very small, thus it will not possess a threat to the structural integrity of bell tower. The resonance phenomena did not occur to the structure because the frequency of bell swing did not match any of the structure's natural frequency. In terms of velocity, the bell swing also did not give any noticeable value that will be critical to the occupant of the structure. Even though the resonance did not occur on the structure, on the next section will be discussed about the possibility of a resonance due to matching structural natural frequencies and due to usage of different mass of bell.

4.3 Case Analysis of Resonance Phenomenon

Another interesting point of view observe is about how big the resonance effect would be if it occurred on the structure. To observe this phenomenon, the time diagrams have to be modified to match the natural frequency of the structure, in this case the first frequency, since it is corresponding to the horizontal bending parallel to the bell swing. Thus, f_0 = 0.969 Hz and T_0 = 1/0.969 = 1.032 sec. The mass of the bell and other properties of the bell remains the same to give the result a reference point. Using same procedures as before, the time dependent analysis is performed again on the structure but this time using different time diagrams.

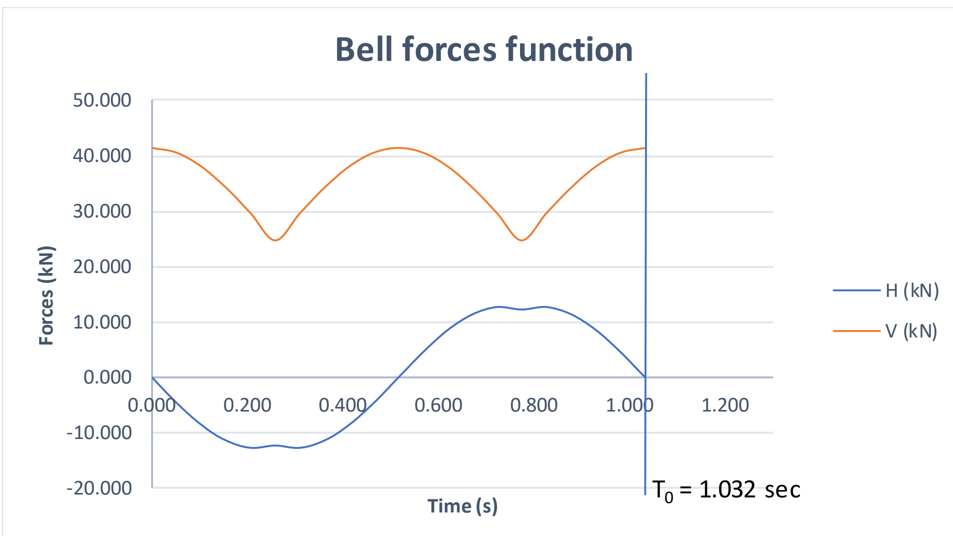

Figure 42 – Modified bell forces

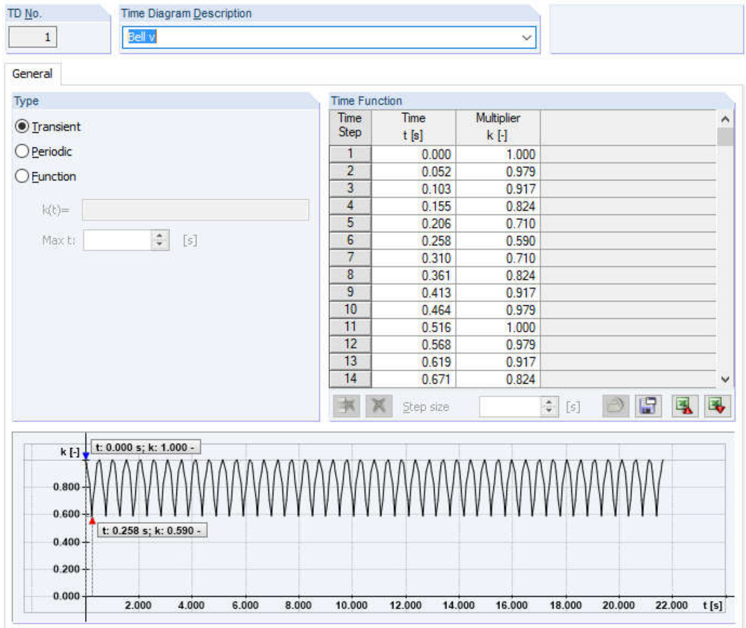

Figure 43 – Modified time diagram for vertical load from the bell swing

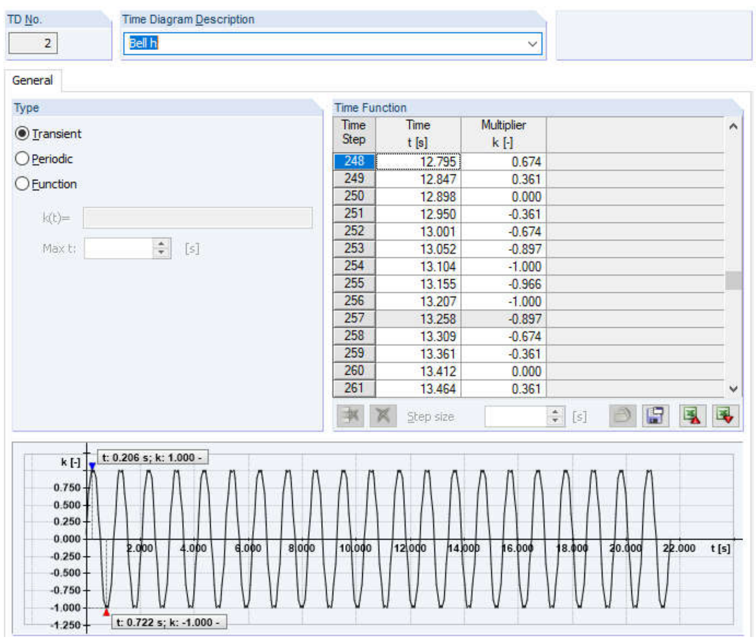

Figure 44 – Modified time diagram for horizontal load from the bell swing

The result of the analysis will be presented on the next page.

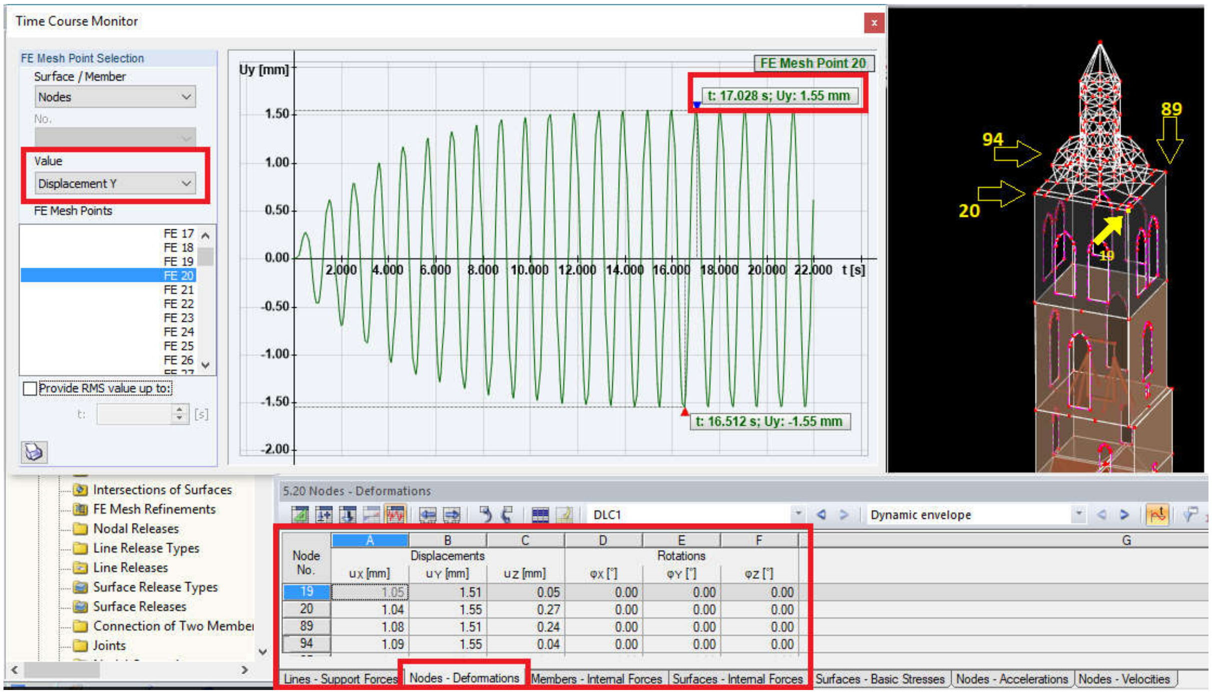

Figure 45 – Top nodal displacements and rotations in case of resonance phenomenon

From the result of the analysis using the same bell weight but with the different bell swing frequency to match one of the structural natural frequency above, it can be seen that the tower will have much larger lateral displacement due to resonance effect. Even though the value of maximum lateral deflection is still small, 1.55 mm on node number 20, but compared to the previous analysis it shows amplification of the deflection up to 6 times. This shows the threat possess by resonance effect on the structure, and such condition must be avoided in the future to ensure the structure integrity and safety.

Another condition worth to look up to is about the usage of the bell with different weight which will create resonanc-like effect on the tower. When a bell with different weight is used, it would have a different swing frequencies that could match natural frequencies of the tower and creating resonance effect. When the bell rings on the tower, it acts with a dynamic force consisting of several harmonic components which the multiplication of it could match one of the natural frequencies of the tower.

If we take a look at the table from DIN 4178 that specifies the relation between mass of the bell and stroke/min below, we can also expand the table to obtain the values of T_0, f_0, and the multiplication values of the frequencies:

Table 9 – Bell mass and stroke/min relation (DIN 4178)

Mass (kg)	stroke/min	T_0=120/(stroke/min)	$f_0=1/T_0$	f_0*2	f_0*3
4000	40	3.00	0.33	0.67	1.00
3000	42	2.86	0.35	0.70	1.05
2500	44	2.73	0.37	0.73	1.10
2000	47	2.55	0.39	0.78	1.18
1600	49	2.45	0.41	0.82	1.23
1150	51	2.35	0.43	0.85	1.28
950	52	2.31	0.43	0.87	1.30
800	54	2.22	0.45	0.90	1.35
660	55	2.18	0.46	0.92	1.38
550	57	2.11	0.48	0.95	1.43
450	58	2.07	0.48	0.97	1.45
400	60	2.00	0.50	1.00	1.50
300	61	1.97	0.51	1.02	1.53
200	65	1.85	0.54	1.08	1.63
150	66	1.82	0.55	1.10	1.65
110	68	1.76	0.57	1.13	1.70
90	69	1.74	0.58	1.15	1.73
50	73	1.64	0.61	1.22	1.83

From the table above, marked with red color are the multiplication of the bell swing frequencies that matches the first three natural frequencies of the bell tower of St. Jakub Church, f1 and f2 respectively. From the table above it can be seen although the phenomenon could occur, the magnitude will be too small to cause a problem on the structure. But if we expand the table to incorporated heavier bell, another critical multiplication value with heavier mass could be found.

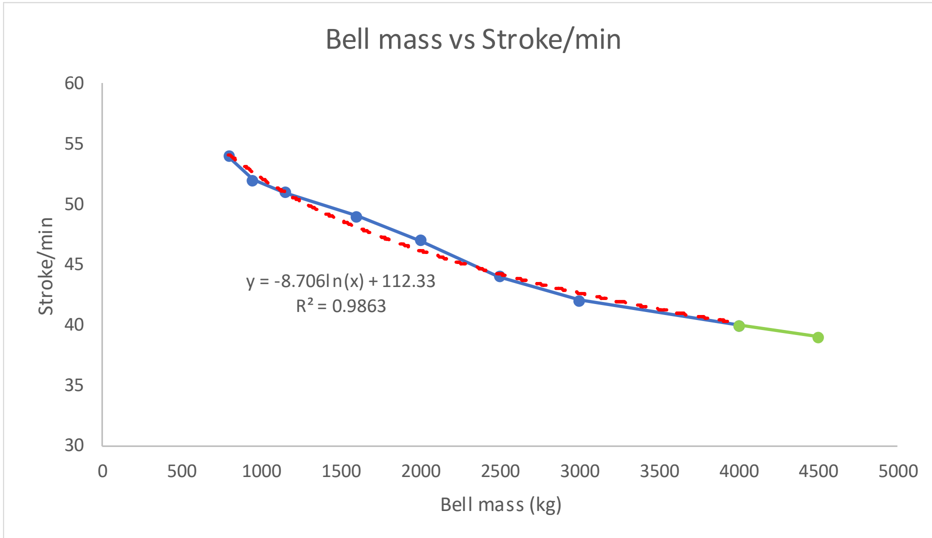

Figure 46 – Plotting and extrapolation of bell mass vs stroke/min relation

From the image above, if the data selection is expanded and interpolated to find the mass of the bell that would require 39 strokes/min, it is found using the trendline equation that the mass of the bell would be approximately 4500 kg.

Table 10 – Bell mass and stroke/min relation with 4500 kg mass of bell

Mass (kg)	stroke/min	T_0=120/(stroke/min)	f_0=1/T_0	f_0*2	f_0*3
4500	39	3.08	0.33	0.65	**0.975**

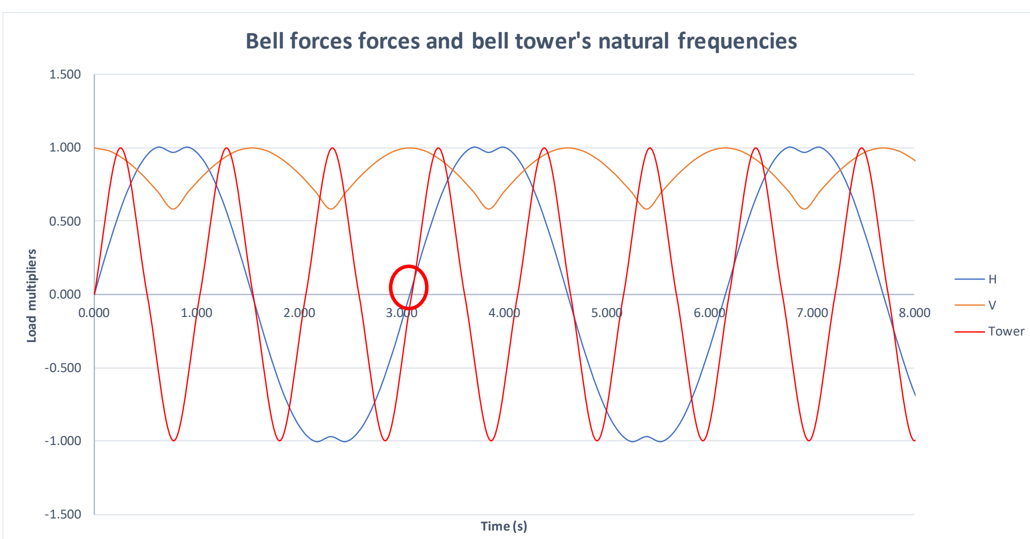

Figure 47 – Bell swing frequencies and bell tower first natural frequency

It can be seen from both table and image above that the bell swing frequency will match the multiplication of the bell tower's first natural frequency, thus will create a resonance-like effect, according to DIN. From here the same time dependent analysis procedure is performed to analyze the resonance effect of 4500 kg swinging bell on the bell tower.

Since the bell now weigh 4500 kg, the maximum bell loads during swinging will also changing. Using equation *(2.9)* and *(2.10)*, it is obtained that the maximum load for horizontal direction is 24.83 kN and 76.88 kN for vertical direction. The analysis result shows that the resonance effect on the tower are as follow:

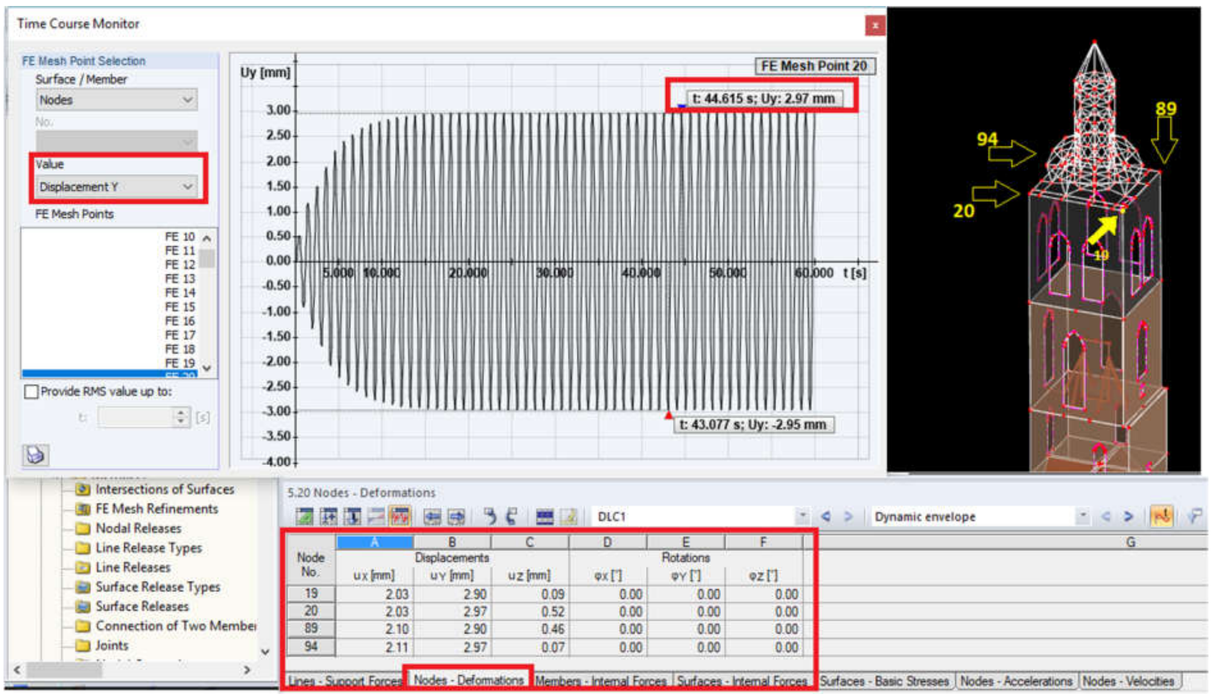

Figure 48 – Top nodal displacements and rotations with a bell weigh 4500 kg

The result shows a maximum top lateral displacement of 2.97 mm in the direction of the bell swing. This value seems small but if the deflection is being added with the deflection caused by the wind load, the result would be different. Deflection caused by the wind load is shown in the picture below:

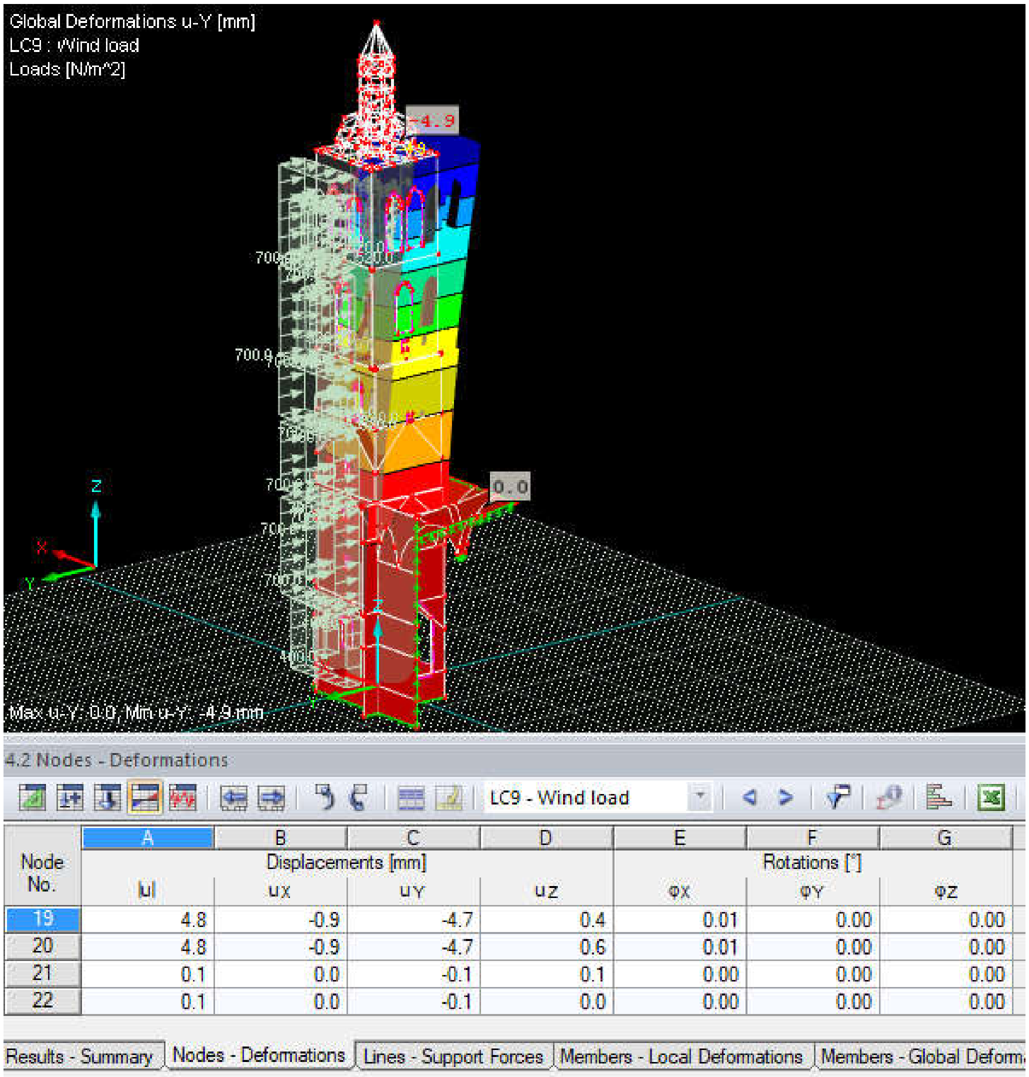

Node No.	A	B	C	D	E	F	G
	Displacements [mm]				Rotations [°]		
	|u|	uX	uY	uZ	φX	φY	φZ
19	4.8	-0.9	-4.7	0.4	0.01	0.00	0.00
20	4.8	-0.9	-4.7	0.6	0.01	0.00	0.00
21	0.1	0.0	-0.1	0.1	0.00	0.00	0.00
22	0.1	0.0	-0.1	0.0	0.00	0.00	0.00

Figure 49 – Horizontal deflection due to wind load in Y direction (parallel to the bell swing)

The total horizontal deflection due to swing of the 4500 kg bell and wind load will be: 4.9+2.97=7.87 mm. Since the deflection will occur in a magnitude twice of the deflection due to 2500 kg bell, the use of heavier bell, in this case 4500 kg bell is not recommended on the bell tower of St. Jakub Church. The deflection that will occur, combined also with the deflection caused by the wind and the actual condition of the structure will make the bell tower more unsafe.

5. CONCLUSION

From the numerical modelling process performed above, there are several things that can be concluded and discussed. The points of conclusion and discussion will be explained below.

- The Masonry Quality Index (MQI) method gave a good result in terms of determining several parameters of the masonry elements of the bell tower. The different values of Young's modulus, compressive strength and shear strength used in the structural model gave a similar stiffness properties on the masonry elements. As a result, the values of the structure's natural frequencies are similar with the experimental modal analysis previously performed
- The result of the structure's first three natural frequencies are similar with the experimental modal analysis previously performed. Not only the values, the mode shapes of the bell tower also matched the result of the experimental modal analysis. The first mode shape corresponds with horizontal deflection in east-west direction, the second mode shape corresponds with horizontal deflection in north-south direction, while the third mode shape corresponds with torsional deformation of the tower.
- The resonance phenomenon is not expected to occur on the bell tower. This mainly caused by the difference between the bell tower natural frequencies and the frequency of the bell swing with the bell weigh 2500 kg. Even though the phenomena is not expected to happen, from another analysis it is known that if the resonance occurs on the structure, it will cause a horizontal deflection up to 6 times higher than the original value. Such thing should be avoided to ensure structural safety and longevity.
- In terms of the usage of heavier bell, it is found that the usage of the bell weighs in around 4500 will create a resonance-like effect due to matching of the bell swing frequency and the multiplication of the bell tower's first natural frequencies. The horizontal deflection caused by the load could be even higher if combined with deflection caused by the wind load. Because of that, the usage of the bell with similar weight is not recommended to be used in the structure.
- It should be noticed that on the analysis performed with 4500 kg of bell, the shape of the bell used remains the same, only the thickness of the bell was changed to achieve the load close to 4500 kg. To get a better result, a true layout of the said bell should be used in order to get a more accurate parameter values of the bell

BIBILOGRAPHY

1. Chopra, Anil K. “Dynamics of structures: theory and applications to earthquake engineering.” Prentice-Hall, 2001.
2. Ivorra, Salvador, Francisco Pallarés, and José Miguel Adam. "Experimental and numerical studies on the belltower of Santa Justa y Rufina (Orihuela-Spain)." Proceedings of the sixth international conference on Structural Analysis of Historic Construction. 2008.
3. Borri, Antonio, et al. "A method for the analysis and classification of historic masonry." Bulletin of Earthquake Engineering 13.9 (2015): 2647.
4. Fajman, Petr, Michal Polàk. "Odborný posudek-vlivu zavěšení zvonu ve věži kostela Sv. Jakub v Kutné Hoře”. Stavebni fakulta, CVUT, 2017.
5. Polàk, Michal, Tomáš Plachý. "Stanovení základních charakteristik vlastního kmitání severní věže kostela svatého jakuba v kutné hoře na havlíčkově náměstí”. Stavebni fakulta, CVUT, 2016.
6. Ivorra, Salvador, Francisco J. Pallarés, and Jose M. Adam. "Masonry bell towers: dynamic considerations." Proceedings of the Institution of Civil Engineers-Structures and Buildings 164.1 (2011): 3-12.
7. Woodhouse, J., et al. "The dynamics of a ringing church bell." *Advances in Acoustics and Vibration* 2012 (2012).
8. Gentile, C., and A. Saisi. "Ambient vibration testing of historic masonry towers for structural identification and damage assessment." *Construction and Building Materials* 21.6 (2007): 1311-1321.
9. British Standards Institution. *Eurocode 2: Design of Concrete Structures: Part 1-1: General Rules and Rules for Buildings*. British Standards Institution, 2004.
10. Brown, Steve, Joon-Pil Hwang, and Andrew Parker. "Assessment of masonry bell tower response to bell ringing using operational modal analysis and numerical modelling." *Proceedings of Acoustics*. 2012.
11. Beconcini, Maria L., Stefano Bennati, and Walter Salvatore. "Structural characterisation of a medieval bell tower: First historical, experimental and numerical investigations." *Proc., 3rd Int. Seminar, Structural Analysis of Historical Constructions, Historical Constructions 2001, Possibilities of Numerical and Experimental Techniques.* Guimarães, Portugal, 2001.
12. Zabel, Volkmar, and Christian Bucher. "Experiences with dynamic investigations of historical bell towers and belfries." *Proceedings of the 20th International Modal Analysis Conference (IMACXX)*. Vol. 2. 2003.
13. Deutsches Institut fur Normung. *DIN 4178: Glockenturme: Berechnung und Ausfuhrung.* Beuth, 1978.

APPENDIX

Appendix 1: Nodal displacement from bell swing load (dynamic load case)

Node	Displacements			Rotations		
No.	u_X [mm]	u_Y [mm]	u_Z [mm]	φ_X [°]	φ_Y [°]	φ_Z [°]
1	0.00	0.00	0.00	0.00	0.00	0.00
2	0.00	0.00	0.00	0.00	0.00	0.00
3	0.00	0.01	0.01	0.00	0.00	0.00
4	0.00	0.01	0.00	0.00	0.00	0.00
5	0.00	0.01	0.00	0.00	0.00	0.00
6	0.02	0.03	0.00	0.00	0.00	0.00
7	0.00	0.00	0.00	0.00	0.00	0.00
8	0.02	0.03	0.02	0.00	0.00	0.00
9	0.03	0.07	0.01	0.00	0.00	0.00
10	0.03	0.07	0.02	0.00	0.00	0.00
11	0.02	0.03	0.00	0.00	0.00	0.00
12	0.04	0.11	0.01	0.00	0.00	0.00
13	0.04	0.11	0.01	0.00	0.00	0.00
14	0.04	0.11	0.02	0.00	0.00	0.00
15	0.06	0.17	0.01	0.00	0.00	0.00
16	0.06	0.18	0.02	0.00	0.00	0.00
17	0.03	0.07	0.02	0.00	0.00	0.00
18	0.07	0.25	0.01	0.00	0.00	0.00
19	0.07	0.24	0.01	0.00	0.00	0.00
20	0.07	0.25	0.02	0.00	0.00	0.00
21	0.00	0.00	0.00	0.00	0.00	0.00
22	0.00	0.00	0.00	0.00	0.00	0.00
23	0.00	0.00	0.00	0.00	0.00	0.00
24	0.00	0.00	0.00	0.00	0.00	0.00
25	0.00	0.01	0.00	0.00	0.00	0.00
26	0.00	0.01	0.00	0.00	0.00	0.00
27	0.00	0.01	0.00	0.00	0.00	0.00
28	0.00	0.01	0.00	0.00	0.00	0.00
29	0.00	0.01	0.00	0.00	0.00	0.00
30	0.00	0.01	0.00	0.00	0.00	0.00
31	0.00	0.01	0.00	0.00	0.00	0.00
32	0.01	0.01	0.01	0.00	0.00	0.00
33	0.01	0.01	0.01	0.00	0.00	0.00
34	0.01	0.02	0.01	0.00	0.00	0.00
35	0.01	0.02	0.01	0.00	0.00	0.00
36	0.01	0.02	0.01	0.00	0.00	0.00
37	0.01	0.03	0.01	0.00	0.00	0.00
38	0.01	0.03	0.01	0.00	0.00	0.00
39	0.01	0.03	0.01	0.00	0.00	0.00
40	0.02	0.04	0.01	0.00	0.00	0.00
41	0.02	0.04	0.01	0.00	0.00	0.00
42	0.02	0.05	0.01	0.00	0.00	0.00
43	0.02	0.05	0.01	0.00	0.00	0.00
44	0.03	0.08	0.01	0.00	0.00	0.00
45	0.03	0.10	0.01	0.00	0.00	0.00
46	0.03	0.10	0.01	0.00	0.00	0.00
47	0.03	0.10	0.01	0.00	0.00	0.00

Node	Displacements			Rotations		
No.	u_X [mm]	u_Y [mm]	u_Z [mm]	φ_X [°]	φ_Y [°]	φ_Z [°]
48	0.03	0.10	0.01	0.00	0.00	0.00
49	0.04	0.10	0.01	0.00	0.00	0.00
50	0.04	0.10	0.01	0.00	0.00	0.00
51	0.04	0.10	0.01	0.00	0.00	0.00
52	0.03	0.10	0.01	0.00	0.00	0.00
53	0.03	0.10	0.01	0.00	0.00	0.00
54	0.03	0.08	0.01	0.00	0.00	0.00
55	0.04	0.12	0.02	0.00	0.00	0.00
56	0.05	0.15	0.01	0.00	0.00	0.00
57	0.05	0.16	0.01	0.00	0.00	0.00
58	0.05	0.16	0.02	0.00	0.00	0.00
59	0.05	0.16	0.02	0.00	0.00	0.00
60	0.05	0.16	0.02	0.00	0.00	0.00
61	0.04	0.11	0.02	0.00	0.00	0.00
62	0.05	0.16	0.02	0.00	0.00	0.00
63	0.05	0.16	0.02	0.00	0.00	0.00
64	0.04	0.12	0.02	0.00	0.00	0.00
65	0.06	0.18	0.01	0.00	0.00	0.00
66	0.06	0.21	0.01	0.00	0.00	0.00
67	0.06	0.22	0.01	0.00	0.00	0.00
68	0.07	0.22	0.01	0.00	0.00	0.00
69	0.07	0.23	0.01	0.00	0.00	0.00
70	0.07	0.22	0.01	0.00	0.00	0.00
71	0.06	0.22	0.01	0.00	0.00	0.00
72	0.06	0.22	0.01	0.00	0.00	0.00
73	0.06	0.18	0.01	0.00	0.00	0.00
74	0.06	0.18	0.02	0.00	0.00	0.00
75	0.06	0.22	0.02	0.00	0.00	0.00
76	0.06	0.22	0.02	0.00	0.00	0.00
77	0.07	0.22	0.02	0.00	0.00	0.00
78	0.07	0.23	0.02	0.00	0.00	0.00
79	0.07	0.22	0.02	0.00	0.00	0.00
80	0.07	0.22	0.02	0.00	0.00	0.00
81	0.06	0.22	0.02	0.00	0.00	0.00
82	0.06	0.18	0.02	0.00	0.00	0.00
84	0.06	0.17	0.02	0.00	0.00	0.00
85	0.00	0.01	0.01	0.00	0.00	0.00
86	0.02	0.03	0.02	0.00	0.00	0.00
87	0.06	0.17	0.02	0.00	0.00	0.00
88	0.04	0.11	0.02	0.00	0.00	0.00
89	0.08	0.24	0.02	0.00	0.00	0.00
90	0.02	0.03	0.00	0.00	0.00	0.00
91	0.03	0.07	0.01	0.00	0.00	0.00
92	0.04	0.11	0.01	0.00	0.00	0.00
93	0.06	0.18	0.01	0.00	0.00	0.00
94	0.08	0.25	0.01	0.00	0.00	0.00
95	0.02	0.03	0.02	0.00	0.00	0.00
96	0.00	0.00	0.00	0.00	0.00	0.00

Node	Displacements			Rotations		
No.	u_X [mm]	u_Y [mm]	u_Z [mm]	φ_X [°]	φ_Y [°]	φ_Z [°]
97	0.06	0.18	0.01	0.00	0.00	0.00
100	0.00	0.00	0.00	0.00	0.00	0.00
101	0.00	0.00	0.00	0.00	0.00	0.00
102	0.00	0.01	0.00	0.00	0.00	0.00
103	0.00	0.01	0.00	0.00	0.00	0.00
104	0.00	0.01	0.01	0.00	0.00	0.00
105	0.00	0.01	0.01	0.00	0.00	0.00
106	0.00	0.00	0.00	0.00	0.00	0.00
107	0.00	0.00	0.00	0.00	0.00	0.00
108	0.06	0.18	0.02	0.00	0.00	0.00
109	0.07	0.22	0.02	0.00	0.00	0.00
110	0.07	0.22	0.02	0.00	0.00	0.00
111	0.00	0.01	0.00	0.00	0.00	0.00
112	0.00	0.01	0.00	0.00	0.00	0.00
113	0.00	0.01	0.00	0.00	0.00	0.00
114	0.00	0.01	0.00	0.00	0.00	0.00
115	0.00	0.01	0.00	0.00	0.00	0.00
116	0.00	0.01	0.00	0.00	0.00	0.00
117	0.00	0.01	0.00	0.00	0.00	0.00
118	0.00	0.01	0.00	0.00	0.00	0.00
119	0.01	0.02	0.00	0.00	0.00	0.00
120	0.01	0.02	0.01	0.00	0.00	0.00
121	0.01	0.02	0.00	0.00	0.00	0.00
122	0.01	0.02	0.01	0.00	0.00	0.00
123	0.02	0.03	0.01	0.00	0.00	0.00
124	0.02	0.03	0.01	0.00	0.00	0.00
125	0.02	0.03	0.00	0.00	0.00	0.00
126	0.02	0.03	0.00	0.00	0.00	0.00
127	0.02	0.03	0.00	0.00	0.00	0.00
128	0.02	0.03	0.00	0.00	0.00	0.00
129	0.02	0.03	0.00	0.00	0.00	0.00
130	0.02	0.03	0.00	0.00	0.00	0.00
131	0.02	0.05	0.02	0.00	0.00	0.00
132	0.02	0.05	0.01	0.00	0.00	0.00
133	0.02	0.05	0.01	0.00	0.00	0.00
134	0.02	0.05	0.02	0.00	0.00	0.00
135	0.03	0.07	0.01	0.00	0.00	0.00
136	0.03	0.07	0.01	0.00	0.00	0.00
137	0.03	0.07	0.01	0.00	0.00	0.00
138	0.03	0.07	0.00	0.00	0.00	0.00
139	0.03	0.07	0.00	0.00	0.00	0.00
140	0.03	0.07	0.01	0.00	0.00	0.00
141	0.03	0.07	0.00	0.00	0.00	0.00
142	0.03	0.07	0.00	0.00	0.00	0.00
143	0.03	0.07	0.00	0.00	0.00	0.00
144	0.03	0.07	0.00	0.00	0.00	0.00
145	0.03	0.07	0.00	0.00	0.00	0.00
146	0.03	0.07	0.00	0.00	0.00	0.00

Node	Displacements			Rotations		
No.	u_X [mm]	u_Y [mm]	u_Z [mm]	φ_X [°]	φ_Y [°]	φ_Z [°]
147	0.08	0.22	0.02	0.00	0.00	0.00
148	0.08	0.23	0.02	0.00	0.00	0.00
149	0.08	0.23	0.02	0.00	0.00	0.00
150	0.07	0.22	0.01	0.00	0.00	0.00
151	0.07	0.22	0.01	0.00	0.00	0.00
152	0.06	0.19	0.01	0.00	0.00	0.00
153	0.06	0.19	0.01	0.00	0.00	0.00
154	0.07	0.22	0.01	0.00	0.00	0.00
155	0.07	0.23	0.01	0.00	0.00	0.00
156	0.08	0.23	0.01	0.00	0.00	0.00
157	0.01	0.01	0.00	0.00	0.00	0.00
158	0.01	0.01	0.00	0.00	0.00	0.00
159	0.01	0.01	0.00	0.00	0.00	0.00
160	0.01	0.01	0.00	0.00	0.00	0.00
161	0.01	0.02	0.00	0.00	0.00	0.00
162	0.01	0.02	0.00	0.00	0.00	0.00
163	0.01	0.03	0.00	0.00	0.00	0.00
164	0.01	0.03	0.00	0.00	0.00	0.00
165	0.02	0.04	0.00	0.00	0.00	0.00
166	0.02	0.04	0.00	0.00	0.00	0.00
167	0.02	0.05	0.00	0.00	0.00	0.00
168	0.02	0.05	0.00	0.00	0.00	0.00
169	0.03	0.07	0.00	0.00	0.00	0.00
170	0.03	0.07	0.00	0.00	0.00	0.00
171	0.04	0.09	0.00	0.00	0.00	0.00
172	0.04	0.10	0.00	0.00	0.00	0.00
173	0.04	0.10	0.00	0.00	0.00	0.00
174	0.04	0.10	0.00	0.00	0.00	0.00
175	0.03	0.10	0.00	0.00	0.00	0.00
176	0.03	0.10	0.00	0.00	0.00	0.00
177	0.03	0.09	0.00	0.00	0.00	0.00
178	0.04	0.12	0.00	0.00	0.00	0.00
179	0.04	0.12	0.01	0.00	0.00	0.00
180	0.05	0.15	0.01	0.00	0.00	0.00
181	0.05	0.16	0.01	0.00	0.00	0.00
182	0.05	0.16	0.01	0.00	0.00	0.00
183	0.05	0.16	0.00	0.00	0.00	0.00
184	0.05	0.16	0.00	0.00	0.00	0.00
185	0.05	0.15	0.00	0.00	0.00	0.00
186	0.05	0.15	0.00	0.00	0.00	0.00
187	0.06	0.18	0.00	0.00	0.00	0.00
188	0.06	0.18	0.01	0.00	0.00	0.00
189	0.07	0.22	0.01	0.00	0.00	0.00
190	0.07	0.22	0.01	0.00	0.00	0.00
191	0.07	0.23	0.01	0.00	0.00	0.00
192	0.07	0.23	0.01	0.00	0.00	0.00
193	0.07	0.23	0.01	0.00	0.00	0.00
194	0.07	0.23	0.00	0.00	0.00	0.00

Node	Displacements			Rotations		
No.	u_X [mm]	u_Y [mm]	u_Z [mm]	φ_X [°]	φ_Y [°]	φ_Z [°]
195	0.07	0.22	0.00	0.00	0.00	0.00
196	0.06	0.18	0.00	0.00	0.00	0.00
197	0.06	0.18	0.00	0.00	0.00	0.00
198	0.07	0.22	0.00	0.00	0.00	0.00
199	0.07	0.23	0.00	0.00	0.00	0.00
200	0.07	0.23	0.00	0.00	0.00	0.00
201	0.07	0.23	0.00	0.00	0.00	0.00
202	0.07	0.23	0.00	0.00	0.00	0.00
203	0.07	0.22	0.00	0.00	0.00	0.00
204	0.07	0.22	0.00	0.00	0.00	0.00
205	0.03	0.07	0.00	0.00	0.00	0.00
206	0.03	0.07	0.00	0.00	0.00	0.00
207	0.03	0.08	0.00	0.00	0.00	0.00
208	0.03	0.08	0.00	0.00	0.00	0.00
209	0.04	0.12	0.00	0.00	0.00	0.00
210	0.04	0.12	0.00	0.00	0.00	0.00
211	0.04	0.12	0.00	0.00	0.00	0.00
212	0.04	0.12	0.00	0.00	0.00	0.00
213	0.05	0.13	0.00	0.00	0.00	0.00
214	0.04	0.13	0.00	0.00	0.00	0.00
215	0.05	0.15	0.00	0.00	0.00	0.00
216	0.05	0.16	0.00	0.00	0.00	0.00
217	0.05	0.16	0.00	0.00	0.00	0.00
218	0.05	0.16	0.00	0.00	0.00	0.00
219	0.05	0.16	0.00	0.00	0.00	0.00
220	0.05	0.16	0.00	0.00	0.00	0.00
221	0.05	0.16	0.00	0.00	0.00	0.00
222	0.06	0.18	0.00	0.00	0.00	0.00
223	0.06	0.18	0.00	0.00	0.00	0.00
224	0.07	0.21	0.00	0.00	0.00	0.00
225	0.07	0.22	0.00	0.00	0.00	0.00
226	0.07	0.22	0.00	0.00	0.00	0.00
227	0.07	0.22	0.00	0.00	0.00	0.00
228	0.07	0.22	0.00	0.00	0.00	0.00
229	0.06	0.21	0.00	0.00	0.00	0.00
230	0.07	0.22	0.00	0.00	0.00	0.00
231	0.06	0.18	0.00	0.00	0.00	0.00
232	0.06	0.18	0.01	0.00	0.00	0.00
233	0.07	0.21	0.01	0.00	0.00	0.00
234	0.07	0.22	0.01	0.00	0.00	0.00
235	0.07	0.22	0.01	0.00	0.00	0.00
236	0.07	0.22	0.00	0.00	0.00	0.00
237	0.07	0.22	0.00	0.00	0.00	0.00
238	0.07	0.21	0.00	0.00	0.00	0.00
239	0.07	0.22	0.00	0.00	0.00	0.00
240	0.08	0.23	0.01	0.00	0.00	0.00
241	0.08	0.23	0.01	0.00	0.00	0.00
242	0.07	0.22	0.01	0.00	0.00	0.00

Node	Displacements			Rotations		
No.	u_X [mm]	u_Y [mm]	u_Z [mm]	φ_X [°]	φ_Y [°]	φ_Z [°]
243	0.07	0.22	0.01	0.00	0.00	0.00
244	0.06	0.19	0.01	0.00	0.00	0.00
247	0.04	0.12	0.02	0.00	0.00	0.00
248	0.05	0.15	0.01	0.00	0.00	0.00
249	0.05	0.16	0.01	0.00	0.00	0.00
250	0.05	0.16	0.01	0.00	0.00	0.00
251	0.06	0.16	0.01	0.00	0.00	0.00
252	0.06	0.16	0.01	0.00	0.00	0.00
253	0.05	0.16	0.01	0.00	0.00	0.00
254	0.05	0.15	0.01	0.00	0.00	0.00
255	0.04	0.12	0.01	0.00	0.00	0.00
256	0.03	0.07	0.01	0.00	0.00	0.00
257	0.03	0.07	0.01	0.00	0.00	0.00
258	0.03	0.10	0.01	0.00	0.00	0.00
259	0.03	0.10	0.01	0.00	0.00	0.00
260	0.03	0.10	0.01	0.00	0.00	0.00
261	0.03	0.10	0.02	0.00	0.00	0.00
262	0.04	0.10	0.02	0.00	0.00	0.00
263	0.04	0.10	0.02	0.00	0.00	0.00
264	0.04	0.10	0.02	0.00	0.00	0.00
265	0.04	0.10	0.02	0.00	0.00	0.00
266	0.03	0.10	0.02	0.00	0.00	0.00
345	0.00	0.00	0.00	0.00	0.00	0.00
346	0.00	0.00	0.00	0.00	0.00	0.00
359	0.00	0.00	0.00	0.00	0.00	0.00
360	0.00	0.00	0.00	0.00	0.00	0.00
361	0.00	0.00	0.00	0.00	0.00	0.00
362	0.00	0.01	0.00	0.00	0.00	0.00
363	0.01	0.03	0.01	0.00	0.00	0.00
370	0.00	0.00	0.00	0.00	0.00	0.00
371	0.01	0.02	0.01	0.00	0.00	0.00
372	0.00	0.00	0.00	0.00	0.00	0.00
373	0.00	0.00	0.00	0.00	0.00	0.00
376	0.00	0.00	0.00	0.00	0.00	0.00
377	0.00	0.01	0.00	0.00	0.00	0.00
378	0.00	0.01	0.00	0.00	0.00	0.00
379	0.00	0.00	0.00	0.00	0.00	0.00
380	0.00	0.00	0.00	0.00	0.00	0.00
381	0.00	0.01	0.01	0.00	0.00	0.00
382	0.00	0.01	0.00	0.00	0.00	0.00
383	0.00	0.00	0.00	0.00	0.00	0.00
384	0.00	0.01	0.01	0.00	0.00	0.00
385	0.02	0.03	0.01	0.00	0.00	0.00
386	0.00	0.00	0.00	0.00	0.00	0.00
387	0.01	0.02	0.01	0.00	0.00	0.00
388	0.00	0.00	0.00	0.00	0.00	0.00
389	0.00	0.01	0.00	0.00	0.00	0.00
390	0.00	0.00	0.00	0.00	0.00	0.00

Node No.	Displacements u_X [mm]	u_Y [mm]	u_Z [mm]	Rotations φ_X [°]	φ_Y [°]	φ_Z [°]
391	0.02	0.03	0.00	0.00	0.00	0.00
392	0.00	0.00	0.00	0.00	0.00	0.00
393	0.01	0.02	0.00	0.00	0.00	0.00
394	0.00	0.00	0.00	0.00	0.00	0.00
395	0.01	0.00	0.00	0.00	0.00	0.00
396	0.00	0.00	0.00	0.00	0.00	0.00
397	0.00	0.00	0.00	0.00	0.00	0.00
398	0.00	0.00	0.00	0.00	0.00	0.00
399	0.00	0.00	0.00	0.00	0.00	0.00
400	0.00	0.02	0.00	0.00	0.00	0.00
401	0.00	0.02	0.00	0.00	0.00	0.00
402	0.00	0.01	0.00	0.00	0.00	0.00
403	0.00	0.00	0.00	0.00	0.00	0.00
404	0.00	0.00	0.00	0.00	0.00	0.00
405	0.00	0.00	0.00	0.00	0.00	0.00
411	0.04	0.11	0.01	0.00	0.00	0.00
412	0.04	0.11	0.02	0.00	0.00	0.00
413	0.04	0.11	0.02	0.00	0.00	0.00
414	0.04	0.11	0.01	0.00	0.00	0.00
415	0.04	0.11	0.00	0.00	0.00	0.00
416	0.04	0.11	0.00	0.00	0.00	0.00
417	0.05	3.67	0.00	0.15	0.00	0.06
418	0.05	3.67	0.00	0.15	0.00	0.06
419	0.05	0.34	0.00	0.05	0.00	0.01
420	0.04	0.12	0.06	0.00	0.00	0.00
421	0.04	0.12	0.06	0.00	0.00	0.00
422	0.05	0.34	0.00	0.05	0.00	0.01
423	0.04	0.12	0.06	0.00	0.00	0.00
424	0.04	0.12	0.06	0.00	0.00	0.00
425	0.05	4.84	0.00	0.15	0.00	0.00
430	0.04	0.11	0.00	0.00	0.00	0.00
431	0.04	0.11	0.00	0.00	0.00	0.00
432	0.04	0.11	0.00	0.00	0.00	0.00
433	0.04	0.11	0.00	0.00	0.00	0.00
667	0.07	0.25	0.02	0.00	0.00	0.00
668	0.07	0.24	0.01	0.00	0.00	0.00
718	0.08	0.25	0.01	0.00	0.00	0.00
719	0.08	0.25	0.01	0.00	0.00	0.00
752	0.08	0.25	0.02	0.00	0.00	0.00
1184	0.08	0.25	0.00	0.00	0.00	0.00
1185	0.08	0.25	0.01	0.00	0.00	0.00
1186	0.07	0.25	0.02	0.00	0.00	0.00
1196	0.07	0.24	0.00	0.00	0.00	0.00
1198	0.07	0.24	0.00	0.00	0.00	0.00
1199	0.08	0.24	0.01	0.00	0.00	0.00
1200	0.08	0.25	0.02	0.00	0.00	0.00
1201	0.08	0.25	0.01	0.00	0.00	0.00
1315	0.07	0.25	0.01	0.00	0.00	0.00

Node	Displacements			Rotations		
No.	u_X [mm]	u_Y [mm]	u_Z [mm]	φ_X [°]	φ_Y [°]	φ_Z [°]
1316	0.07	0.25	0.02	0.00	0.00	0.00
1398	0.01	0.02	0.00	0.00	0.00	0.00
1399	0.01	0.03	0.00	0.00	0.00	0.00
1400	0.01	0.01	0.00	0.00	0.00	0.00
1401	0.01	0.02	0.01	0.00	0.00	0.00
1402	0.01	0.02	0.00	0.00	0.00	0.00
1403	0.01	0.02	0.00	0.00	0.00	0.00
1405	0.00	0.00	0.00	0.00	0.00	0.00
1406	0.00	0.01	0.00	0.00	0.00	0.00
1407	0.01	0.02	0.01	0.00	0.00	0.00
1408	0.01	0.02	0.00	0.00	0.00	0.00
1409	0.01	0.01	0.00	0.00	0.00	0.00
1410	0.01	0.01	0.00	0.00	0.00	0.00
1411	0.01	0.02	0.00	0.00	0.00	0.00
1412	0.01	0.02	0.00	0.00	0.00	0.00
1413	0.01	0.01	0.00	0.00	0.00	0.00
1414	0.01	0.02	0.01	0.00	0.00	0.00
1415	0.01	0.02	0.01	0.00	0.00	0.00
1416	0.00	0.01	0.00	0.00	0.00	0.00
1417	0.01	0.01	0.00	0.00	0.00	0.00
1418	0.01	0.01	0.00	0.00	0.00	0.00
1419	0.00	0.00	0.00	0.00	0.00	0.00
1420	0.00	0.01	0.00	0.00	0.00	0.00
1421	0.00	0.02	0.00	0.00	0.00	0.00
1422	0.01	0.01	0.00	0.00	0.00	0.00
1424	0.00	0.02	0.00	0.00	0.00	0.00
1426	0.01	0.02	0.01	0.00	0.00	0.00
1427	0.01	0.02	0.01	0.00	0.00	0.00
1428	0.01	0.02	0.01	0.00	0.00	0.00
1429	0.00	0.01	0.01	0.00	0.00	0.00
1430	0.00	0.01	0.00	0.00	0.00	0.00
1432	0.01	0.02	0.01	0.00	0.00	0.00
1433	0.01	0.02	0.00	0.00	0.00	0.00
1434	0.01	0.02	0.00	0.00	0.00	0.00
1435	0.01	0.02	0.01	0.00	0.00	0.00
1436	0.01	0.02	0.01	0.00	0.00	0.00
1439	0.00	0.03	0.00	0.00	0.00	0.00
1440	0.00	0.03	0.01	0.00	0.00	0.00
1509	0.01	0.00	0.00	0.00	0.00	0.00
1513	0.02	0.00	0.00	0.00	0.00	0.00
1514	0.01	0.00	0.00	0.00	0.00	0.00
1521	0.01	0.01	0.00	0.00	0.00	0.00
1523	0.01	0.00	0.00	0.00	0.00	0.00
1524	0.01	0.00	0.00	0.00	0.00	0.00
1527	0.00	0.00	0.00	0.00	0.00	0.00
1532	0.01	0.00	0.00	0.00	0.00	0.00
1558	0.01	0.02	0.01	0.00	0.00	0.00
1559	0.01	0.02	0.00	0.00	0.00	0.00

Node No.	Displacements u_X [mm]	u_Y [mm]	u_Z [mm]	Rotations φ_X [°]	φ_Y [°]	φ_Z [°]
1562	0.01	0.02	0.00	0.00	0.00	0.00
1563	0.01	0.03	0.00	0.00	0.00	0.00
1564	0.01	0.03	0.01	0.00	0.00	0.00
1565	0.01	0.02	0.00	0.00	0.00	0.00
1566	0.01	0.02	0.01	0.00	0.00	0.00
1567	0.00	0.00	0.00	0.00	0.00	0.00
1568	0.00	0.00	0.00	0.00	0.00	0.00
1571	0.01	0.00	0.00	0.00	0.00	0.00

Appendix 2: Nodal displacement from wind load

Node	Displacements [mm]				Rotations [°]		
No.	|u|	u_X	u_Y	u_Z	φ_X	φ_Y	φ_Z
1	0.0	0.0	0.0	0.0	0.00	0.00	0.00
2	0.0	0.0	0.0	0.0	0.00	0.00	0.00
3	0.2	0.0	-0.2	0.2	0.00	0.00	0.00
4	0.2	0.0	-0.2	0.1	0.00	0.00	0.00
5	0.2	0.0	-0.2	0.0	0.00	0.00	0.00
6	0.7	-0.2	-0.6	0.1	0.00	0.00	0.00
7	0.0	0.0	0.0	0.0	0.00	0.00	0.00
8	0.8	-0.2	-0.7	0.3	0.00	0.00	0.00
9	1.4	-0.3	-1.3	0.3	0.01	0.00	0.00
10	1.4	-0.4	-1.3	0.5	0.01	0.00	0.00
11	0.7	-0.2	-0.7	0.2	0.00	0.00	0.00
12	2.0	-0.5	-1.9	0.3	0.01	0.00	0.00
13	2.0	-0.5	-2.0	0.3	0.01	0.00	0.00
14	2.1	-0.5	-2.0	0.5	0.01	0.00	0.00
15	3.3	-0.7	-3.2	0.4	0.01	0.00	0.00
16	3.4	-0.7	-3.3	0.6	0.01	0.00	0.00
17	1.4	-0.4	-1.3	-0.4	0.01	0.00	0.00
18	5.0	-0.9	-4.9	0.5	0.01	0.00	0.00
19	4.8	-0.9	-4.7	0.4	0.01	0.00	0.00
20	4.8	-0.9	-4.7	0.6	0.01	0.00	0.00
21	0.1	0.0	-0.1	0.1	0.00	0.00	0.00
22	0.1	0.0	-0.1	0.0	0.00	0.00	0.00
23	0.1	0.0	-0.1	0.0	0.00	0.00	0.00
24	0.2	0.0	-0.1	0.1	0.00	0.00	0.00
25	0.2	0.0	-0.2	0.1	0.00	0.00	0.00
26	0.2	0.0	-0.1	0.1	0.00	0.00	0.00
27	0.2	0.0	-0.1	0.1	0.00	0.00	0.00
28	0.2	0.0	-0.1	0.1	0.00	0.00	0.00
29	0.2	0.0	-0.2	0.1	0.00	0.00	0.00
30	0.2	0.0	-0.1	0.1	0.00	0.00	0.00
31	0.2	0.0	-0.1	0.1	0.00	0.00	0.00
32	0.4	-0.1	-0.3	0.1	0.00	0.00	0.00
33	0.4	-0.1	-0.3	0.1	0.00	0.00	0.00
34	0.4	-0.1	-0.4	0.2	0.00	0.00	0.00
35	0.4	-0.1	-0.4	0.2	0.00	0.00	0.00
36	0.6	-0.1	-0.5	0.2	0.00	0.00	0.00
37	0.6	-0.1	-0.5	0.2	0.00	0.00	0.00
38	0.7	-0.2	-0.6	0.2	0.00	0.00	0.00
39	0.7	-0.2	-0.6	0.2	0.00	0.00	0.00
40	0.9	-0.2	-0.8	0.3	0.00	0.00	0.00
41	0.9	-0.2	-0.8	0.3	0.00	0.00	0.00
42	1.0	-0.3	-0.9	0.3	0.00	0.00	0.00
43	1.0	-0.3	-0.9	0.3	0.00	0.00	0.00
44	1.4	-0.3	-1.3	0.3	0.01	0.00	0.00
45	1.8	-0.4	-1.7	0.4	0.01	0.00	0.00
46	1.8	-0.4	-1.7	0.4	0.01	0.00	0.00
47	1.8	-0.4	-1.7	0.4	0.01	0.00	0.00

No.	|u|	u_X	u_Y	u_Z	φ_X	φ_Y	φ_Z
48	1.8	-0.4	-1.7	0.4	0.01	0.00	0.00
49	1.8	-0.4	-1.7	0.4	0.01	0.00	0.00
50	1.8	-0.4	-1.7	0.4	0.01	0.00	0.00
51	1.8	-0.4	-1.7	0.4	0.01	0.00	0.00
52	1.8	-0.4	-1.7	0.4	0.01	0.00	0.00
53	1.8	-0.4	-1.7	0.4	0.01	0.00	0.00
54	1.4	-0.4	-1.4	0.3	0.01	0.00	0.00
55	2.2	-0.5	-2.1	0.4	0.01	0.00	0.00
56	3.0	-0.6	-2.9	0.5	0.01	0.00	0.00
57	3.0	-0.6	-2.9	0.5	0.01	0.00	0.00
58	3.1	-0.6	-3.0	0.5	0.01	0.00	0.00
59	3.2	-0.6	-3.0	0.5	0.01	0.00	0.00
60	3.1	-0.6	-3.0	0.5	0.01	0.00	0.00
61	2.1	-0.5	-1.9	-0.5	0.01	0.00	0.00
62	3.0	-0.6	-2.9	0.5	0.01	0.00	0.00
63	3.0	-0.6	-2.9	0.5	0.01	0.00	0.00
64	2.2	-0.5	-2.1	0.4	0.01	0.00	0.00
65	3.5	-0.7	-3.4	0.4	0.01	0.00	0.00
66	4.3	-0.8	-4.2	0.5	0.01	0.00	0.00
67	4.4	-0.8	-4.3	0.5	0.01	0.00	0.00
68	4.4	-0.8	-4.4	0.5	0.01	0.00	0.00
69	4.6	-0.8	-4.5	0.5	0.01	0.00	0.00
70	4.5	-0.8	-4.4	0.5	0.01	0.00	0.00
71	4.5	-0.8	-4.4	0.5	0.01	0.00	0.00
72	4.4	-0.8	-4.3	0.5	0.01	0.00	0.00
73	3.6	-0.7	-3.5	0.5	0.01	0.00	0.00
74	3.6	-0.7	-3.5	0.5	0.01	0.00	0.00
75	4.4	-0.8	-4.3	0.5	0.01	0.00	0.00
76	4.5	-0.8	-4.4	0.5	0.01	0.00	0.00
77	4.5	-0.8	-4.4	0.5	0.01	0.00	0.00
78	4.6	-0.8	-4.4	0.5	0.01	0.00	0.00
79	4.5	-0.8	-4.4	0.5	0.01	0.00	0.00
80	4.4	-0.8	-4.3	0.6	0.01	0.00	0.00
81	4.3	-0.8	-4.2	0.6	0.01	0.00	0.00
82	3.6	-0.7	-3.5	0.5	0.01	0.00	0.00
84	3.4	-0.7	-3.2	-0.5	0.01	0.00	0.00
85	0.2	0.0	-0.2	-0.2	0.00	0.00	0.00
86	0.8	-0.2	-0.7	-0.3	0.00	0.00	0.00
87	3.4	-0.7	-3.2	-0.5	0.01	0.00	0.00
88	2.1	-0.5	-2.0	-0.5	0.01	0.00	0.00
89	4.8	-0.9	-4.7	-0.5	0.01	0.00	0.00
90	0.6	-0.2	-0.6	-0.1	0.00	0.00	0.00
91	1.4	-0.3	-1.3	-0.2	0.01	0.00	0.00
92	2.0	-0.5	-2.0	-0.3	0.01	0.00	0.00
93	3.4	-0.7	-3.3	-0.4	0.01	0.00	0.00
94	4.8	-0.9	-4.7	-0.4	0.01	0.00	0.00
95	0.8	-0.2	-0.7	-0.3	0.00	0.00	0.00
96	0.0	0.0	0.0	0.0	0.00	0.00	0.00
97	3.4	-0.7	-3.3	-0.3	0.01	0.00	0.00

Node	Displacements [mm]				Rotations [°]		
No.	|u|	u_X	u_Y	u_Z	φ_X	φ_Y	φ_Z
100	0.1	0.0	-0.1	0.1	0.00	0.00	0.00
101	0.1	0.0	-0.1	0.0	0.00	0.00	0.00
102	0.2	0.0	-0.2	0.1	0.00	0.00	0.00
103	0.2	0.0	-0.2	0.1	0.00	0.00	0.00
104	0.2	0.0	-0.2	-0.1	0.00	0.00	0.00
105	0.2	0.0	-0.2	-0.2	0.00	0.00	0.00
106	0.1	0.0	-0.1	0.0	0.00	0.00	0.00
107	0.1	0.0	-0.1	-0.1	0.00	0.00	0.00
108	3.6	-0.7	-3.4	-0.5	0.01	0.00	0.00
109	4.3	-0.8	-4.2	-0.5	0.01	0.00	0.00
110	4.4	-0.8	-4.2	-0.5	0.01	0.00	0.00
111	0.2	0.0	-0.2	0.0	0.00	0.00	0.00
112	0.2	0.0	-0.2	0.1	0.00	0.00	0.00
113	0.2	0.0	-0.2	0.0	0.00	0.00	0.00
114	0.2	0.0	-0.2	-0.1	0.00	0.00	0.00
115	0.2	0.0	-0.2	0.0	0.00	0.00	0.00
116	0.2	0.0	-0.2	0.0	0.00	0.00	0.00
117	0.2	0.0	-0.2	0.0	0.00	0.00	0.00
118	0.2	0.0	-0.2	0.0	0.00	0.00	0.00
119	0.5	-0.1	-0.4	0.1	0.00	0.00	0.00
120	0.5	-0.1	-0.4	0.3	0.00	0.00	0.00
121	0.4	-0.1	-0.4	-0.1	0.00	0.00	0.00
122	0.6	-0.1	-0.5	-0.3	0.00	0.00	0.00
123	0.8	-0.2	-0.7	0.2	0.00	0.00	0.00
124	0.7	-0.2	-0.7	-0.2	0.00	0.00	0.00
125	0.7	-0.2	-0.6	0.1	0.00	0.00	0.00
126	0.7	-0.2	-0.7	-0.1	0.00	0.00	0.00
127	0.7	-0.2	-0.7	-0.1	0.00	0.00	0.00
128	0.7	-0.2	-0.6	0.1	0.00	0.00	0.00
129	0.7	-0.2	-0.7	0.0	0.00	0.00	0.00
130	0.7	-0.2	-0.7	0.0	0.00	0.00	0.00
131	1.0	-0.3	-0.9	0.4	0.00	0.00	0.00
132	0.9	-0.3	-0.9	-0.2	0.00	0.00	0.00
133	1.0	-0.2	-0.9	0.2	0.00	0.00	0.00
134	1.0	-0.3	-0.9	-0.4	0.00	0.00	0.00
135	1.4	-0.3	-1.3	0.3	0.01	0.00	0.00
136	1.4	-0.3	-1.3	0.3	0.01	0.00	0.00
137	1.4	-0.4	-1.3	-0.3	0.00	0.00	0.00
138	1.3	-0.4	-1.3	0.1	0.00	0.00	0.00
139	1.3	-0.4	-1.3	0.1	0.00	0.00	0.00
140	1.4	-0.4	-1.3	-0.3	0.00	0.00	0.00
141	1.4	-0.4	-1.3	-0.1	0.00	0.00	0.00
142	1.4	-0.4	-1.3	-0.1	0.00	0.00	0.00
143	1.4	-0.4	-1.3	0.0	0.00	0.00	0.00
144	1.4	-0.4	-1.3	0.0	0.00	0.00	0.00
145	1.4	-0.4	-1.3	0.0	0.00	0.00	0.00
146	1.4	-0.4	-1.3	0.0	0.00	0.00	0.00
147	4.4	-0.8	-4.3	-0.5	0.01	0.00	0.00

Node	Displacements [mm]				Rotations [°]		
No.	|u|	u_X	u_Y	u_Z	φ_X	φ_Y	φ_Z
148	4.5	-0.9	-4.4	-0.5	0.01	0.00	0.00
149	4.5	-0.8	-4.4	-0.5	0.01	0.00	0.00
150	4.4	-0.8	-4.3	-0.5	0.01	0.00	0.00
151	4.3	-0.8	-4.2	-0.5	0.01	0.00	0.00
152	3.6	-0.7	-3.5	-0.4	0.01	0.00	0.00
153	3.6	-0.7	-3.5	-0.4	0.01	0.00	0.00
154	4.3	-0.8	-4.2	-0.4	0.01	0.00	0.00
155	4.4	-0.8	-4.3	-0.4	0.01	0.00	0.00
156	4.5	-0.8	-4.4	-0.4	0.01	0.00	0.00
157	0.3	-0.1	-0.3	0.1	0.00	0.00	0.00
158	0.3	-0.1	-0.3	0.1	0.00	0.00	0.00
159	0.3	-0.1	-0.3	0.1	0.00	0.00	0.00
160	0.3	-0.1	-0.3	0.1	0.00	0.00	0.00
161	0.5	-0.1	-0.5	0.1	0.00	0.00	0.00
162	0.5	-0.1	-0.5	0.1	0.00	0.00	0.00
163	0.6	-0.2	-0.6	0.1	0.00	0.00	0.00
164	0.6	-0.2	-0.5	0.1	0.00	0.00	0.00
165	0.8	-0.2	-0.7	0.1	0.00	0.00	0.00
166	0.8	-0.2	-0.7	0.1	0.00	0.00	0.00
167	1.0	-0.3	-0.9	0.1	0.00	0.00	0.00
168	0.9	-0.3	-0.9	0.1	0.00	0.00	0.00
169	1.4	-0.4	-1.3	0.1	0.00	0.00	0.00
170	1.4	-0.4	-1.3	0.1	0.00	0.00	0.00
171	1.7	-0.4	-1.7	0.1	0.01	0.00	0.00
172	1.8	-0.4	-1.7	0.1	0.01	0.00	0.00
173	1.8	-0.4	-1.7	0.1	0.00	0.00	0.00
174	1.8	-0.4	-1.8	0.1	0.00	0.00	0.00
175	1.8	-0.4	-1.7	0.1	0.00	0.00	0.00
176	1.8	-0.4	-1.7	0.1	0.01	0.00	0.00
177	1.7	-0.4	-1.7	0.1	0.01	0.00	0.00
178	2.1	-0.5	-2.0	0.1	0.00	0.00	0.00
179	2.1	-0.5	-2.0	0.2	0.00	0.00	0.00
180	2.9	-0.6	-2.8	0.2	0.01	0.00	0.00
181	2.9	-0.6	-2.9	0.2	0.01	0.00	0.00
182	3.0	-0.6	-2.9	0.2	0.01	0.00	0.00
183	3.0	-0.6	-3.0	0.1	0.00	0.00	0.00
184	3.0	-0.6	-2.9	0.1	0.01	0.00	0.00
185	2.9	-0.6	-2.9	0.1	0.01	0.00	0.00
186	2.9	-0.6	-2.8	0.1	0.01	0.00	0.00
187	3.5	-0.7	-3.4	0.2	0.00	0.00	0.00
188	3.5	-0.7	-3.4	0.3	0.01	0.00	0.00
189	4.2	-0.8	-4.1	0.3	0.01	0.00	0.00
190	4.3	-0.8	-4.2	0.3	0.01	0.00	0.00
191	4.3	-0.8	-4.2	0.3	0.01	0.00	0.00
192	4.4	-0.8	-4.3	0.2	0.00	0.00	0.00
193	4.3	-0.8	-4.3	0.2	0.01	0.00	0.00
194	4.3	-0.8	-4.2	0.2	0.01	0.00	0.00
195	4.2	-0.8	-4.2	0.2	0.01	0.00	0.00

Node	Displacements [mm]				Rotations [°]		
No.	|u|	u_X	u_Y	u_Z	φ_X	φ_Y	φ_Z
196	3.5	-0.7	-3.4	-0.1	0.01	0.00	0.00
197	3.5	-0.7	-3.4	0.1	0.00	0.00	0.00
198	4.2	-0.8	-4.2	0.1	0.01	0.00	0.00
199	4.3	-0.8	-4.2	0.1	0.01	0.00	0.00
200	4.3	-0.8	-4.3	0.0	0.01	0.00	0.00
201	4.4	-0.8	-4.3	0.0	0.01	0.00	0.00
202	4.3	-0.8	-4.2	-0.1	0.01	0.00	0.00
203	4.3	-0.8	-4.2	-0.1	0.01	0.00	0.00
204	4.2	-0.8	-4.1	-0.1	0.01	0.00	0.00
205	1.4	-0.4	-1.3	-0.1	0.00	0.00	0.00
206	1.4	-0.4	-1.3	-0.1	0.00	0.00	0.00
207	1.4	-0.4	-1.4	-0.1	0.00	0.00	0.00
208	1.4	-0.4	-1.4	-0.1	0.00	0.00	0.00
209	2.1	-0.5	-2.1	0.0	0.00	0.00	0.00
210	2.1	-0.5	-2.1	-0.1	0.00	0.00	0.00
211	2.3	-0.5	-2.2	-0.1	0.01	0.00	0.00
212	2.3	-0.5	-2.2	0.0	0.01	0.00	0.00
213	2.4	-0.5	-2.3	0.0	0.01	0.00	0.00
214	2.4	-0.5	-2.3	-0.1	0.01	0.00	0.00
215	2.9	-0.6	-2.9	-0.1	0.01	0.00	0.00
216	3.0	-0.6	-2.9	-0.1	0.01	0.00	0.00
217	3.0	-0.6	-3.0	-0.1	0.00	0.00	0.00
218	3.1	-0.6	-3.0	0.0	0.00	0.00	0.00
219	3.0	-0.6	-3.0	0.0	0.00	0.00	0.00
220	3.0	-0.6	-2.9	0.0	0.01	0.00	0.00
221	3.0	-0.6	-2.9	0.0	0.01	0.00	0.00
222	3.5	-0.7	-3.4	0.2	0.01	0.00	0.00
223	3.5	-0.7	-3.4	0.0	0.01	0.00	0.00
224	4.2	-0.8	-4.1	0.0	0.01	0.00	0.00
225	4.3	-0.8	-4.2	0.0	0.01	0.00	0.00
226	4.3	-0.9	-4.3	0.0	0.01	0.00	0.00
227	4.4	-0.9	-4.3	0.1	0.00	0.00	0.00
228	4.3	-0.9	-4.2	0.2	0.01	0.00	0.00
229	4.2	-0.8	-4.1	0.2	0.01	0.00	0.00
230	4.3	-0.9	-4.2	0.1	0.01	0.00	0.00
231	3.5	-0.7	-3.4	-0.1	0.00	0.00	0.00
232	3.5	-0.7	-3.4	-0.3	0.01	0.00	0.00
233	4.2	-0.8	-4.1	-0.3	0.01	0.00	0.00
234	4.3	-0.8	-4.2	-0.3	0.01	0.00	0.00
235	4.3	-0.8	-4.2	-0.3	0.01	0.00	0.00
236	4.4	-0.8	-4.3	-0.2	0.01	0.00	0.00
237	4.3	-0.8	-4.3	-0.1	0.01	0.00	0.00
238	4.2	-0.8	-4.2	-0.1	0.01	0.00	0.00
239	4.3	-0.8	-4.2	-0.1	0.01	0.00	0.00
240	4.5	-0.8	-4.4	-0.4	0.01	0.00	0.00
241	4.4	-0.8	-4.3	-0.4	0.01	0.00	0.00
242	4.3	-0.8	-4.2	-0.4	0.01	0.00	0.00
243	4.3	-0.8	-4.2	-0.4	0.01	0.00	0.00

Node	Displacements [mm]				Rotations [°]		
No.	|u|	u_X	u_Y	u_Z	φ_X	φ_Y	φ_Z
244	3.6	-0.7	-3.5	-0.4	0.01	0.00	0.00
247	2.2	-0.5	-2.1	-0.4	0.01	0.00	0.00
248	3.0	-0.6	-2.9	-0.4	0.01	0.00	0.00
249	3.0	-0.6	-2.9	-0.4	0.01	0.00	0.00
250	3.1	-0.7	-3.0	-0.4	0.01	0.00	0.00
251	3.1	-0.7	-3.0	-0.4	0.01	0.00	0.00
252	3.1	-0.6	-3.0	-0.4	0.01	0.00	0.00
253	3.0	-0.6	-2.9	-0.4	0.01	0.00	0.00
254	3.0	-0.6	-2.9	-0.4	0.01	0.00	0.00
255	2.2	-0.5	-2.1	-0.4	0.01	0.00	0.00
256	1.4	-0.4	-1.3	-0.3	0.01	0.00	0.00
257	1.4	-0.4	-1.3	-0.3	0.01	0.00	0.00
258	1.8	-0.4	-1.7	-0.4	0.01	0.00	0.00
259	1.8	-0.4	-1.7	-0.4	0.01	0.00	0.00
260	1.8	-0.4	-1.7	-0.4	0.01	0.00	0.00
261	1.8	-0.4	-1.7	-0.4	0.01	0.00	0.00
262	1.8	-0.4	-1.7	-0.4	0.01	0.00	0.00
263	1.8	-0.4	-1.7	-0.4	0.01	0.00	0.00
264	1.8	-0.4	-1.7	-0.4	0.01	0.00	0.00
265	1.8	-0.4	-1.7	-0.4	0.01	0.00	0.00
266	1.8	-0.4	-1.7	-0.4	0.01	0.00	0.00
345	0.0	0.0	0.0	0.0	0.00	0.00	0.00
346	0.0	0.0	0.0	0.0	0.00	0.00	0.00
359	0.0	0.0	0.0	0.0	0.00	0.00	0.00
360	0.0	0.0	0.0	0.0	0.00	0.00	0.00
361	0.0	0.0	0.0	0.0	0.00	0.00	0.00
362	0.2	0.0	-0.2	0.1	0.00	0.00	0.00
363	0.7	-0.1	-0.6	0.2	0.00	0.00	0.00
370	0.1	0.0	-0.1	0.1	0.00	0.00	0.00
371	0.5	0.0	-0.5	0.2	0.00	0.00	0.00
372	0.0	0.0	0.0	0.0	0.00	0.00	0.00
373	0.0	0.0	0.0	0.0	0.00	0.00	0.00
376	0.0	0.0	0.0	0.0	0.00	0.00	0.00
377	0.1	0.0	-0.1	0.0	0.00	0.00	0.00
378	0.2	0.0	-0.1	-0.1	0.00	0.00	0.00
379	0.0	0.0	0.0	0.0	0.00	0.00	0.00
380	0.0	0.0	0.0	0.0	0.00	0.00	0.00
381	0.2	0.0	-0.1	-0.1	0.00	0.00	0.00
382	0.1	0.0	-0.1	0.0	0.00	0.00	0.00
383	0.0	0.0	0.0	0.0	0.00	0.00	0.00
384	0.2	0.0	-0.2	0.1	0.00	0.00	0.00
385	0.7	-0.2	-0.6	0.2	0.00	0.00	0.00
386	0.1	0.0	-0.1	0.1	0.00	0.00	0.00
387	0.5	-0.1	-0.4	0.2	0.00	0.00	0.00
388	0.0	0.0	0.0	0.0	0.00	0.00	0.00
389	0.2	0.0	-0.2	0.0	0.00	0.00	0.00
390	0.0	0.0	0.0	0.0	0.00	0.00	0.00
391	0.6	-0.2	-0.6	-0.1	0.00	0.00	0.00

Node	Displacements [mm]				Rotations [°]		
No.	|u|	u_X	u_Y	u_Z	φ_X	φ_Y	φ_Z
392	0.1	0.0	-0.1	0.0	0.00	0.00	0.00
393	0.4	-0.1	-0.4	0.0	0.00	0.00	0.00
394	0.0	0.0	0.0	0.0	0.00	0.00	0.00
395	0.2	-0.2	0.0	0.0	0.00	0.00	-0.01
396	0.0	0.0	0.0	0.0	0.00	0.00	0.00
397	0.0	0.0	0.0	0.0	0.00	0.00	0.00
398	0.0	0.0	0.0	0.0	0.00	0.00	0.00
399	0.0	0.0	0.0	0.0	0.00	0.00	0.00
400	0.4	0.0	-0.4	0.0	0.00	0.00	0.00
401	0.4	0.0	-0.4	0.0	0.00	0.00	0.00
402	0.2	0.0	-0.2	0.0	0.00	0.00	0.00
403	0.1	0.0	-0.1	0.0	0.00	0.00	0.00
404	0.0	0.0	0.0	0.0	0.00	0.00	0.00
405	0.0	0.0	0.0	0.0	0.00	0.00	0.00
411	2.1	-0.5	-2.0	-0.3	0.01	0.00	0.00
412	2.1	-0.5	-2.0	0.4	0.01	0.00	0.00
413	2.1	-0.5	-2.0	-0.4	0.01	0.00	0.00
414	2.1	-0.5	-2.0	0.4	0.01	0.00	0.00
415	2.0	-0.5	-2.0	0.0	0.00	0.00	0.00
416	2.0	-0.5	-2.0	0.0	0.00	0.00	0.00
417	2.5	-0.6	-2.5	0.0	0.00	0.00	0.00
418	2.5	-0.6	-2.5	0.0	0.00	0.00	0.00
419	2.4	-0.6	-2.3	0.0	0.00	0.00	0.00
420	2.0	-0.5	-2.0	0.3	0.01	0.00	0.00
421	2.0	-0.5	-2.0	-0.2	0.01	0.00	0.00
422	2.4	-0.6	-2.3	0.0	0.00	0.00	0.00
423	2.0	-0.5	-2.0	-0.2	0.01	0.00	0.00
424	2.0	-0.5	-2.0	0.2	0.01	0.00	0.00
425	2.5	-0.6	-2.5	0.0	0.00	0.00	0.00
430	2.0	-0.5	-2.0	-0.1	0.00	0.00	0.00
431	2.0	-0.5	-1.9	0.1	0.00	0.00	0.00
432	2.0	-0.5	-2.0	0.0	0.00	0.00	0.00
433	2.0	-0.5	-2.0	0.1	0.00	0.00	0.00
667	4.8	-0.9	-4.7	0.6	0.01	0.00	0.00
668	4.8	-0.9	-4.7	0.4	0.01	0.00	0.00
718	4.8	-0.9	-4.7	-0.4	0.01	0.00	0.00
719	4.8	-0.9	-4.7	-0.3	0.01	0.00	0.00
752	4.8	-0.9	-4.7	-0.5	0.01	0.00	0.00
1184	4.7	-0.9	-4.7	0.0	0.01	0.00	0.00
1185	4.7	-0.9	-4.7	0.3	0.01	0.00	0.00
1186	4.8	-0.9	-4.7	0.5	0.01	0.00	0.00
1196	4.8	-0.9	-4.7	0.3	0.01	0.00	0.00
1198	4.8	-0.9	-4.7	0.1	0.01	0.00	0.00
1199	4.7	-0.9	-4.7	-0.2	0.01	0.00	0.00
1200	4.9	-0.9	-4.8	-0.5	0.01	0.00	0.00
1201	4.9	-0.9	-4.8	-0.4	0.01	0.00	0.00
1315	5.0	-0.9	-4.9	0.5	0.01	0.00	0.00
1316	5.0	-0.9	-4.9	0.5	0.01	0.00	0.00

Node	Displacements [mm]				Rotations [°]		
No.	|u|	u_X	u_Y	u_Z	φ_X	φ_Y	φ_Z
1398	0.4	-0.1	-0.4	0.1	0.00	0.00	0.00
1399	0.5	-0.2	-0.5	-0.1	0.00	0.00	0.00
1400	0.2	-0.1	-0.2	0.0	0.00	0.00	0.00
1401	0.4	-0.1	-0.3	-0.2	0.00	0.00	0.00
1402	0.4	-0.2	-0.4	0.0	0.00	0.01	-0.01
1403	0.3	-0.1	-0.3	-0.1	0.00	0.01	0.00
1405	0.0	0.0	0.0	0.0	0.00	-0.01	0.00
1406	0.2	0.0	-0.2	0.0	0.00	0.00	0.00
1407	0.5	-0.2	-0.4	-0.2	0.00	0.00	0.00
1408	0.5	-0.1	-0.4	0.1	0.00	0.00	0.00
1409	0.3	-0.2	-0.2	0.1	0.00	0.00	-0.01
1410	0.3	-0.1	-0.3	0.1	0.00	0.00	0.00
1411	0.4	-0.1	-0.4	0.1	0.00	0.00	0.00
1412	0.3	-0.1	-0.3	-0.1	0.00	0.00	0.00
1413	0.3	-0.2	-0.2	0.0	0.01	0.00	0.00
1414	0.5	-0.2	-0.4	-0.2	0.00	0.00	0.00
1415	0.5	-0.2	-0.4	-0.2	0.00	0.00	0.00
1416	0.2	0.0	-0.2	0.0	-0.01	0.00	0.00
1417	0.2	-0.2	-0.1	0.0	0.00	-0.01	0.00
1418	0.3	-0.2	-0.2	0.0	0.00	0.00	0.00
1419	0.0	0.0	0.0	0.0	0.00	-0.01	0.00
1420	0.1	0.0	-0.1	0.0	0.00	0.00	0.00
1421	0.5	0.0	-0.5	0.0	0.00	0.00	0.00
1422	0.2	-0.1	-0.2	-0.1	0.00	0.00	0.00
1424	0.5	0.0	-0.5	0.0	0.00	0.00	0.00
1426	0.5	-0.2	-0.4	-0.2	0.00	0.00	0.00
1427	0.5	-0.2	-0.3	-0.2	0.00	0.01	0.00
1428	0.5	-0.2	-0.4	-0.2	0.00	0.00	0.00
1429	0.3	-0.1	-0.3	-0.2	0.00	0.00	0.00
1430	0.2	-0.1	-0.2	-0.1	0.00	0.01	-0.01
1432	0.5	-0.1	-0.5	-0.2	0.00	0.00	0.00
1433	0.5	-0.1	-0.5	-0.1	0.00	0.00	0.00
1434	0.5	-0.1	-0.5	-0.1	0.00	0.00	0.00
1435	0.6	-0.1	-0.5	-0.3	0.00	0.00	0.00
1436	0.4	-0.1	-0.3	-0.2	0.00	0.00	0.00
1439	0.5	0.0	-0.5	0.0	-0.01	0.00	0.00
1440	0.7	-0.1	-0.7	-0.3	0.00	0.00	0.00
1509	0.1	-0.1	0.0	0.0	0.00	0.00	-0.01
1513	0.2	-0.2	0.0	0.0	0.00	0.00	0.00
1514	0.2	-0.2	0.0	0.0	0.00	0.00	0.01
1521	0.2	-0.1	-0.2	0.0	0.00	0.00	0.00
1523	0.1	-0.1	0.0	0.0	0.00	0.00	0.01
1524	0.1	-0.1	0.0	0.0	0.00	0.00	0.00
1527	0.0	0.0	0.0	0.0	0.00	0.00	0.00
1532	0.1	-0.1	0.0	0.0	0.00	0.00	0.00
1558	0.4	-0.1	-0.4	-0.3	0.00	0.00	0.00
1559	0.4	-0.1	-0.3	-0.1	0.00	0.00	0.00
1562	0.4	-0.1	-0.4	0.1	0.00	0.00	0.00

Node	Displacements [mm]				Rotations [°]		
No.	|u|	u_X	u_Y	u_Z	φ_X	φ_Y	φ_Z
1563	0.6	-0.1	-0.5	0.1	0.00	0.00	0.00
1564	0.6	-0.2	-0.5	-0.3	0.00	0.00	0.00
1565	0.5	-0.1	-0.4	0.1	0.00	0.00	0.00
1566	0.6	-0.1	-0.5	-0.3	0.00	0.00	0.00
1567	0.0	0.0	0.0	0.0	0.00	-0.01	0.00
1568	0.0	0.0	0.0	0.0	0.00	-0.01	0.00
1571	0.1	-0.1	0.0	0.0	0.00	0.00	0.00
Max	**5.0**	**0.0**	**0.0**	**0.6**	**0.01**	**0.01**	**0.01**
Min	**0.0**	**-0.9**	**-4.9**	**-0.5**	**-0.01**	**-0.01**	**-0.01**

Appendix 3: Static loads summary

	Description	Value	Unit	Comment
	LC1 - Self-weight			
	Sum of loads in X	0.000	kN	
	Sum of support forces in X	-0.485	kN	
	Sum of loads in Y	0.000	kN	
	Sum of support forces in Y	0.140	kN	
	Sum of loads in Z	-8.26E+04	kN	
	Sum of support forces in Z	-8.26E+04	kN	Deviation: 0.00 %
	Resultant of reactions about X	-133.794	kNm	At center of gravity of model (X: 4927.790, Y: -4292.740, Z: 20754.300 mm)
	Resultant of reactions about Y	157.731	kNm	At center of gravity of model
	Resultant of reactions about Z	-6.110	kNm	At center of gravity of model
	Maximum displacement in X-direction	4.6	mm	FE Node No. 395 (X: -6570.9, Y: 0.0, Z: 20270.0 mm)
	Maximum displacement in Y-direction	4.9	mm	FE Node No. 400 (X: 10160.0, Y: -13500.0, Z: 20270.0 mm)
	Maximum displacement in Z-direction	-17.7	mm	FE Node No. 22463 (X: 5520.3, Y: -4321.2, Z: 46145.8 mm)
	Maximum vectorial displacement	18.2	mm	FE Node No. 22462 (X: 5822.7, Y: -4321.2, Z: 46144.2 mm)
	Maximum rotation about X-axis	-0.29	°	FE Node No. 1406 (X: 129.1, Y: -13495.2, Z: 19400.0 mm)
	Maximum rotation about Y-axis	0.18	°	FE Node No. 33834 (X: -1670.9, Y: -10561.9, Z: 19000.0 mm)
	Maximum rotation about Z-axis	-0.09	°	FE Node No. 34076 (X: -407.0, Y: -12244.7, Z: 18953.4 mm)
	Method of analysis	Large		Large Deformation Analysis (Newton-Raphson)
	Consider favorable effects due to tension forces of members	+		
	Divide results by LC Factor	-		
	Reduction of stiffness	-		
	Number of load increments	5		
	Number of iterations	3		
	Maximum value of element of stiffness matrix on diagonal	4.804E+11		
	Minimum value of element of stiffness matrix on diagonal	10000		
	Stiffness matrix determinant	5.024E+2035255		
	Infinity Norm	1.139E+12		
	Incrementally increasing loading	-		

	LC4 - Bell			
	Description	Value	Unit	Comment
	Sum of loads in X	0.000	kN	
	Sum of support forces in X	0.000	kN	
	Sum of loads in Y	0.000	kN	
	Sum of support forces in Y	0.000	kN	
	Sum of loads in Z	-26.500	kN	
	Sum of support forces in Z	-26.500	kN	Deviation: 0.00 %
	Resultant of reactions about X	4.843	kNm	At center of gravity of model (X: 4927.790, Y: -4292.740, Z: 20754.300 mm)
	Resultant of reactions about Y	18.304	kNm	At center of gravity of model
	Resultant of reactions about Z	-0.002	kNm	At center of gravity of model
	Maximum displacement in X-direction	-0.3	mm	Member No. 133, x: 769.6 mm
	Maximum displacement in Y-direction	0.0	mm	Member No. 161, x: 3028.2 mm
	Maximum displacement in Z-direction	-1.5	mm	Member No. 157, x: 1300.0 mm
	Maximum vectorial displacement	1.5	mm	FE Node No. 425 (X: 5618.5, Y: -4475.5, Z: 41090.0 mm)
	Maximum rotation about X-axis	0.00	°	Member No. 164, x: 1641.0 mm
	Maximum rotation about Y-axis	-0.06	°	Member No. 157, x: 433.3 mm
	Maximum rotation about Z-axis	0.00	°	FE Node No. 23204 (X: 8792.3, Y: -4774.8, Z: 35170.0 mm)
	Method of analysis	Large		Large Deformation Analysis (Newton-Raphson)
	Consider favorable effects due to tension forces of members	+		
	Divide results by LC Factor	-		
	Reduction of stiffness	-		
	Number of load increments	5		
	Number of iterations	2		
	Maximum value of element of stiffness matrix on diagonal	4.804E+11		
	Minimum value of element of stiffness matrix on diagonal	10000		
	Stiffness matrix determinant	1.293E+2035263		
	Infinity Norm	1.139E+12		
	Incrementally increasing loading	-		

	LC6 - SIDL			
	Description	Value	Unit	Comment
	Sum of loads in X	0.000	kN	
	Sum of support forces in X	-0.002	kN	
	Sum of loads in Y	0.000	kN	
	Sum of support forces in Y	0.003	kN	
	Sum of loads in Z	-1584.440	kN	
	Sum of support forces in Z	-1584.440	kN	Deviation: 0.00 %
	Resultant of reactions about X	349.124	kNm	At center of gravity of model (X: 4927.790, Y: -4292.740, Z: 20754.300 mm)
	Resultant of reactions about Y	666.912	kNm	At center of gravity of model
	Resultant of reactions about Z	-0.050	kNm	At center of gravity of model
	Maximum displacement in X-direction	0.1	mm	Member No. 171, x: 3821.5 mm
	Maximum displacement in Y-direction	0.1	mm	FE Node No. 12891 (X: 6394.0, Y: -8907.0, Z: 49290.0 mm)
	Maximum displacement in Z-direction	-2.8	mm	FE Node No. 26485 (X: 4952.3, Y: -4573.4, Z: 0.0 mm)
	Maximum vectorial displacement	2.8	mm	FE Node No. 26485 (X: 4952.3, Y: -4573.4, Z: 0.0 mm)
	Maximum rotation about X-axis	-0.05	°	FE Node No. 26781 (X: 4953.5, Y: -7326.9, Z: 0.0 mm)
	Maximum rotation about Y-axis	0.05	°	FE Node No. 26475 (X: 1898.1, Y: -4587.2, Z: 0.0 mm)
	Maximum rotation about Z-axis	0.00	°	FE Node No. 1429 (X: 129.1, Y: -10395.2, Z: 17500.0 mm)
	Method of analysis	Large		Large Deformation Analysis (Newton-Raphson)
	Consider favorable effects due to tension forces of members	+		
	Divide results by LC Factor	-		
	Reduction of stiffness	-		
	Number of load increments	5		
	Number of iterations	3		
	Maximum value of element of stiffness matrix on diagonal	4.804E+11		
	Minimum value of element of stiffness matrix on diagonal	10000		
	Stiffness matrix determinant	8.110E+2035262		
	Infinity Norm	1.139E+12		
	Incrementally increasing loading	-		

	LC7 - Live Load			
	Description	Value	Unit	Comment
	Sum of loads in X	0.000	kN	
	Sum of support forces in X	-0.002	kN	
	Sum of loads in Y	0.000	kN	
	Sum of support forces in Y	0.003	kN	
	Sum of loads in Z	-1584.440	kN	
	Sum of support forces in Z	-1584.440	kN	Deviation: 0.00 %
	Resultant of reactions about X	349.124	kNm	At center of gravity of model (X: 4927.790, Y: -4292.740, Z: 20754.300 mm)
	Resultant of reactions about Y	666.912	kNm	At center of gravity of model
	Resultant of reactions about Z	-0.050	kNm	At center of gravity of model
	Maximum displacement in X-direction	0.1	mm	Member No. 171, x: 3821.5 mm
	Maximum displacement in Y-direction	0.1	mm	FE Node No. 12891 (X: 6394.0, Y: -8907.0, Z: 49290.0 mm)
	Maximum displacement in Z-direction	-2.8	mm	FE Node No. 26485 (X: 4952.3, Y: -4573.4, Z: 0.0 mm)
	Maximum vectorial displacement	2.8	mm	FE Node No. 26485 (X: 4952.3, Y: -4573.4, Z: 0.0 mm)
	Maximum rotation about X-axis	-0.05	°	FE Node No. 26781 (X: 4953.5, Y: -7326.9, Z: 0.0 mm)
	Maximum rotation about Y-axis	0.05	°	FE Node No. 26475 (X: 1898.1, Y: -4587.2, Z: 0.0 mm)
	Maximum rotation about Z-axis	0.00	°	FE Node No. 1429 (X: 129.1, Y: -10395.2, Z: 17500.0 mm)
	Method of analysis	Large		Large Deformation Analysis (Newton-Raphson)
	Consider favorable effects due to tension forces of members	+		
	Divide results by LC Factor	-		
	Reduction of stiffness	-		
	Number of load increments	5		
	Number of iterations	3		
	Maximum value of element of stiffness matrix on diagonal	4.804E+11		
	Minimum value of element of stiffness matrix on diagonal	10000		
	Stiffness matrix determinant	8.110E+2035262		
	Infinity Norm	1.139E+12		
	Incrementally increasing loading	-		

	LC9 - Wind load			
	Description	Value	Unit	Comment
	Sum of loads in X	0.000	kN	
	Sum of support forces in X	0.000	kN	
	Sum of loads in Y	-491.971	kN	
	Sum of support forces in Y	-491.971	kN	Deviation: 0.00 %
	Sum of loads in Z	0.000	kN	
	Sum of support forces in Z	0.000	kN	
	Resultant of reactions about X	5367.430	kNm	At center of gravity of model (X: 4927.790, Y: -4292.740, Z: 20754.300 mm)
	Resultant of reactions about Y	0.000	kNm	At center of gravity of model
	Resultant of reactions about Z	-247.499	kNm	At center of gravity of model
	Maximum displacement in X-direction	-0.9	mm	FE Node No. 8545 (X: 1075.0, Y: -2366.4, Z: 57250.0 mm)
	Maximum displacement in Y-direction	-4.9	mm	FE Node No. 5002 (X: 5617.9, Y: 0.0, Z: 57250.0 mm)
	Maximum displacement in Z-direction	0.6	mm	FE Node No. 4964 (X: 10363.8, Y: 0.0, Z: 50331.4 mm)
	Maximum vectorial displacement	5.0	mm	FE Node No. 5002 (X: 5617.9, Y: 0.0, Z: 57250.0 mm)
	Maximum rotation about X-axis	0.01	°	FE Node No. 5327 (X: 5267.8, Y: 0.0, Z: 49008.8 mm)
	Maximum rotation about Y-axis	0.01	°	FE Node No. 33245 (X: -1670.9, Y: -6071.4, Z: 18600.0 mm)
	Maximum rotation about Z-axis	-0.01	°	FE Node No. 35352 (X: -3952.2, Y: -5064.2, Z: 17808.0 mm)
	Method of analysis	Linear		Geometrically Linear Analysis
	Reduction of stiffness	-		
	Number of load increments	1		
	Number of iterations	1		
	Maximum value of element of stiffness matrix on diagonal	4.805E+11		
	Minimum value of element of stiffness matrix on diagonal	10000		
	Stiffness matrix determinant	4.421E+2039026		
	Infinity Norm	1.139E+12		
	Incrementally increasing loading	-		

	Summary			
	Description	Value	Unit	Comment
	Calculation Status	OK		
	Maximum displacement in X-direction	4.6	mm	LC1, FE Node No. 395 (X: -6570.9, Y: 0.0, Z: 20270.0 mm)
	Maximum displacement in Y-direction	-4.9	mm	LC9, FE Node No. 5002 (X: 5617.9, Y: 0.0, Z: 57250.0 mm)
	Maximum displacement in Z-direction	-17.7	mm	LC1, FE Node No. 22463 (X: 5520.3, Y: -4321.2, Z: 46145.8 mm)
	Maximum vectorial displacement	18.2	mm	LC1, FE Node No. 22462 (X: 5822.7, Y: -4321.2, Z: 46144.2 mm)
	Maximum rotation about X-axis	-0.29	°	LC1, FE Node No. 1406 (X: 129.1, Y: -13495.2, Z: 19400.0 mm)
	Maximum rotation about Y-axis	0.18	°	LC1, FE Node No. 33834 (X: -1670.9, Y: -10561.9, Z: 19000.0 mm)
	Maximum rotation about Z-axis	-0.09	°	LC1, FE Node No. 34076 (X: -407.0, Y: -12244.7, Z: 18953.4 mm)
	Number of 1D finite elements (member elements)	179		
	Number of 2D finite elements (surface elements)	41755		
	Number of 3D finite elements (solid elements)	0		
	Number of FE nodes	38687		
	Number of equations	232122		
	Matrix solver method	Direct		
	Maximum number of iterations	100		
	Number of divisions for member results	10		
	Number of divisions of members with cable, elastic foundation, taper,	10		
	Activate shear stiffness of members (A-y, A-z)	+		
	Plate bending theory	Mindlin		
	Precision of convergence criteria of nonlinear calculation	1.0		